Smart Planning and Operation in Cellular Networks

by

Jonah Ho

A thesis
presented to the University of Waterloo
in fulfillment of the
thesis requirement for the degree of
Master of Applied Science
in
Electrical and Computer Engineering

Waterloo, Ontario, Canada, 2020

Author's Declaration

I hereby declare that I am the sole author of this thesis. This is a true copy of the thesis, including any required final revisions, as accepted by my examiners.

I understand that my thesis may be made electronically available to the public.

Abstract

Cellular networks are less and less regular as operators add base stations (BSs) to increase coverage and performance. Given these facts, we explore the network planning and operation stages of the downlink of a multi-cell Orthogonal Frequency Division Multiple Access (OFDMA)-based network. In the planning stage, which is an offline process, we look at improving expected performance while maintaining good coverage. To do so, we parameterize offline a simple power map assignment to be used by all BSs. In the operation stage, which is an online process, we look at improving performance by handling load imbalance and hotspots in the network. To do so, we propose a heuristic that modifies the power map (from the planning stage) by allocating subchannels to BSs, and specifying for each BS the transmit power to use on the subchannels.

The research questions are as follows: i) Is conventional planning good enough in view of the fact that networks are less and less regular? ii) BS subchannel allocation is typically done only in the planning stage, can we (re)do it more often (i.e., during the operation stage) to improve performance? iii) How can we take load imbalance and hotspots into account when operating a network?

To answer these questions, we propose and investigate one planning scheme and one simple and practical operation scheme in the downlink. We evaluate these schemes on three different network topologies (i.e., 19-cell regular, highly irregular, and lightly irregular). For each we consider both uniform and non-uniform distributions of users (i.e., hotspots). The simulations take place in a dynamic setting with arriving and departing users.

The contributions are as follows: i) We propose a simple power map assignment that we parameterize to offer good performance and good coverage even in highly irregular networks, ii) We propose a heuristic based on BS coordination that allocates subchannels to BSs and specifies for each BS the transmit power to use on the subchannels to handle load imbalance and hotspots, and iii) A practical heuristic implementation that reduces BS coordination.

Acknowledgements

I would like to thank my supervisor Prof. Catherine Rosenberg for her focus and guidance. The meetings, emails, Skype calls and chats, lab presentations, lunches, and teaching assistant experience were all meaningful. It was an eye-opening experience doing research with you and the sharpened skills I gained will last a lifetime.

I would like to thank Yigit Ozcan for being my mentor and his collaboration on this topic. I learned from the best.

I would like to thank Ara Shaverdian for the lunches, dinners, and late night company working in the lab.

I would like to thank Duncan Ho for introducing me to the cellular world, and looking after my best interests.

I would like to thank Charisse Ho for her incessantly funny text messages. Good luck in AP Chemistry!

Special thanks to the AMPL Google Group for their expertise on AMPL, MINOS, and amplpy.

Dedication

This is dedicated to my family, and friends.

Table of Contents

List of Figures

List of Tables

List of Abbreviations

AR augmented reality 1

BBU baseband unit 3

BSs base stations iii

C-RAN Centralized - Radio Access Network 2

EP equal power 17

FDD Frequency Division Duplexing 13

FFR Fractional Frequency Reuse 5

ICI inter-cell interference 6

IP Internet Protocol 3

LTE Long Term Evolution 10

OFDMA Orthogonal Frequency Division Multiple Access iii

PF proportional fair 16

RB resource block 13

RL-LSTM Reinforcement Learning - Long Short-Term Memory 11

RR round robin 10

RRHs remote radio heads 3

RSRP Reference Signal Received Power 10

RSRQ Reference Signal Received Quality 10

SFR Soft Frequency Reuse 5

SINR Signal to Interference and Noise Ratio 2

SISO Single In Single Out 13

SO Smart Operation 57

TS time-slot 13

UA user association 3

UE user equipment 10

US user scheduling 3

Chapter 1

Introduction

1.1 Overview

Networks are less and less regular as operators add base stations (BSs) to increase radio access coverage and capacity. This is due to the explosive growth of cellular traffic and can be seen in Ericsson Mobility Reports. In Q1 2014, global cellular traffic was only 2 exabytes per month [32]. As of Q4 2019, global cellular traffic was 40 exabytes per month [32]. For example in 2019, Finland's mobile traffic was 8,000 terabytes (TB) per day, surpassing the 6,000 TB/day of global fixed internet traffic in 2001 [21]!

The main driver of traffic is video which consumes 65% of global cellular downlink traffic today [35][1]. This is not suprising given the rise of streaming services like Netflix and YouTube, instant messaging services like WhatsApp and WeChat, and social games like Pokémon Go and TikTok. Even Apple, whose stock performance was almost exclusively tied to iPhone shipments, has been forced to diversify itself as a services company with the launch of services like Apple Music, Arcade, News+, and TV+ monthly subscriptions. Meanwhile Google, which generates 40% of global internet traffic, launched its streaming video game service Stadia in 2019. Similarly, Microsoft is expected to launch its own in September 2020 as part of Xbox Game Pass Ultimate. Today, the top three global cellular traffic applications in the downlink are YouTube (27%), FaceBook (23%), and Instagram (7%) [35][1]. To exacerbate the issue, the mobile augmented reality (AR) market is expected to hit $24 billion by 2030 [38]. Clearly there is a lot of traffic today and there will be even more tomorrow.

[1] [35] excludes data from China and India.

Given the fact that networks are less and less regular, we explore planning and operation to see if we can improve system performance in an OFDMA (Orthogonal Frequency Division Multiple Access)-based cellular network. We focus on the downlink. Planning is an offline process that in its basic form can be described as: how many BSs and what placement to offer good service to an area? Unfortunately, this problem is hard and somewhat meaningless because locations cannot be chosen freely (it is more and more difficult for operators to find sites to place their BSs). Clearly planning also depends on the service demand, which is not uniformly distributed and is quite diverse and dynamic [18], and the frequency bands that are available. Thus the question is often stated as: given an area to cover, a set $\mathcal{X}$ of BS locations, BSs of a certain type (we focus on BS with omnidirectional antennas here) with a certain maximum transmit power budget, some ideas (maybe vague) on the traffic, a licensed band, how to allocate portions of the band to BSs and how to use the transmit power budget to ensure a good level of coverage (which we describe as: all devices in the area see a Signal to Interference and Noise Ratio (SINR) greater than a certain threshold β with a high probability) and good performance. Note that for performance, the rule of thumb is more channels is better. However, this means the spreading the power which might cause problems for users at the edge (a coverage issue). Once planning is done, the network enters the (online) operation phase which includes processes such as scheduling, and user association.

The conventional way for planning is Reuse 1 (all the BSs use the full band), the use of the full power budget at each BS and a pre-allocated equal power per resource block[2] However, it is not always possible that the coverage meets our target β especially if the network is very irregular. Then the network is operated without changing the power allocated to resource blocks and the allocation of subchannels to BSs. Another way is to try a higher reuse factor (e.g. 2 or 3) if the coverage is not good enough. In that case, each BS uses less subchannels and more power per subchannel. In that case, the network is also operated without playing with the maximum power per resource block and BS subchannel allocation. One of our research questions is: Is this simple planning method good enough in view of the fact that networks are less and less regular? Two other research questions related to the operation of the network are: How can we take load imbalance and hotspots into account when operating a network? Should we allocate subchannels in a more dynamic fashion (since typically it is only done once and in the planning stage)?

The picture becomes more interesting with the architectural shift of cellular networks to a Centralized - Radio Access Network (C-RAN). Typically, operators deploy BSs that

[2]In an OFDMA system, the time is slotted and a frame is made of several time-slots. The band is divided in several sub-channels. A resource block is the smallest scheduling unit consisting of a subchannel and a time-slot.

operate independently. A BS typically consists of a baseband unit (BBU) and up to three remote radio heads (RRHs) [25]. The BBU is the brain of the BS and terminates the connection from the core network. On the downlink, the BBU takes the Internet Protocol (IP) packets and converts them into a digital signal for the RRH. Then the RRH modulates the digital signal for transmitting over the air. In 4G networks, the RRH also broadcasts reference signals used for cell selection, cell re-selection, and handover measurements. However with C-RAN, the BBUs are centralized which, among many advantages, opens up the possibility of coordination between BSs. Figure 1.1 compares the traditional distributed RAN and C-RAN.

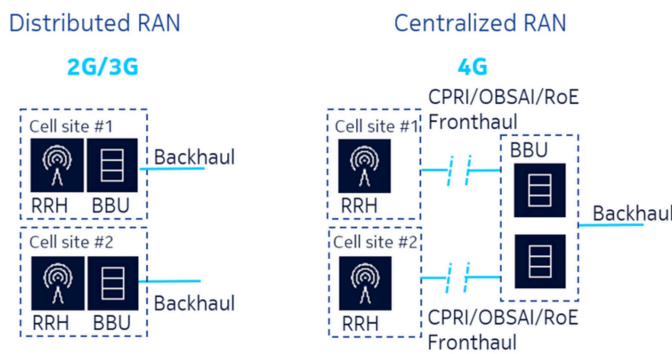

Figure 1.1: Comparing distributed RAN with C-RAN [28].

To answer the above research questions, we explore and define planning and operation as follows:

> **Planning:** Offline process that decides, given BS locations and area to cover, which frequency subchannels to allocate to each BS and what is the power budget for each BS, and the power constraints for each BS if any.

> **Operation:** Online process that is in charge of user association (UA), user scheduling (US), and possibly further constraints to reflect instantaneous load imbalance between BSs.

We will propose methods to perform planning and operation smartly. We call our approach Smart Planning and Smart Operation respectively and investigate the performance gains in the downlink with respect to conventional benchmarks. We consider three different topologies which are the 19-cell regular, a highly irregular, and a lightly irregular network. For each, we test against uniform and non-uniform distributions of users (i.e., hotspots), and two service scenarios which are fixed delay and file download. In the fixed delay scenario, users arrive and stay for Q seconds before departing. We record the average throughput of every departing user as a performance metric. In the file download scenario, users arrive and download a file of F bits before departing. We record the time spent downloading the file, known as delay, of every departing user as a performance metric.

1.2 Contributions

The contributions are as follows:

1. In Smart Planning, we parameterize offline a simple power map assignment to be used by all BSs to improve performance while maintaining good coverage even in highly irregular networks.

2. In Smart Operation, we propose given the power map obtained by planning, a heuristic based on BS coordination that allocates subchannels to BSs dynamically (while respecting the power map), and specifies for each BS the transmit power to use on the subchannels.

3. A practical implementation of Smart Operation that reduces coordination between BSs. This means less communication overhead and higher scalability because the computations can be done by the BSs. We show that we can still achieve good performance.

The main message is that conventional planning and operation are not good enough in view of the fact that networks are less and less regular. By smartly planning and operating networks, we can improve system performance while maintaining good coverage both in the presence and absence of load imbalance and hotspots for regular and irregular networks.

1.3 Literature Review

The big picture is that the vast majority of papers on planning and operation only consider the regular network deployment. In a regular deployment, the BS locations follow a regular pattern such that the cell radius and inter-site distance are consistent. Figure 1.2 shows the 19-cell regular network where the BSs are the black circles.

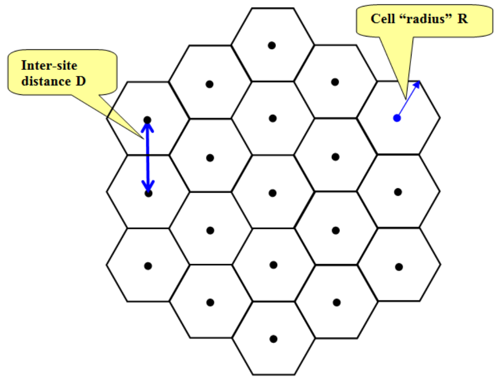

Figure 1.2: Regular network deployment [31].

This makes planning and operation easy to visualize and analyze because all BSs serve the same area, cells are clearly defined, and cells align perfectly together. For example, frequency reuse schemes used in planning like Reuse 1/2/3, Fractional Frequency Reuse (FFR) [8] [30], and Soft Frequency Reuse (SFR) [27] [30] are all introduced using regular networks. Unfortunately, irregular networks offer no such benefits making them harder to visualize and analyze as in Figure 1.3.

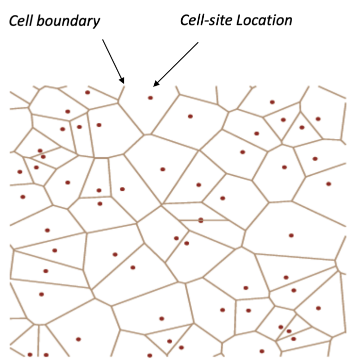

Figure 1.3: Irregular network deployment [19].

As a result, irregular networks are not as widely used in analysis and hence are not the de facto standard in literature. Therefore this is a topic that deserves more attention in the academic research community, especially as operators make their networks more irregular to handle increased traffic and the scarcity of sites to place BSs.

1.3.1 Planning

In practice, planning involves dimensioning, positioning, and configuring BSs to achieve a certain quality of service and coverage [18]. However, as aforementioned, we believe that the problem is hard and somewhat meaningless because the BS locations cannot be freely chosen. Therefore we focus on the configuration phase of planning.

Approaches in planning typically focus on reducing inter-cell interference (ICI) for users near cell edges. This is done by computing a power map. A power map specifies for each BS which subchannels to use and with how much power. By smartly computing a power map such that neighbour BSs do not use the same subchannels with high power, ICI can be reduced. ICI is a problem for cell edge users because the signal strength from a neighbour BS is as strong as the signal coming from their BSs and is seen as interference. In the conventional scheme called Reuse 1, equal power per subchannel is used and all BSs use all subchannels (i.e., the full band B). Under this scheme, the cell edge users might experience heavy interference. Basically, any Reuse n scheme can be thought of as n-colouring a set of cells where cells of same colour use the same set of subchannels. Figure 1.4 shows the power map for Reuse 1 with some cell edges marked in a 3-cell topology.

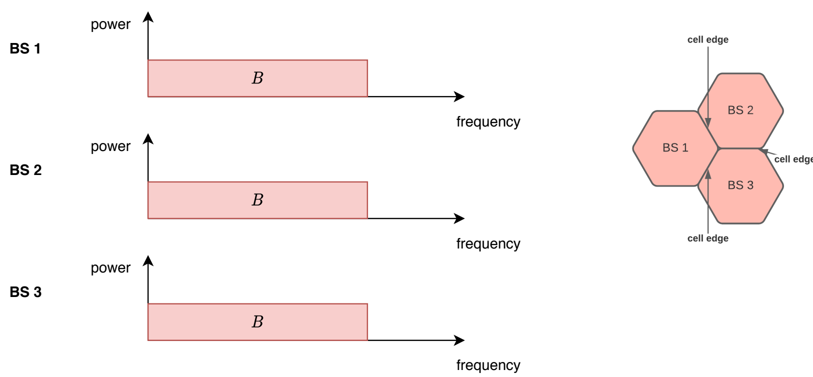

Figure 1.4: Reuse 1 power map.

Naturally, the alternatives to Reuse 1 are Reuse 2, Reuse 3, and higher values of reuse. In Reuse 2, the full band is divided into 2 bands B_1 and B_2 containing the first and latter half of subchannels respectively. BSs transmit on either B_1 or B_2. Likewise in Reuse 3, the full band is divided into 3 bands B_1, B_2 and B_3 containing the first, second, and third tierce of subchannels respectively. By applying a proper n-colouring to a set of cells for Reuse n, neighbour cells will have different colours and thus decrease the ICI for cell edge users. However, the drawback is low spectrum efficiency because no BS has access to the full band. Figure 1.5 shows the power map for Reuse 3 with a 3-cell topology.

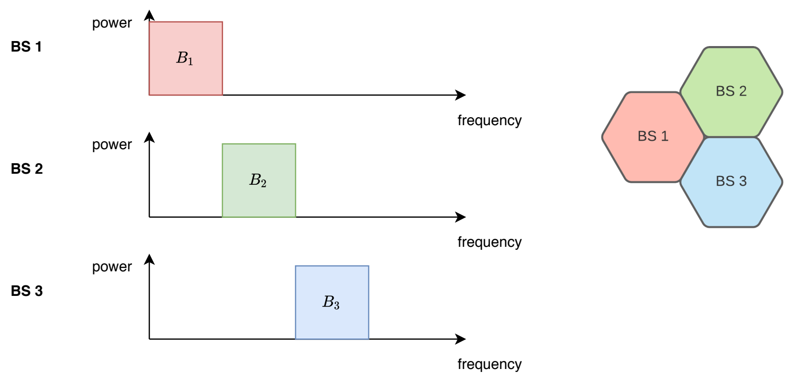

Figure 1.5: Reuse 3 power map.

Another way to manage ICI is called FFR. There are two types of FFR: distance-based FFR [41], and SINR-based FFR [29]. In distance-based FFR, the cells are partitioned into cell centre and cell edge regions. Users are classified as cell centre or cell edge users based on their location in the cell. In SINR-based FFR, users are classified as cell centre users if their SINR is above a threshold or cell edge users if below a threshold. In both types of FFR, the full band is typically divided into 4 sub-bands: B_1, B_2, B_3, and B_4 each containing a number of subchannels. Typically, B_1 is the largest size, and the remaining sub-bands are of equal size and smaller than B_1. The transmit power in B_1 is typically lower than the other sub-bands. BSs use B_1 to transmit to cell centre users, and either B_2, B_3, or B_4 to transmit to cell edge users. A FFR power map applied to a distance-based FFR scheme is shown in Figure 1.6.

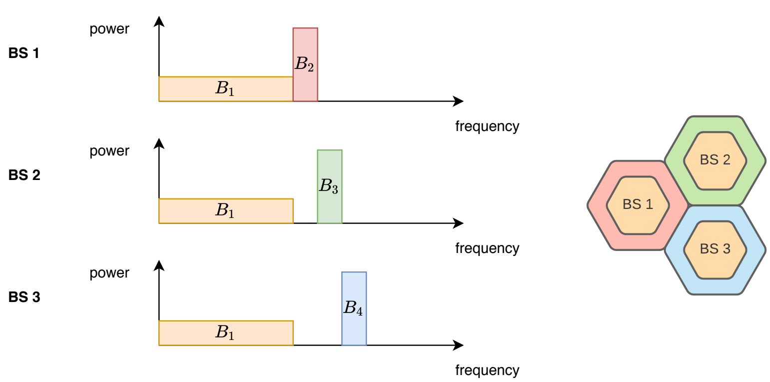

Figure 1.6: FFR power map.

The idea is that cell centre users have good SINR and hence all BSs can afford to use the same sub-band to transmit to them. Since cell edge users have worse SINR, BSs use different sub-bands to transmit to them (to reduce interference). However, the drawback is not all BSs have access to the full band. Also, the reservation of sub-bands for cell centre and cell edge regions is fixed. This makes it inflexible to account for various ratios of cell centre to edge users.

In [22], the authors studied the coverage and performance of FFR. However, their criteria for performance were Bit Error Rate and SINR. There was no analysis on average system throughput. In [11], the authors also studied the performance of FFR. But they did not consider coverage. Furthermore, they only worked with a regular network deployment. They also express performance using the metric Bits Per Second Per Hertz Per Cell which is very granular. An operator is probably more concerned with the average system throughput. In [23], the authors studied the performance of FFR but they only considered cell edge users. They also did not consider coverage. In [14], the authors applied FFR to irregular networks but do not simulate with any users to determine performance. They also did not consider coverage.

SFR is another technique based on and typically seen as an improvement to FFR. It addresses the weakness of FFR's spectrum inefficiency by allowing BSs access to to the full band. In SFR, the full band is typically divided into 3 sub-bands B_1, B_2, and B_3 of equal size. Every BS dedicates 1 sub-band to cell edge users and the other sub-bands to cell centre users. Typically, BSs transmit using high power to cell edge users and low power to cell centre users. However, the reservation of spectrum for cell centre and edge users is still fixed. Figure 1.7 shows a SFR power map applied to a distance-based SFR scheme.

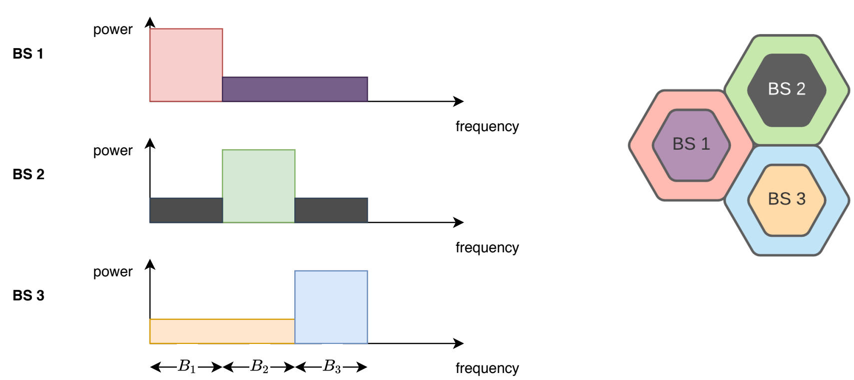

Figure 1.7: SFR power map.

In [20], the authors studied the performance of SFR but did not consider coverage and only worked with a regular network deployment. In addition, they did not consider low-level processes such as user scheduling. In [30], the authors considered an irregular placement of BSs but only evaluated coverage. They briefly mentioned a performance metric but only with respect to cell edge users and have no results for it. Also, their performance metric was solely based on user rates derived from SINR and did not include user scheduling to obtain user throughputs. The work in [15] included user scheduling for their SFR scheme but only looked at performance and did not consider coverage. In [13], the authors applied SFR to irregular networks but did not simulate with any users to determine performance. They also did not consider coverage.

In [44], the authors created a power map to manage ICI in irregular networks. They stated that their power map "can be considered as a generalization of the traditional SFR method" [44] since SFR is typically limited to Reuse 3 for the cell users and two power-levels (i.e., low and high power for cell centre and edge users respectively). Their power map is shown in Figure 1.8.

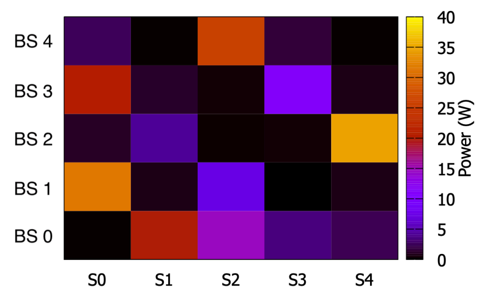

Figure 1.8: Power map in [44] (BS labels have been modified for clarity).

The power map splits the full band into five sub-bands S0 to S4 of equal size, and each sub-band consists of a fixed set of subchannels. The BS indices are in the vertical axis, and sub-band indices in the horizontal axis. A darker colour indicates lower per subchannel power and a brighter colour indicates higher per subchannel power. Intuitively, when a BS transmits with high power on a given subchannel, the other BSs transmit with a lower power. Its continuous power levels give it more flexibility in tuning for better coverage and performance [44] unlike SFR which typically has two power-levels. However, they only considered performance when computing the power map, There was no analysis on coverage. In addition, it was painful to compute because it required solving a non-convex non-linear optimization problem.

In our work in planning, we consider performance and coverage in both regular and irregular networks. We propose a simple method for the offline computation of a power map with results that quantify its performance and coverage. Lastly, our performance metric is average throughput which translates better to real world performance than metrics like bits per second per hertz per cell.

1.3.2 Operation

Processes in operation involve user association (UA), user scheduling (US), and possibly further constraints to reflect instantaneous load imbalance between BSs. For example, another process could be the subchannel (re)allocation to BSs. In fact, our work considers subchannel (re)allocation to BSs as an operation process while it is typically a planning process (while still respecting the power map). The UA, US, and subchannel allocation can be separately or jointly computed [37] as tradeoffs between low complexity and optimal performance.

UA is the process of finding a suitable cell after the user equipment (UE) turns on and starts Initial Cell Selection. In practice, UEs choose the cell with the highest Reference Signal Received Power (RSRP) as in 3GPP Release 8 [2]. In Release 10 [4], UEs choose the best cell based on RSRP and Reference Signal Received Quality (RSRQ). The behaviour remains the same in Release 16 [5], which is the latest release and devoted to 3GPP's initial 5G system. Meanwhile in the literature, the consensus is that Best SINR is the benchmark [40] [36]. Therefore many papers try to propose a UA that also takes into account the number of users at each BS as a form of load balancing [40] [36]. In the case of heterogenous networks, more complex schemes exist such as Small Cell First [17], and Cell Range Extension [3]. UA can also be determined by machine learning approaches [26].

US is a real-time process typically performed independently by each BS every few milliseconds (i.e., every frame) to allocate resource blocks among its users. A resource block is the smallest scheduling unit that can be assigned to a user. In Long Term Evolution (LTE) networks, one resource block is 0.5ms wide in time domain and 180 kHz wide in frequency domain. US can also determine the transmit power per resource block (in that case, the power map can be seen as specifying the maximum power levels per resource block). In practice, these algorithms are proprietary among the BS vendors such as Nokia, Huawei, and Ericsson. A well-known scheduling algorithm in literature is round robin (RR) scheduling with equal power per resource block. This means that each user of a given BS gets the same number of resource blocks, and the total power budget of a given BS is divided equally among its resource blocks. Another type of scheduler is max-min [39] where a given BS tries to maximize the minimum throughput among its users. In the proportional fair scheduler [24], the scheduling maximizes the sum of of the logarithms of the user throughputs.

For subchannel allocation to BSs, Challita et al. [10] used a Reinforcement Learning - Long Short-Term Memory (RL-LSTM) framework so that BSs can learn which Wi-Fi subchannels to use when sharing spectrum with Wi-Fi access point deployments. Basically, they formulated the problem as a noncooperative game where the players are the BSs, the action is the subchannel selection, and the goal for each BS is to maximize their throughput over the subchannels. The key idea was that RL-LSTM allows the BSs to learn which channels to pick in the future based on a sequence of historical traffic load (i.e., measured traffic activity on subchannels). However, they did not consider coverage and irregular networks at all. They also did not consider fairness among users associated to the same BS, and non-uniform user distributions. Furthermore, their training dataset only has traffic activity over several days.

Post and Borst [33] proposed load-aware dynamic frequency allocation in irregular networks. Basically, BSs would acquire and relinquish frequencies (i.e., subchannels) based on its load. They first start by creating an non fully-connected interference graph (it was not clear how they created it). Then BSs would acquire and relinquish subchannels to keep their load within an interval. The idea is that when a BS acquires additional subchannels, it cannot acquire the subchannels used by a neighbour BS as per the interference graph. This paper stood out because they simulated in a dynamic setting with arriving/departing users, and a single moving hotspot. However, their simulation area was only 500x1000m which is small and with only 10 BSs. In addition, they only simulate with one hotspot. Another drawback is the need to choose multiple parameters carefully. For example, when keeping the load within an interval, the interval must be defined. They also did not consider coverage at all.

Elwekial et al. in [16] split the entire frequency band into sub-bands where each sub-band contained a number of subchannels. Then they proposed adaptive FFR where the BSs could choose the sub-bands for the cell edge and centre regions. But their assumptions were too basic such as assuming the number of users in each cell are equal, having a uniform user distribution, and using a regular network deployment. The BSs choose the sub-bands such that the total interference for its users is minimized according to an optimization problem. But this requires users to measure and report interference from neighbour cells. Having the radio perform more measuring on top of existing handover-related measurements might be too much overhead. Also, their algorithm cannot be run in real-time because it takes 2 seconds for all BSs in the network to finish choosing the sub-bands. They also did not consider coverage at all.

In our work on operation, we focus on performance having already solved the coverage problem during planning. We do this by playing with subchannel allocation to BSs while considering both regular and irregular networks with uniform and non-uniform user distributions. We also consider user fairness, and use average throughput and average delay as metrics that translate better to real world performance. Therefore our work which considers planning and operation is more comprehensive, and is evaluated in more network topologies.

1.4 Outline

In Chapter 2, we present the system model and simulation setting used throughout the thesis. In Chapter 3, we introduce and present the results of Smart Planning. In Chapter 4, we introduce and present the results of Smart Operation. Finally, we conclude the research in Chapter 5.

Chapter 2

System Model and Simulation Setting

2.1 Network model

We consider the downlink of a cellular OFDMA network with a set $\mathcal{J}$ of macro BSs operating in Frequency Division Duplexing (FDD) mode in licensed spectrum. FDD means the downlink and uplink traffic are transmitted on separate frequency bands. We also consider Single In Single Out (SISO) as opposed to MIMO (Multiple In Multiple Out) communications. This means there is a single omnidirectional antenna at the BSs and at the users.

In the time domain, time is slotted. We assume everything stays constant in a time-slot (TS). A TS is of duration τ (s). There are N TSs in a frame. For example, TS 0 to TS $N-1$ make up frame 0. In the frequency domain, the frequency band is divided into smaller units called subchannels. Let $\mathcal{M}$ be the set of subchannels in the network, and $M = |\mathcal{M}|$ the number of subchannels in the network. One TS and one subchannel is known as a resource block (RB). One RB is the smallest resource unit that can be allocated by a BS to a user for data transmission, and its size is determined by the subchannel bandwidth b (kHz) and TS duration τ (s) as in Figure 2.1.

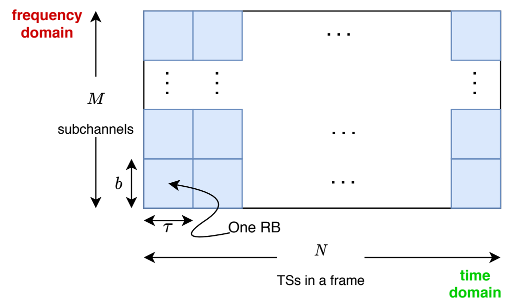

Figure 2.1: RB representation in time and frequency domain.

Let $\mathcal{U}(t)$ be the set of users in the network in TS t. Now we make the following assumptions:

- Each user is fixed (i.e., no mobility) and can only associate with one BS at a time (i.e., no dual connectivity)
- UA is given and $\mathcal{U}_j(t)$ is the set of users associated with BS j in TS t. A user remains associated to the same BS as long as it remains in the system.
- Each BS $j, \forall j \in \mathcal{J}$ has a total transmit power of P_{max} watts, and uses all its transmit power when transmitting
- BSs with no users do not transmit (i.e., per subchannel transmit power is zero for all subchannels and hence do not cause interference)
- Let $G^c_{u,j}(t)$ be the subchannel gain with shadowing between user $u \in \mathcal{U}(t)$ and BS $j \in \mathcal{J}$ on subchannel $c \in \mathcal{M}$ in TS t. We assume flat fading across subchannels, and henceforth drop the the superscript c.
- Let $M_j(t)$ be the number of subchannels used by BS j in TS t
- Let $x^c_j(t)$ be 1 if BS j transmits on subchannel c in TS t, else 0
- The rate function $f(\cdot)$ is the same for all BSs (see Sections 2.2 and 2.7 for more details)
- Full buffer traffic (i.e., users are always downloading)
- Infinite backhaul capacity. In a cellular network, every BS connects to the operator's core network via the S1 interface. We call this link the backhaul and assume that it does not bottleneck traffic.

- Perfect channel state information (e.g. all subchannel gains from any BS to any user are known)
- C-RAN network architecture (described in Section 1.1)

2.2 SINR and rate models

Assuming the power budget is spread evenly across all the subchannels of a BS given $P_{max}, M_j(t), x_j^c(t)$, $G_{u,j}(t)$, the SINR for user u associated to BS j on subchannel c in TS t is:

$$\Omega_{u,j}^c(t) = \frac{\frac{P_{max}}{M_j(t)} x_j^c(t) G_{u,j}(t)}{\mu + \sum_{j' \neq j, j' \in \mathcal{J}} \frac{P}{M_{j'}(t)} x_{j'}^c(t) G_{u,j'}(t)} \tag{2.1}$$

Equation 2.1 only holds when all BSs have at least one user. BSs with no users are omitted from the interference calculation. μ is the additive white gaussian noise and is assumed to be a constant. $G_{u,j}(t)$ is the subchannel gain between user u and BS j in TS t and accounts for the pathloss $\Gamma_{u,j}$, antenna gain AG, equipment loss EL, and shadowing $S_{u,j}(t)$ as shown in Equations 2.2 and 2.3.

$$G_{u,j}(t) = 10^{(-\overline{G}_{u,j}(t)/10)} \tag{2.2}$$

$$\overline{G}_{u,j}(t) = \Gamma_{u,j} - AG + EL + S_{u,j}(t) \tag{2.3}$$

The pathloss $\Gamma_{u,j}$ (dB) has the form $\Gamma_{u,j} = a + b \cdot log(d_{u,j}/1000)$ where a and b are coefficients, and $d_{u,j}$ is the distance between user u and BS j in metres. The antenna gain AG (dB) and equipment loss EL (dB) are both constants. The shadowing $S_{u,j}(t)$ (dB) between user u and BS j in TS t is assumed to be a normal random variable with zero mean and standard deviation σ.

Given the SINR $\Omega_{u,j}^c(t)$, we use a continuous rate mapping function $f(\cdot)$ to obtain the rate (Mbit/s) $r_{u,j}^c(t) = f(\Omega_{u,j}^c(t))$ of user u associated to BS j on subchannel c if allocated subchannel c by BS j in TS t (i.e., it is the per RB (subchannel c, TS t) rate. Although a discrete mapping function is used in practice, the continuous function provides an upper-bound approximation and makes it easier to use in an optimization problem. This approach is borrowed from [44]. The rate mapping function is shown in Equation 2.4 where η and Δ are constant scalar parameters chosen to account for the subchannel bandwidth b and

TS duration τ, and R_{max} is the maximum achievable rate (Mbit/s) set by the modulation and coding scheme.

$$r^c_{u,j}(t) = f(\Omega^c_{u,j}(t)) = \min(\eta(\Omega^c_{u,j}(t))^{\Delta}, R_{max}) \tag{2.4}$$

2.3 User scheduling

User scheduling is a process done independently by each BS in every frame to allocate RBs to its users. This is called local scheduling. To explain precisely, we consider a BS j that is allocated M_j subchannels and assume that the power per subchannel is P_{max}/M_j. We will adjust scheduling to other power maps later. Consider frame k. With M_j subchannels and N TSs in a frame, there are M_jN RBs to allocate. To simplify, we assume that the subchannels within a frame are flat. Given a user u associated to BS j, this means the per RB rates are the same across subchannels:

$$r^c_{u,j}(t) = r_{u,j}(t), \forall t = kN\tau + i\tau, \forall i = 0, .., N-1 \tag{2.5}$$

We also assume that the subchannel gains within a frame are time-invariant which means the per RB rates are time-invariant:

$$r_{u,j}(t) = r^k_{u,j}, \forall t = kN\tau + i\tau, \forall i = 0, .., N-1 \tag{2.6}$$

Hence, the per RB rates do not change within a frame and we end up with $r^k_{u,j}$, the per RB rate in frame k for user u associated to BS j. In that case, instead of allocating RBs, we allocate all M_j subchannels to user u of BS j in frame k for a proportion of time equal to $\alpha_{u,j}(k)$ where $\sum_{u\in\mathcal{U}_j} \alpha_{u,j}(k) = 1$. $\mathcal{U}_j$ is the set of users associated to BS j. We compute the $\alpha_{u,j}(k)$ so as to be proportional fair (PF). In that case, the throughput of user u in frame k is:

$$\lambda^k_u = M_j\alpha_{u,j}(k)r^k_{u,j} \tag{2.7}$$

2.4 User scheduling in simulation

When we simulate, we assume that the subchannel gains are time-invariant (not only on a frame basis but forever). Under this assumption, this means that the per frame throughput are constant between user arrivals/departures. Therefore instead of doing simulation based on frames, we do it based on periods. A period is the time interval between two successive user arrivals/departures as in Figure 2.2.

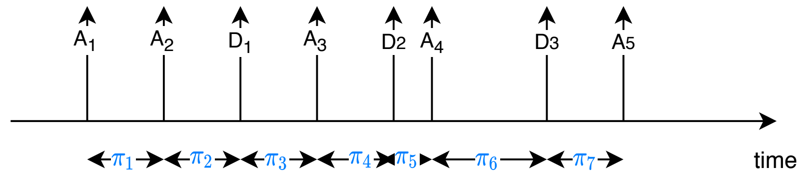

Figure 2.2: Simulation periods π_l.

In Figure 2.2, the user arrival events are $A_1, A_2, A_3, ...$, and the user departure events are $D_1, D_2, D_3, ...$ We call π_l the lth period. Scheduling is done at the beginning of a period. The resulting user throughputs are unchanged within a period.

2.5 Benchmarks

We now present two benchmarks: Reuse 1 with equal power (EP) per subchannel, and Reuse 2 with EP per subchannel. For both benchmarks and throughout this thesis, the UA is Best Channel Gain. We define Best Channel Gain UA as a given user u associates to the BS with the highest subchannel gain. That is, user u arriving in TS t associates to BS $j^* = \text{argmax}_{j,\forall j\in\mathcal{J}} G_{u,j}(t)$.

2.5.1 Reuse 1 with EP per subchannel

Every BS uses M subchannels, so the per subchannel power for each BS is P_{max}/M. Under the assumption that subchannel gains are time-invariant, the per subchannel rate $\gamma^c_{u,j}$for user u associated to BS j on subchannel c can be computed as:

$$\gamma^c_{u,j} = f(\frac{\frac{P_{max}}{M} G_{u,j}}{\mu + \sum_{j'\neq j, j'\in\mathcal{J}} \frac{P_{max}}{M} G_{u,j'}}), \qquad \forall u \in \mathcal{U}_j, \forall j \in \mathcal{J}, \forall c \in \mathcal{M} \tag{2.8}$$

Note that the per subchannel rate $\gamma^c_{u,j} = r^k_{u,j}$ because both are user rates on one subchannel. Equation 2.8 only holds when all BS have at least one user. BSs with no users are omitted from the interference calculation.

Given M, $\gamma^c_{u,j}, \forall u \in \mathcal{U}_j, \forall j \in \mathcal{J}, \forall c \in \mathcal{M}$, we do local PF scheduling within a frame by solving $\mathcal{P}_{\text{reuse1}}$ at each BS.

$$\mathcal{P}_{\text{reuse1}}: \max_{\lambda_u, \alpha^c_{u,j}, \forall u \in \mathcal{U}_j} \sum_{u \in \mathcal{U}_j} log(\lambda_u) \tag{2.9}$$

$$\lambda_u = M \alpha^c_{u,j} \gamma^c_{u,j}, \qquad \forall u \in \mathcal{U}_j \tag{2.10}$$

$$\sum_{u \in \mathcal{U}_j} \alpha^c_{u,j} \leq 1, \tag{2.11}$$

$$\alpha^c_{u,j} \geq 0, \lambda_u \geq 0, \qquad \forall u \in \mathcal{U}_j \tag{2.12}$$

λ_u is the throughput of user u, and $\alpha^c_{u,j}$ is the proportion of time allocated to user u associated to BS j on subchannel c. Constraint (2.10) defines the throughput seen by user u, and constraint (2.11) says that the total proportion of time allocated to users of a BS is less than or equal to 1. In [17], the authors showed that local PF scheduling is equivalent to local equal-time scheduling. Therefore an easier to way to compute the user throughputs is:

$$\lambda_u = \frac{1}{|\mathcal{U}_j|} M \gamma^c_{u,j}, \qquad \forall u \in \mathcal{U}_j \tag{2.13}$$

2.5.2 Reuse 2 with EP per subchannel

It is the same as Reuse 1 with EP per subchannel except that BSs use half the number of subchannels and the per subchannel power is doubled, and a user receives interference only from the co-subchannel BSs.

2.6 Simulation setting

We consider two different dynamic scenarios for performance evaluation known as *fixed delay* and *file download*. We assume that users arrive according to a Poisson process and are placed on a grid of points $\mathcal{G}$ overlaid on the network at random based on a probability distribution described later. Arriving users that have no coverage (i.e., SINR < -6.5 dB) are discarded and a new user is created. The simulation updates the user throughputs after every arrival and departure event. In the fixed delay setting, users depart after Q seconds, and we record their throughputs as the number of bits downloaded divided by Q. We analyze the system performance in terms of the average throughput (i.e., arithmetic mean) of the users. In the file download setting, users depart after downloading a file of

F bits, and we record their delay as the time spent downloading the file. We analyze the system performance in terms of the average delay of the users.

For both dynamic scenarios, the simulation starts at time $t = 0$ with zero users, and has a warmup period of t_{warmup} seconds. During the warmup period, we do not record any data. We begin recording data starting with the first user arrival after time $t = t_{warmup}$. The simulation runs until it has a confidence interval of 5%, which means the system performance metric (e.g., average throughput, or average delay) and per BS performance metric for all BSs did not change by more than 5% over the previous W seconds (i.e., a stable system). As a result, the simulation performs the first stability check at time $t = t_{warmup} + W$ where it records the system performance metric and the per BS performance metric for all BSs. Since there is no past system performance metric and per BS performance metric to compare it to, the earliest time the simulation can terminate is at time $t = t_{warmup} + 2W$ where it performs the second stability check. Until the system is stable, the simulation checks for stability every W seconds. The simulation runs until the system is stable, and then outputs the system performance metric.

For each dynamic scenario, we simulate with uniform and non-uniform distribution of users. The latter case is meant to create hotspots. For the uniform case, the probability of placing a user at any point is $1/|\mathcal{G}|$. For the non-uniform case, we define the following parameters:

- x, the hotspot probability multiplier
- $\mathcal{H}$, the set of hotspot points on the grid
- $N_H = |\mathcal{H}|$, the number of hotspot points on the grid
- $N_C = |\mathcal{G} \backslash \mathcal{H}|$, the number of coldspot points (i.e., not in a hotspot) on the grid
- p', the probability of choosing a coldspot point
- p, the probability of choosing a hotspot point

Then we have $(1 + x)p'N_H + p'N_C = 1$ (i.e., probabilities sum to 1), we can solve for p' and p in Equations 2.14 and 2.15 respectively.

$$p' = \frac{1}{N_C + (1 + x)N_H} \tag{2.14}$$

$$p \triangleq (1 + x)p' \tag{2.15}$$

As a result, each arriving user is assigned to a hotspot or coldspot with probability pN_H and $1 - pN_H$ respectively. If assigned to hotspots, the user location is chosen uniformly among the points in $\mathcal{H}$. Otherwise, it is selected uniformly among the points in $\mathcal{G} \backslash \mathcal{H}$. Note that the uniform user distribution case occurs when $x = 0$.

We now present the networks and the hotspot locations.

2.6.1 Regular network

The topology for the regular network is in Figure 2.3.

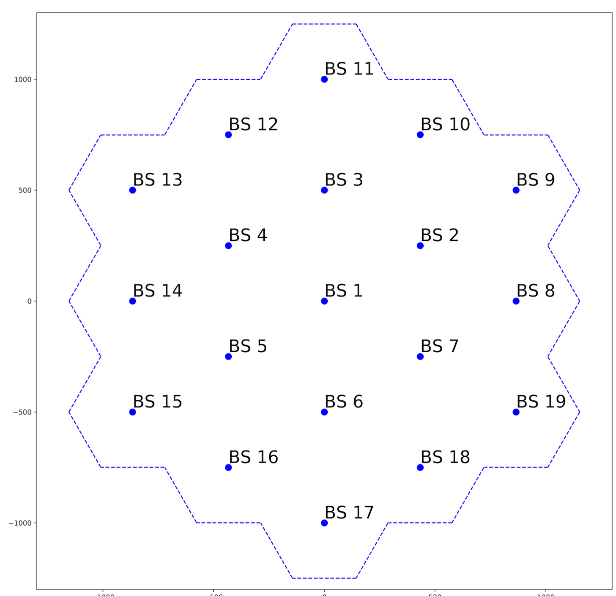

Figure 2.3: Regular network topology.

The network has 19 BSs placed regularly with an inter-site distance of 500m. The area under consideration is outlined by the dashed blue borders for a total area of $4,113,620\text{m}^2$. The area is not the entire square because we use a wraparound model. The hotspot locations are shown in Figure 2.4 where each hotspot (i.e., the red square) is 300x300m with an area of 90,000m^2.

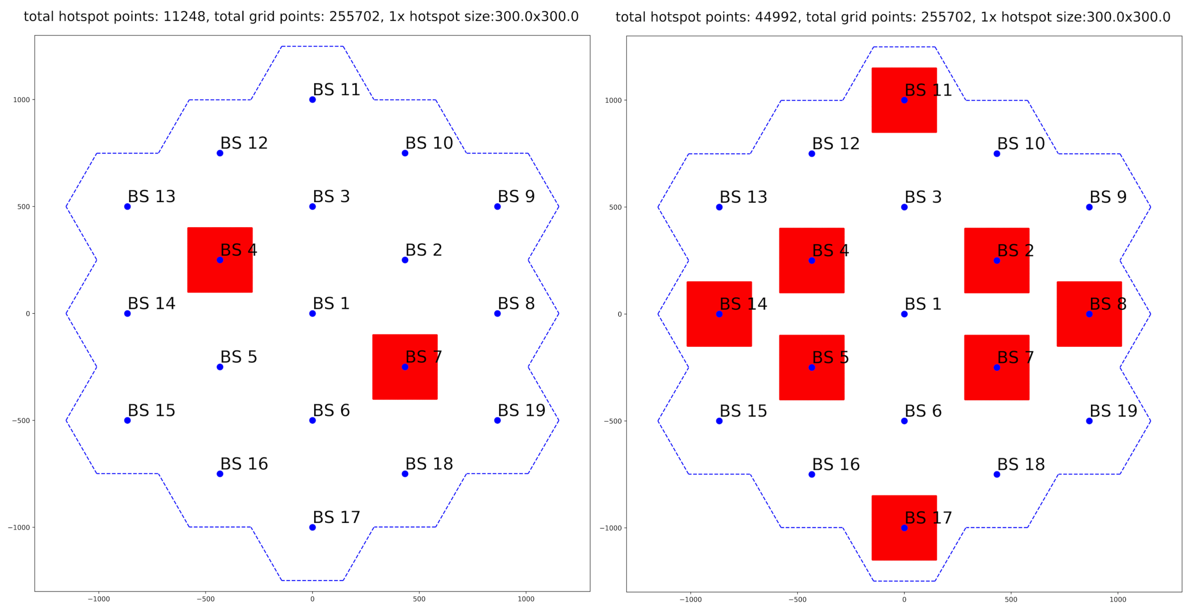

Figure 2.4: Regular network hotspot locations.

2.6.2 Lightly irregular network

The topology for the lightly irregular network is in Figure 2.5.

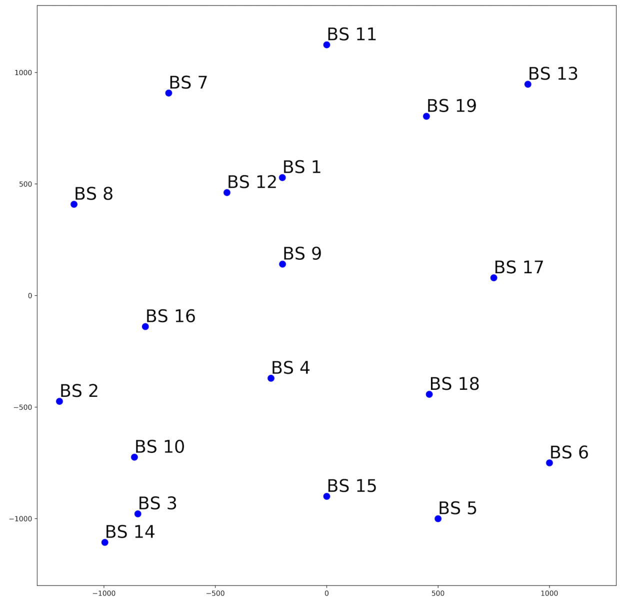

Figure 2.5: Lightly irregular network topology.

The area under consideration is the entire square which is 2600x2600m for a total area of $6,760,000\text{m}^2$. The hotspot locations are shown in Figure 2.6 where each hotspot (i.e., the red square) is 400x400m with an area of 160,000m^2.

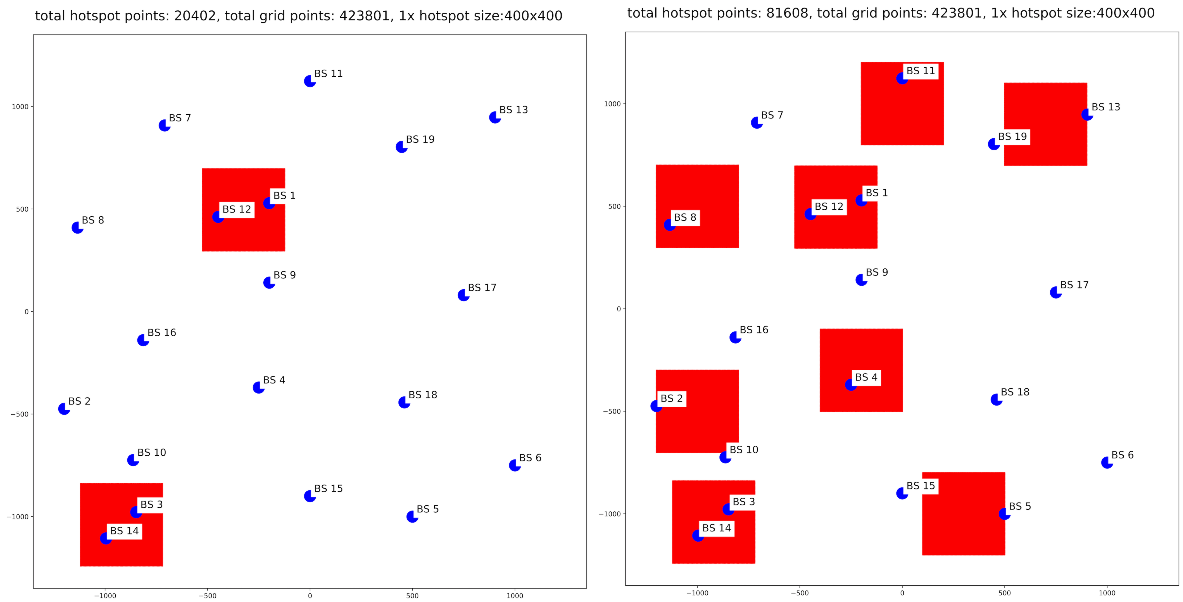

Figure 2.6: Lightly irregular network hotspot locations.

2.6.3 Highly irregular network

The topology for the highly irregular network is in Figure 2.7.

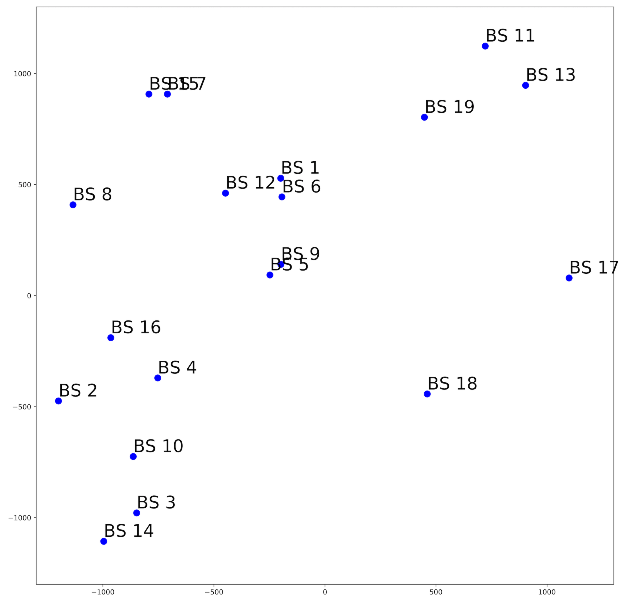

Figure 2.7: Highly irregular network topology.

The area under consideration is the entire square which is 2600x2600m for a total area of $6,760,000\text{m}^2$. The hotspot locations are shown in Figure 2.8 where each hotspot (i.e., the red square) is 400x400m with an area of 160,000m^2.

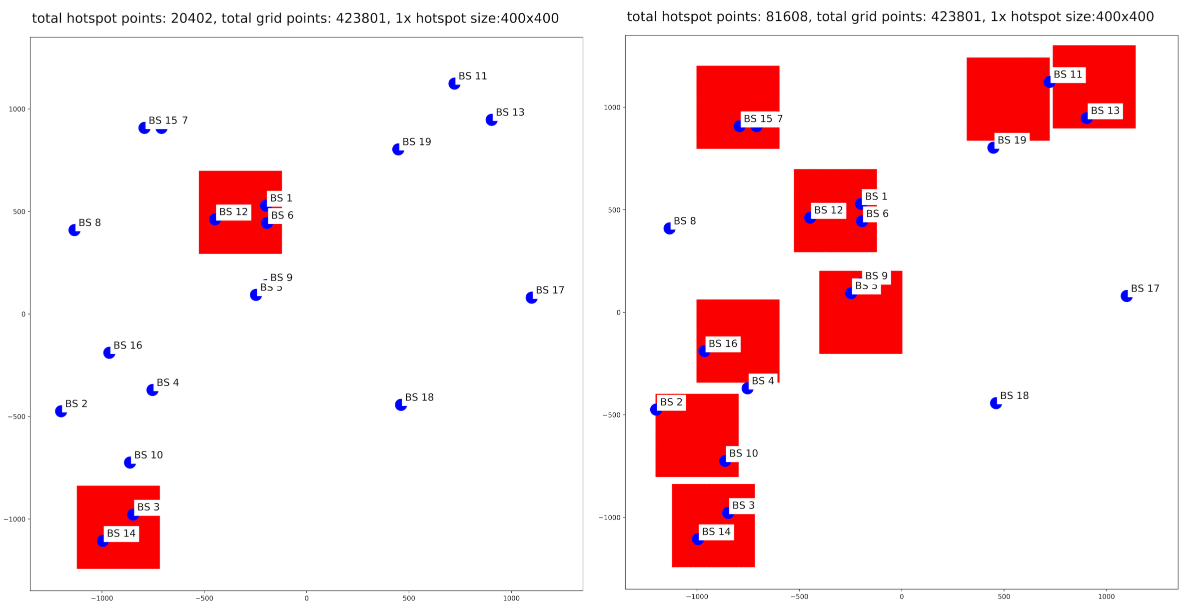

Figure 2.8: Highly irregular network hotspot locations.

2.7 Simulation parameters

We use the simulation parameters shown in Tables 2.1, and 2.2.

Table 2.1: Simulation parameters

Parameter	Value
Q (fixed delay)	60 seconds
F (file size)	10 MB
W (stability check periodicity)	1000 seconds
t_{warmup}	2000 seconds
η	0.168
Δ	0.43
R_{max}	0.9324 Mbit/s

The values of η and Δ account for the system model parameters where the subchannel bandwidth is 180 kHz and TS duration is 0.001s (1ms). The chosen values also closely approximate the LTE rate function on one RB. This is shown in Figure 2.9 in the red curve.

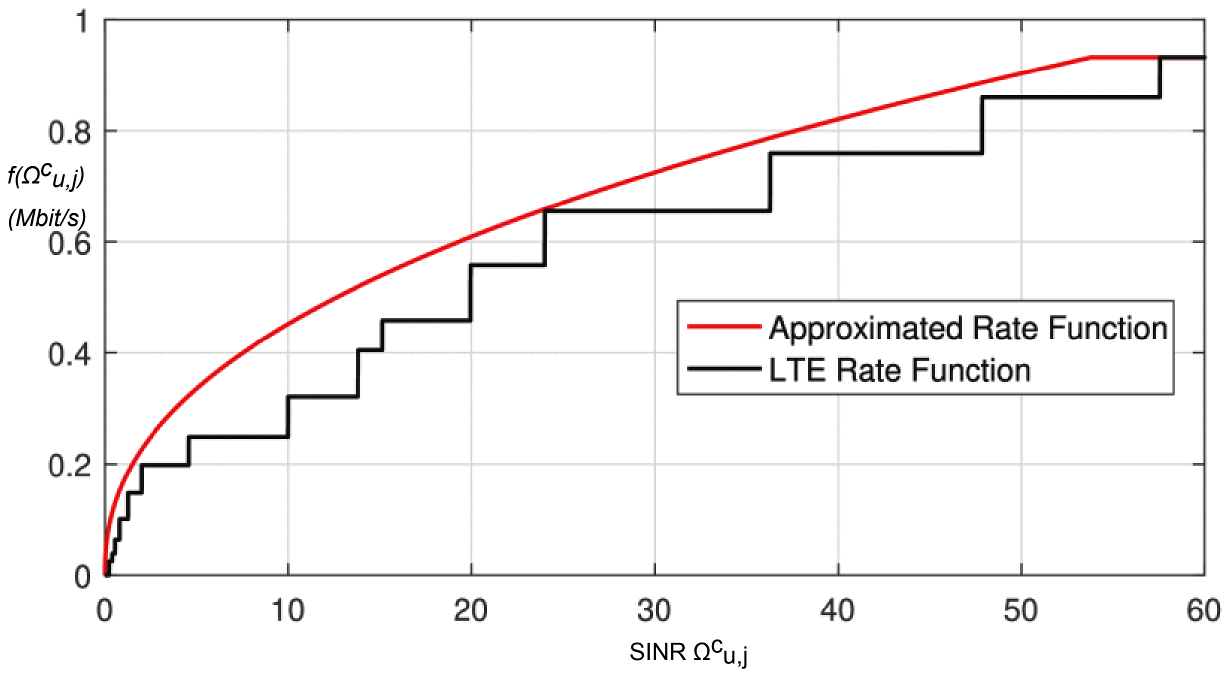

Figure 2.9: Rate mapping function [44] (axis labels modified for notation purposes).

Table 2.2: Simulation parameters for x

Network type	Fixed delay	File download
Regular - 0 hotspot	0	0
Regular - 2 hotspots	3	0.5
Regular - 8 hotspots	3	0.5
Lightly irregular - 0 hotspot	0	0
Lightly irregular - 2 hotspots	3	5
Lightly irregular - 8 hotspots	3	5
Highly irregular - 0 hotspot	0	0
Highly irregular - 2 hotspots	3	18
Highly irregular - 8 hotspots	3	18

For the fixed delay scenario, we chose $x = 3$ to get a good number of users at the hotspots. For the regular network, this equates to roughly 15% and 45% of users are placed in a hotspot for 2 and 8 hotspots respectively. For the irregular networks, roughly 17% and 49% of users are placed in a hotspot for 2 and 8 hotspots respectively.

Note that we used different values of x for the file download scenarios involving hotspots. This was done to create hotspots in the file download scenario. Ideally, we would keep the values of x consistent. However, if we had used the same values as in the fixed delay scenario, there either would not be enough users in the hotspots or there would be too many. For example in the regular network, we had to step down from $x = 3$ to $x = 0.5$ because there were too many users. In the irregular networks, we had to increase the value of x because there were too few users. The new values of x were chosen by trial-and-error.

Chapter 3

Smart Planning

Let us recall the definition of planning.

> **Planning:** Offline process that decides, given BS locations and area to cover, which frequency subchannels to allocate to each BS and what is the power budget for each BS, and the power constraints for each BS if any.

First we plan for coverage. Then given sufficient coverage, we plan for performance.

3.1 Planning for coverage

We consider the concept of β-coverage. That is, given a network topology, a set of grid points representing all possible user locations, and a reuse scheme (e.g., Reuse 1 with EP per subchannel), do a high percentage (say $X\%$) of grid points see an SINR above β dB? If it does, then we say the network has β-coverage. Else, it does not and we have to use a different frequency reuse scheme. Note that this step is often ignored in research papers while it is critical to ensure that the results are meaningful. We do this for the three network topologies.

The coverage planning parameters are in Table 3.1 and system model parameters are in Table 3.2.

Table 3.1: Coverage planning parameters

Parameter	Value
β	-2 dB
X	95 %
Grid spacing	4m

With a grid spacing of 4m, there are a total of 255702 points in the grid of the regular network, and 423801 points in each grid of the irregular networks.

Table 3.2: System model parameters

Parameter	Value
μ	5.722e-15 W (-112.4245 dBm)
P_{max}	39.81 W (46 dBm)
M	90
$\Gamma_{u,j}$	$128.1 + 37.6 \cdot \log(d_{u,j}/1000)$ dB
AG	15 dB
EL	20 dB
σ	8 dB
Subchannel bandwidth	180 kHz
TS duration	0.001s (1ms)

We chose $\beta = -2$ dB because the minimum SINR for a non-zero rate is -6.5 dB. Since we do not account for shadowing when computing coverage, -2 dB gives us some buffer above the -6.5 dB threshold. Our coverage target is X = 95% for all networks which we picked for good measure. If the coverage is below, we consider it a fail. Else, a pass. We only consider the effects of wraparound for the regular network.

3.1.1 Regular network

Figure 3.1 shows the coverage of Reuse 1 with EP per subchannel for the regular network.

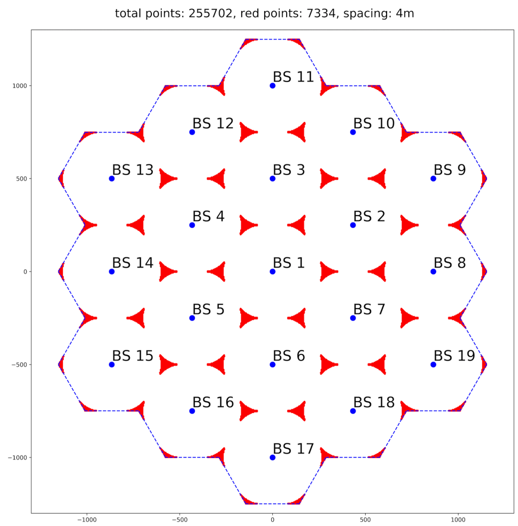

Figure 3.1: Reuse 1 with EP per subchannel coverage.

The red points are the locations without coverage. With a total of 255702 grid points and 7334 red points, the coverage is 97%. Therefore we can use Reuse 1 with EP per subchannel for the regular network.

Reuse 1 β-coverage: Pass

3.1.2 Lightly irregular network

Figure 3.2 shows the coverage of Reuse 1 with EP per subchannel for the lightly irregular network.

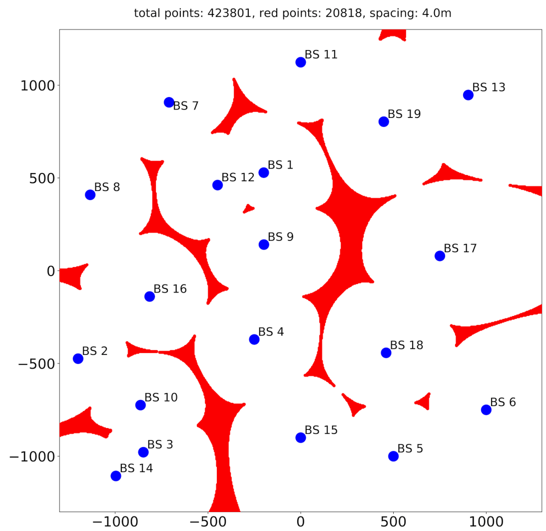

Figure 3.2: Reuse 1 with EP per subchannel coverage.

The red points are the locations without coverage. With a total of 423801 grid points and 20818 red points, the coverage is 95%. Therefore we can use Reuse 1 with EP per subchannel for the lightly irregular network, though it is borderline.

Reuse 1 β-coverage: Pass

3.1.3 Highly irregular network

Figure 3.3 shows the coverage of Reuse 1 with EP per subchannel for the highly irregular network.

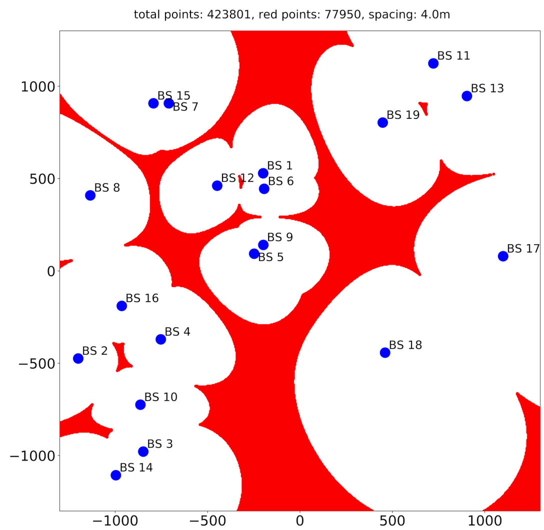

Figure 3.3: Reuse 1 with EP per subchannel coverage.

The red points are the locations without coverage. With a total of 423801 grid points and 77950 red points, the coverage is 81%. Therefore we cannot use Reuse 1 with EP per subchannel for the highly irregular network.

Reuse 1 β-coverage: **Fail**

Since Reuse 1 with EP per subchannel has insufficient coverage, we try Reuse 2 with EP per subchannel. We divide the band into 2 equal bands B_1 and B_2. The question now is: Which BSs transmit in frequency band B_1 and which in frequency band B_2? To solve this, we propose a simple heuristic that assigns the BSs to a frequency band. Let $\mathcal{L}_1$ and $\mathcal{L}_1$ be two distinct sets of points on the grid. We define the distance between these two sets as the minimum distance over all pairs of points (one for each set):

$$D(\mathcal{L}_1, \mathcal{L}_2) = \min\{d(x_1, x_2) \mid x_1 \in \mathcal{L}_1, x_2 \in \mathcal{L}_2\} \tag{3.1}$$

In Equation 3.1, $d(x, y)$ is the Euclidean distance between points x and y. Given $\mathcal{L}_1$ and $\mathcal{L}_2$, the closest point to $\mathcal{L}_1$ among the points in $\mathcal{L}_2$ is denoted $c(\mathcal{L}_1, \mathcal{L}_2)$. We propose the following heuristic to allocate two colors (blue and orange) to any network. Let $\mathcal{L}$ be the set of points corresponding to the BS positions.

Step 1: Select the initial point in $\mathcal{L}$ to be the one closest to the centre of the area to cover. Call it x_1 and make it blue. Let $\mathcal{L}_1 = \{x_1\}$ and $\mathcal{L}_2 = \overline{\mathcal{L}_1}$. Let $n = 1$.

As long as $\mathcal{L}_2 \neq \emptyset$, repeat Step 2:

Step 2: Let $x_{n+1} = c(\mathcal{L}_1, \mathcal{L}_2)$. If the closest point to x_{n+1} in $\mathcal{L}_1$ is blue, then x_{n+1} is orange, otherwise x_{n+1} is blue. Let $\mathcal{L}_1 = \mathcal{L}_1 \cup \{x_{n+1}\}$, $\mathcal{L}_2 = \overline{\mathcal{L}_1}$ and $n = n + 1$.

Verify that the number of blue points is about the same as the number of orange points. If they are not the same, we could cluster (based on euclidean distance) a dense group of blue or orange points (whichever colour is dominating the unbalanced colouring) and then re-run the heuristic on those points.

The resulting colouring and coverage is shown in Figure 3.4 for the highly irregular network. Note that the power per subchannel in a BS is doubled with respect to what it was for Reuse 1.

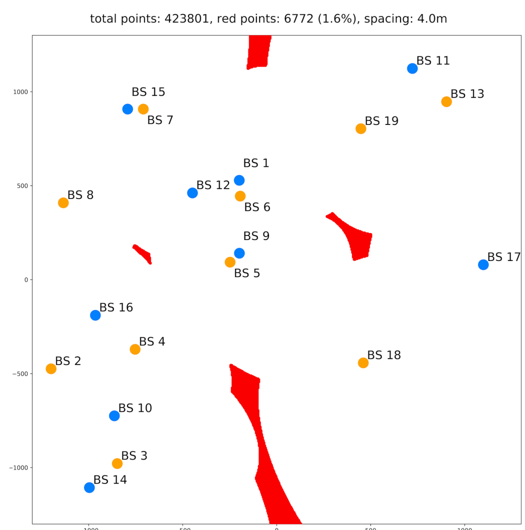

Figure 3.4: Reuse 2 with EP per subchannel coverage.

There are 9 blue BSs and 10 orange BSs which is what we want. No corrective action is needed. With a total of 423801 grid points and 6772 red points, the coverage is 98%. Therefore we can use Reuse 2 with EP per subchannel for the highly irregular network.

Reuse 2 β-coverage: Pass

3.2 Planning for performance

In this section, we investigate a simple way to provide better system performance than Reuse 1 with EP per subchannel for the regular and lightly irregular networks, and better than Reuse 2 with EP per subchannel for the highly irregular network. This is what we call Generalized Reuse 1.

3.2.1 Generalized Reuse 1

We propose *Generalized Reuse 1* which uses non-equal power per subchannel. Let $\mathcal{J}$ be the set of BSs in the system, and $\mathcal{J}_1, \mathcal{J}_2$ be the set of BSs coloured blue and orange respectively. We do this for all 3 networks. Then J is the number of BSs in the system, and J_1, J_2 are the number of BSs in blue and orange groups respectively. Assume there are M subchannels in the system where M is divisible by 3. We create 3 sub-bands B_1, B_2, B_3 of equal size. If M is not divisible by 3, we would have to slightly adjust what we are doing. Let $\mathcal{U}_j$ be the set of users associated to BS j as given by the UA. All BSs in $\mathcal{J}$ transmit with per subchannel power P in B_1 (i.e., subchannels 1 to $M/3$ inclusive). All BSs in $\mathcal{J}_1$ and $\mathcal{J}_2$ transmit with per subchannel power P and δP in B_2 respectively (i.e., subchannels $M/3+1$ to $2M/3$ inclusive) where δ is a small positive number. All BSs in $\mathcal{J}_1$ and $\mathcal{J}_2$ transmit with per subchannel power δP and P in B_3 respectively (i.e., subchannels $2M/3+1$ to M inclusive). An illustration of the per subchannel transmit power is shown in Figure 3.5.

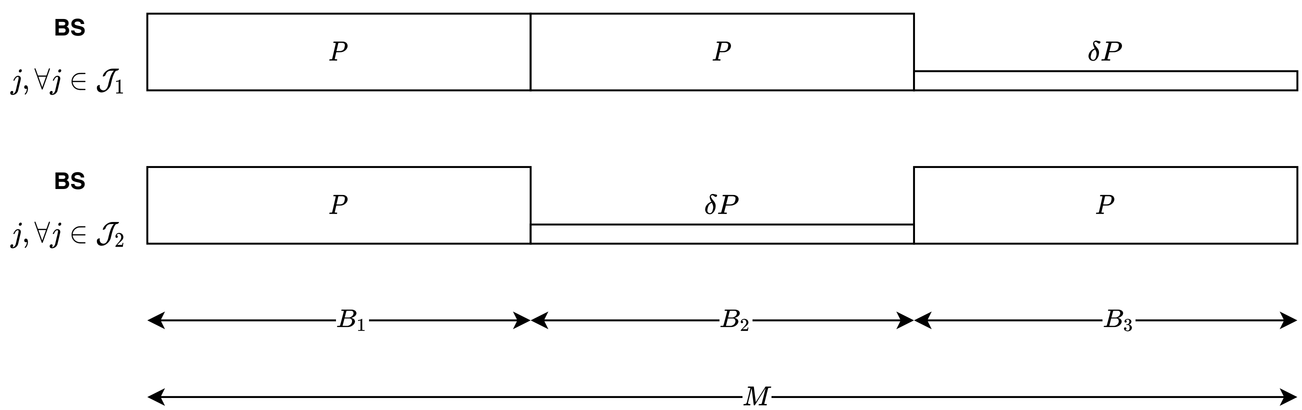

Figure 3.5: Per subchannel power for Generalized Reuse 1.

Given P_{max}, M and δ, the per subchannel power P can be computed using Equation 3.2.

$$(2+\delta)\frac{PM}{3} = P_{max} \tag{3.2}$$

We now present the per subchannel user rates under the assumption that the subchannel gains are time-invariant. The per subchannel user rates $\gamma_{u,j}^c$ in B_1 can be computed using Equation 3.3 given P, μ, and $G_{u,j}, \forall u \in \mathcal{U}_j \forall j \in \mathcal{J}$:

$$\gamma_{u,j}^c = f\big(\frac{PG_{u,j}}{\mu + \sum_{j' \neq j, j' \in \mathcal{J}} PG_{u,j'}}\big), \qquad \forall u \in \mathcal{U}_j, \forall j \in \mathcal{J}, \forall c \in B_1 \tag{3.3}$$

The per subchannel user rates $\gamma_{u,j}^c$ in B_2 can be computed using Equations 3.4 and 3.5 given δ, P, μ, and $G_{u,j}, \forall u \in \mathcal{U}_j \forall j \in \mathcal{J}$.

$$\gamma_{u,j}^c = f\big(\frac{PG_{u,j}}{\mu + \sum_{j' \neq j, j' \in \mathcal{J}_1} PG_{u,j'} + \sum_{j' \in \mathcal{J}_2} \delta PG_{u,j'}}\big), \forall u \in \mathcal{U}_j, \forall j \in \mathcal{J}_1, \forall c \in B_2 \tag{3.4}$$

$$\gamma_{u,j}^c = f\big(\frac{\delta PG_{u,j}}{\mu + \sum_{j' \in \mathcal{J}_1} PG_{u,j'} + \sum_{j' \neq j, j' \in \mathcal{J}_2} \delta PG_{u,j'}}\big), \forall u \in \mathcal{U}_j, \forall j \in \mathcal{J}_2, \forall c \in B_2 \tag{3.5}$$

The per subchannel user rates $\gamma_{u,j}^c$ in B_3 can be computed using Equations 3.6 and 3.7 given δ, P, μ, and $G_{u,j}, \forall u \in \mathcal{U}_j \forall j \in \mathcal{J}$.

$$\gamma_{u,j}^c = f\big(\frac{\delta PG_{u,j}}{\mu + \sum_{j' \neq j, j' \in \mathcal{J}_1} \delta PG_{u,j'} + \sum_{j' \in \mathcal{J}_2} PG_{u,j'}}\big), \forall u \in \mathcal{U}_j, \forall j \in \mathcal{J}_1, \forall c \in B_3 \tag{3.6}$$

$$\gamma_{u,j}^c = f\big(\frac{PG_{u,j}}{\mu + \sum_{j' \in \mathcal{J}_1} \delta PG_{u,j'} + \sum_{j' \neq j, j' \in \mathcal{J}_2} PG_{u,j'}}\big), \forall u \in \mathcal{U}_j, \forall j \in \mathcal{J}_2, \forall c \in B_3 \tag{3.7}$$

Again, the equations for the user rates only hold when all BSs have at least one user. BSs that have no users are omitted from the interference calculation.

Given M, and $\gamma_{u,j}^c, \forall u \in \mathcal{U}_j, \forall j \in \mathcal{J}, \forall c \in \mathcal{M}$, we do local user scheduling within a frame by solving $\mathcal{P}_{\text{generalized\_reuse1}}$ at each BS. Let $\alpha_{u,l}$ be the proportion of time given to user u in B_l (user u receives all the $M/3$ subchannels during that time), $\forall u \in \mathcal{U}_j, \forall l \in \{1, 2, 3\}$. Let $y_{u,l}$ be the per subchannel rate of user $u, \forall u \in \mathcal{U}_j$ in $B_l, \forall l \in \{1, 2, 3\}$. Note that $y_{u,1} = \gamma_{u,j}^c, \forall u \in \mathcal{U}_j, \forall j \in \mathcal{J}, \forall c \in B_1$, $y_{u,2} = \gamma_{u,j}^c, \forall u \in \mathcal{U}_j, \forall j \in \mathcal{J}, \forall c \in B_2$, and $y_{u,3} = \gamma_{u,j}^c, \forall u \in \mathcal{U}_j, \forall j \in \mathcal{J}, \forall c \in B_3$.

$$\mathcal{P}_{\text{generalized\_reuse1}}: \max_{\alpha_{u,l}, \forall u \in \mathcal{U}_j, \forall l \in \{1,2,3\}} \sum_{u \in \mathcal{U}_j} log(\lambda_u) \tag{3.8}$$

$$\lambda_u = \sum_{l \in \{1,2,3\}} \frac{M}{3} \alpha_{u,l} y_{u,l}, \qquad \forall u \in \mathcal{U}_j \tag{3.9}$$

$$\sum_{u \in \mathcal{U}_j} \alpha_{u,l} \leq 1, \qquad \forall l \in \{1,2,3\} \tag{3.10}$$

$$\alpha_{u,l} \geq 0, \qquad \forall u \in \mathcal{U}_j, \forall l \in \{1,2,3\} \tag{3.11}$$

The problem is a simple linear problem, and we solve it using the commercial solver MINOS 5.51 [1].

Finding the best δ

In the above, the performance of Generalized Reuse 1 depends on the parameter δ. The larger the δ, the more interference the BSs in $\mathcal{J}_2$ create in B_2, and the more interference the BSs in $\mathcal{J}_1$ create in B_3. At the same time, the larger the δ, the more per subchannel power the BSs in $\mathcal{J}_2$ use in B_2, and the more per subchannel power the BSs in $\mathcal{J}_1$ use in B_3. Therefore there is a tradeoff between rate and interference. The best δ also depends on the network and hotspot configuration.

We found the best δ by trial-and-error. This method is practical because $0 \leq \delta \leq 1$ which means the range of values to try is limited. To evaluate the system performance of a given δ, we use the fixed delay scenario. We find the best δ for all networks and their hotspot configurations. We tried 6 values of δ: 0, 0.05, 0.1, 0.15, 0.5, and 0.75.

The system model parameters are the same as in Table 3.2. The simulation parameters are the same as in Tables 2.1 and 2.2. The results for the regular, lightly irregular, and highly irregular network are shown in Sections 3.2.2, 3.2.3, and 3.2.4 respectively.

3.2.2 Regular network

We find the best δ for 0, 2, and 8 hotspots. First, we colour the BSs using the heuristic described in Section 3.1.3. The resulting colouring is in Figure 3.6, and the results for the different values of δ tried are in Figures 3.7, 3.8, and 3.9.

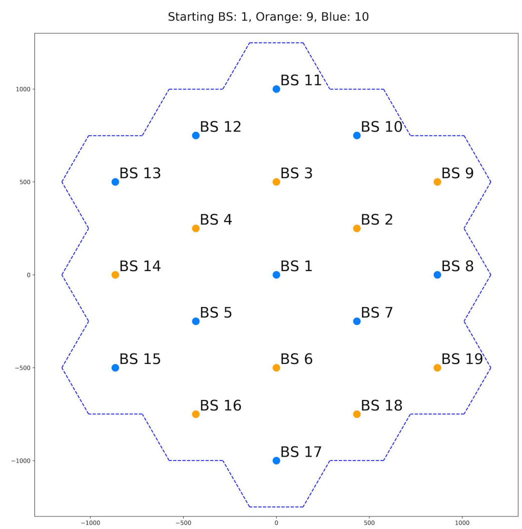

Figure 3.6: Regular network colouring.

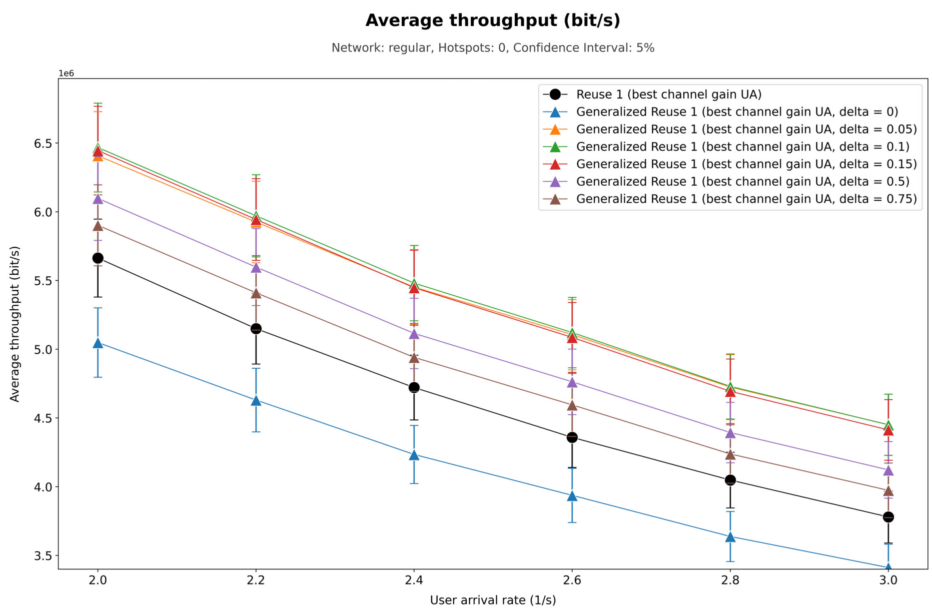

Figure 3.7: Finding the best δ for regular network (0 hotspot).

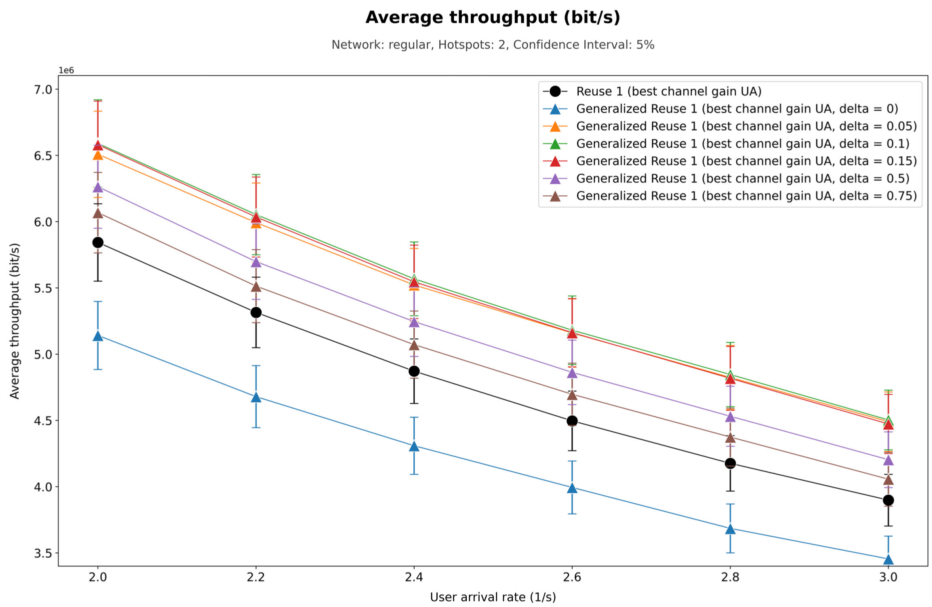

Figure 3.8: Finding the best δ for regular network (2 hotspots).

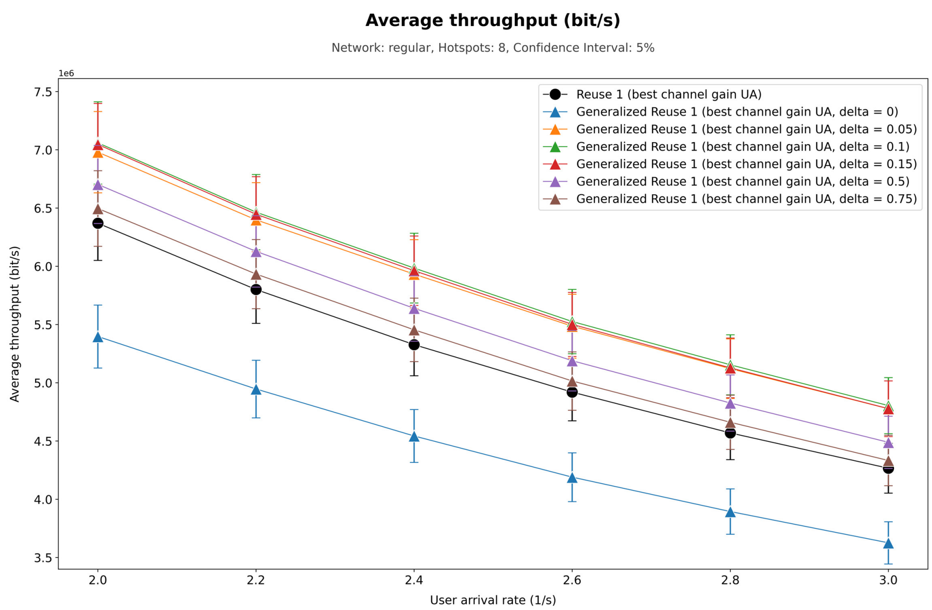

Figure 3.9: Finding the best δ for regular network (8 hotspots).

The results show that performance peaks at about $\delta = 0.1$ for 0, 2, and 8 hotspots.

Therefore we keep $\delta = 0.1$ as the best δ for the regular network. The gains of Generalized Reuse 1 for $\delta = 0.1$ are summarized in Table 3.3 with Reuse 1 with EP per subchannel as the baseline.

Table 3.3: Gains for regular network with Generalized Reuse 1 ($\delta = 0.1$).

User arrival rate λ (1/s)	0 hotspot	2 hotspots	8 hotspots
2.0	1.142021	1.127850	1.108335
2.2	1.159446	1.138913	1.114536
2.4	1.160871	1.143027	1.123411
2.6	1.174973	1.152146	1.123241
2.8	1.168345	1.160497	1.128055
3.0	1.177413	1.155147	1.126067

We see that Generalized Reuse 1 has better performance than Reuse 1 by roughly 10-18% depending on the arrival rate and hotspot configuration. We also verify the resulting coverage with $\delta = 0.1$ as shown in Figure 3.10.

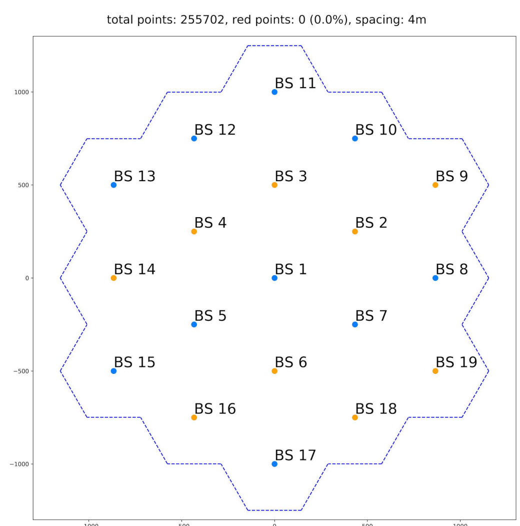

Figure 3.10: Regular network coverage with Generalized Reuse 1.

The coverage with Generalized Reuse 1 is 100% which is better than with Reuse 1.

Generalized Reuse 1 β-coverage: Pass

3.2.3 Lightly irregular network

We find the best δ for 0, 2, and 8 hotspots. First, we colour the BSs using the heuristic described in Section 3.1.3. The resulting colouring is in Figure 3.11, and the results for the different values of δ tried are in Figures 3.12, 3.13, and 3.14.

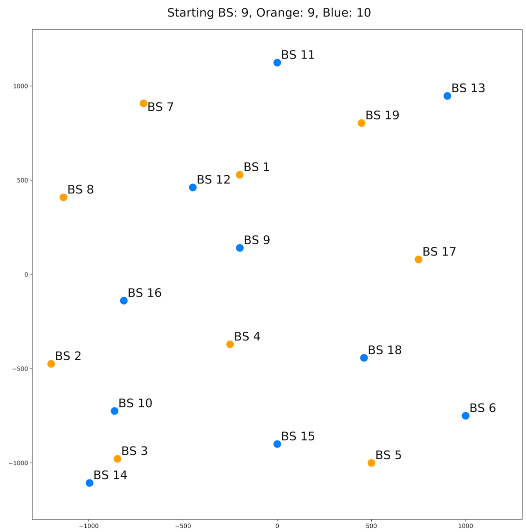

Figure 3.11: Lightly irregular network colouring.

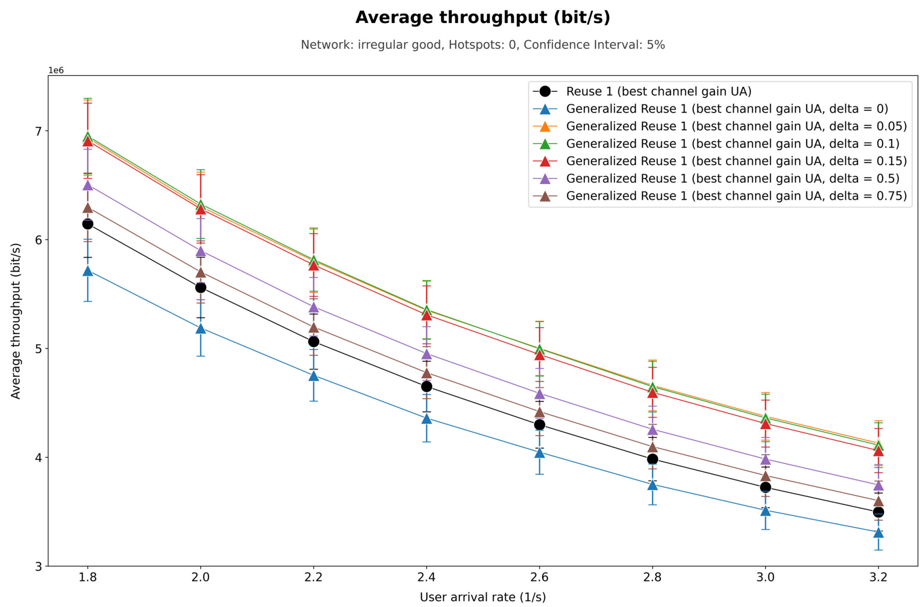

Figure 3.12: Finding the best δ for lightly irregular network (0 hotspot).

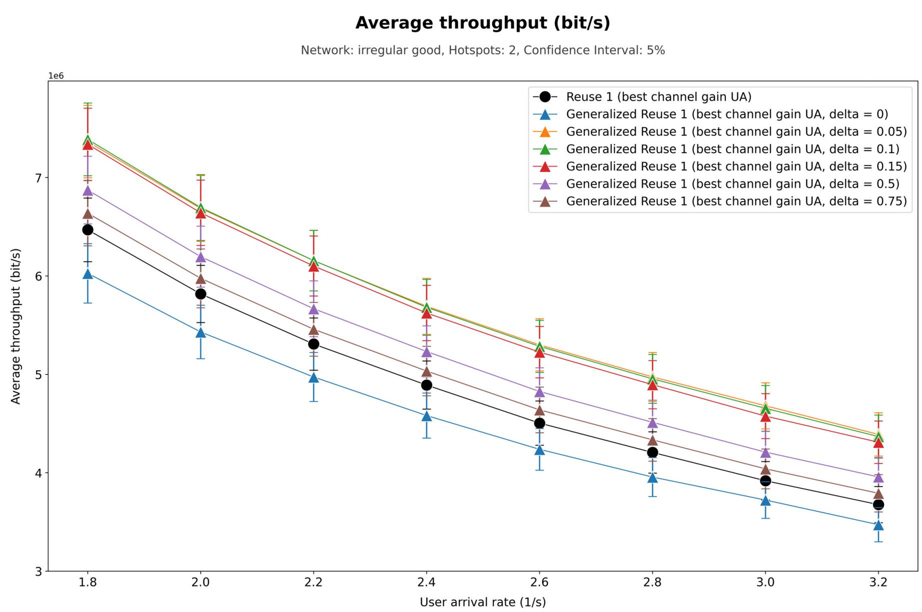

Figure 3.13: Finding the best δ for lightly irregular network (2 hotspots).

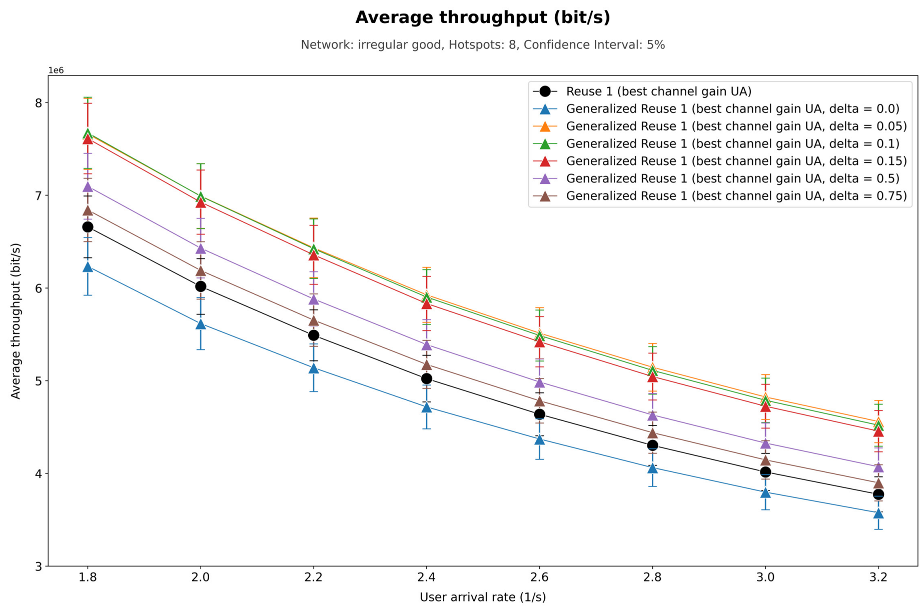

Figure 3.14: Finding the best δ for lightly irregular good network (8 hotspots).

The results show that performance peaks at about $\delta = 0.05$ for 0, 2, and 8 hotspots. Therefore we keep $\delta = 0.05$ as the best δ for the lightly irregular network. The gains of Generalized Reuse 1 for $\delta = 0.05$ are summarized in Table 3.4 with Reuse 1 with EP per subchannel as the baseline.

Table 3.4: Gains for lightly irregular network with Generalized Reuse 1 ($\delta = 0.05$).

User arrival rate λ (1/s)	0 hotspot	2 hotspots	8 hotspots
1.8	1.128751	1.138609	1.150490
2.0	1.133690	1.149289	1.162067
2.2	1.146593	1.159636	1.171791
2.4	1.150617	1.163772	1.180012
2.6	1.163246	1.176497	1.188551
2.8	1.169937	1.182459	1.195806
3.0	1.175308	1.194415	1.201359
3.2	1.180947	1.194013	1.207909

We see that Generalized Reuse 1 has better performance than Reuse 1 by roughly 12-20% depending on the arrival rate and hotspot configuration. We also verify the resulting coverage with $\delta = 0.05$ as shown in Figure 3.15.

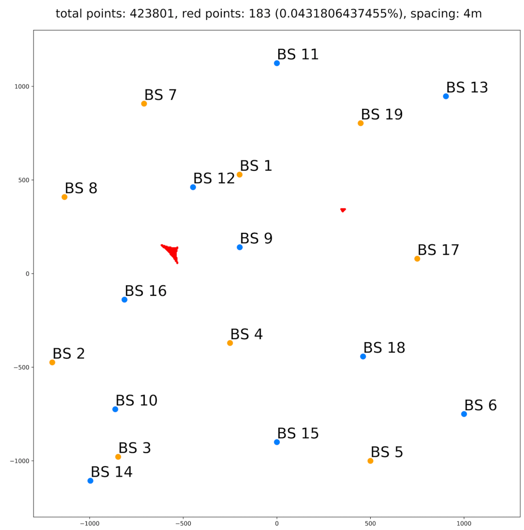

Figure 3.15: Lightly irregular network coverage with Generalized Reuse 1.

The coverage with Generalized Reuse 1 is 99% which is better than with Reuse 1.

Generalized Reuse 1 β-coverage: Pass

3.2.4 Highly irregular network

We find the best δ for 0, 2, and 8 hotspots. First, we colour the BSs using the heuristic described in Section 3.1.3. The resulting colouring is in Figure 3.16, and the results for the different values of δ tried are in Figures 3.17, 3.18, and 3.19.

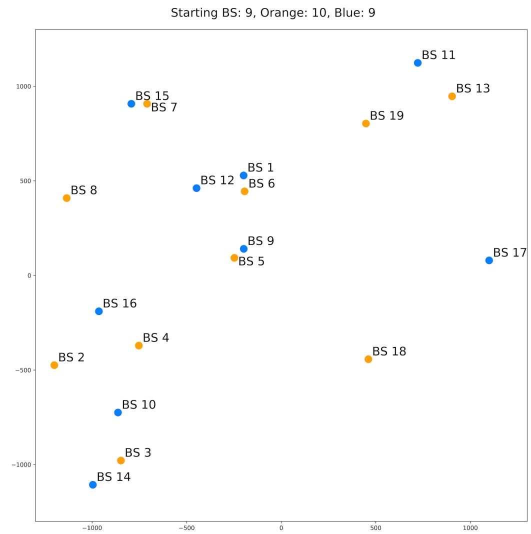

Figure 3.16: Highly irregular network colouring.

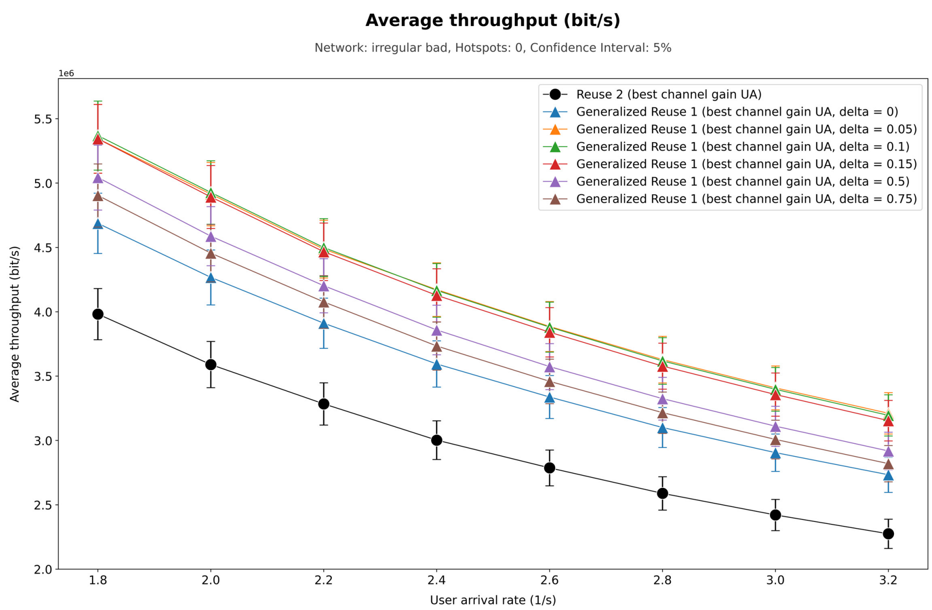

Figure 3.17: Finding the best δ for highly irregular network (0 hotspot).

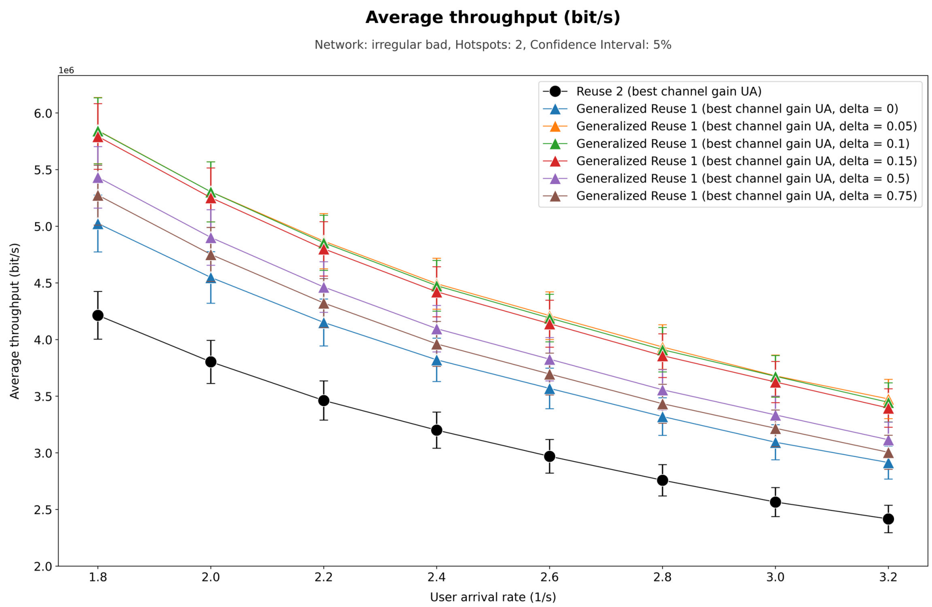

Figure 3.18: Finding the best δ for highly irregular network (2 hotspots).

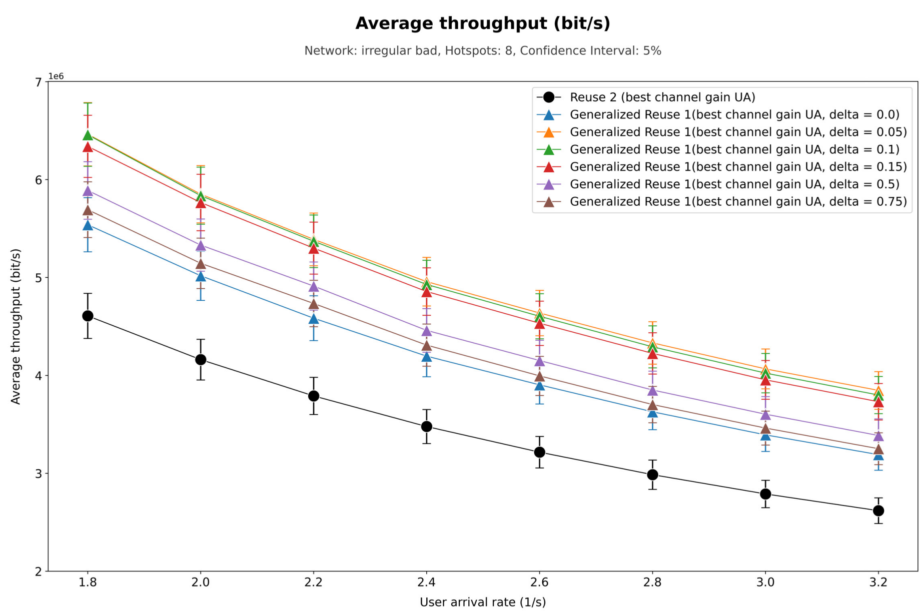

Figure 3.19: Finding the best δ for highly irregular network (8 hotspots).

The results show that performance peaks at about $\delta = 0.05$ for 0, 2, and 8 hotspots.

Therefore we keep $\delta = 0.05$ as the best δ for the highly irregular network. The gains of Generalized Reuse 1 for $\delta = 0.05$ are summarized in Table 3.5 with Reuse 2 with EP per subchannel as the baseline.

Table 3.5: Gains for highly irregular network with Generalized Reuse 1 ($\delta = 0.05$).

User arrival rate λ (1/s)	0 hotspot	2 hotspots	8 hotspots
1.8	1.342295	1.387022	1.402616
2.0	1.368956	1.394636	1.406039
2.2	1.366213	1.406236	1.421825
2.4	1.389577	1.403873	1.425555
2.6	1.394324	1.418237	1.441940
2.8	1.401524	1.426370	1.450791
3.0	1.407947	1.434161	1.457905
3.2	1.411556	1.438205	1.469081

We see that Generalized Reuse 1 has better performance than Reuse 2 by roughly 34-47% depending on the arrival rate and hotspot configuration. We also verify the resulting coverage with $\delta = 0.05$ as shown in Figure 3.20.

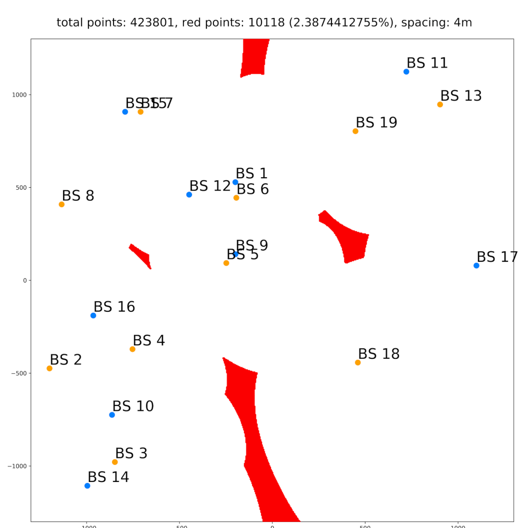

Figure 3.20: Highly irregular network coverage with Generalized Reuse 1.

The coverage with Generalized Reuse 1 is 98% which slightly less than Reuse 2 but worth it considering the gain in performance.

Generalized Reuse 1 β-coverage: Pass

3.3 Results summary

To summarize the results, Generalized Reuse 1 improved performance and coverage relative to Reuse 1 in the regular and lightly irregular networks where Reuse 1 was viable. For the highly irregular network, Generalized Reuse 1 significantly improved performance while slightly decreasing coverage relative to Reuse 2. Therefore at this point, Generalized Reuse 1 is the clear preference over either of the benchmarks Reuse 1 and Reuse 2.

Chapter 4

Smart Operation

Let us recall the definition of operation.

> **Operation:** Online process that is in charge of user association (UA), user scheduling (US), and possibly further constraints to reflect instantaneous load imbalance between BSs.

In Smart Operation, we want to further improve the performance obtained in Smart Planning. This is possible by using the available network information (e.g., user subchannel gains, number of users at each BS) in a C-RAN. The C-RAN with global network state can smartly modify the power map obtained in Smart Planning for better performance. For example, overcrowded BSs may use more subchannels and BSs with fewer users may use fewer subchannels. This is known as subchannel allocation and contrary to doing it in the planning stage as conventional planning dictates, we propose to do it in the operation stage in a periodic fashion. The key idea is that we obey the per BS max power budget P_{max} W. We do not use more than P_{max} at each BS. In fact, BSs with fewer users may use less power to reduce interference to help overcrowded BSs. In effect, Smart Operation builds on Smart Planning (seen later) by differentiating between currently lightly and highly loaded BSs, and users with excellent and poor radio conditions at the global level.

A problem with this global state approach is that it involves taking a snapshot of the entire network, and using the information to modify the power map. Ideally, a snapshot is taken every time the network changes. But this is impractical because it would mean updating the power map for every user arriving and leaving the network. Therefore to be practical, the power map is changed periodically which means that snapshots are also taken periodically.

The questions to answer are summarized as:

- Which subchannels do BSs use with high power given the network state?
- Which subchannels do BSs use with low power given the network state?
- What value to use for high power, what value to use for low power?
- How often do we take a snapshot of the network to update the power map?

We now introduce the Smart Operation variants of the three schemes described in Smart Planning: Reuse 1 + Smart Operation, Reuse 2 + Smart Operation, and Generalized Reuse 1 + Smart Operation. Think of it as taking the power map from planning (call it the original) for a given scheme and making changes to it. The result is a new power map that is derived from the original power map as will be explained next.

4.1 Reuse 1 with Smart Operation

In this section, we assume that the network under consideration is β-covered when Reuse 1 is used. At a given time (we will discuss timing in more details later), we order the BSs such that the most loaded BS (based on number of users) is called BS 1 and the least loaded one is called BS J. Right now, somewhat unrealistically, we assume that we do this every time there is a change in the number of users (either an arrival or departure). We propose that BS j will use M_j subchannels starting from subchannel 1. Hence, all BSs use the first M_J subchannels, all BSs except BS J use the subchannels numbered $M_J + 1$ to M_{J-1}, etc. As a result, the BSs allowed to use the subchannels with high numbering will see much less interference on those subchannels.

Given an order, we compute the per subchannel rates $\gamma_{u,j}(k)$ on block k $(1 \leq k \leq J)$ for user $i \in \mathcal{U}_j$ where block 1 is of size $M_1 - M_2$, block 2 is of size $M_2 - M_3$, and block k is of size $M_k - M_{k+1}$. Here we adopt a 2-level subchannel power allocation scheme. Specifically, BS $j \in \mathcal{J}$ transmits with per subchannel power P_{max}/M on its allocated M_j subchannels, and with per subchannel power $P_\epsilon = \epsilon P_{max}/M$ on the remaining $M - M_j$ subchannels where ϵ is a small positive number as shown in Figure 4.1.

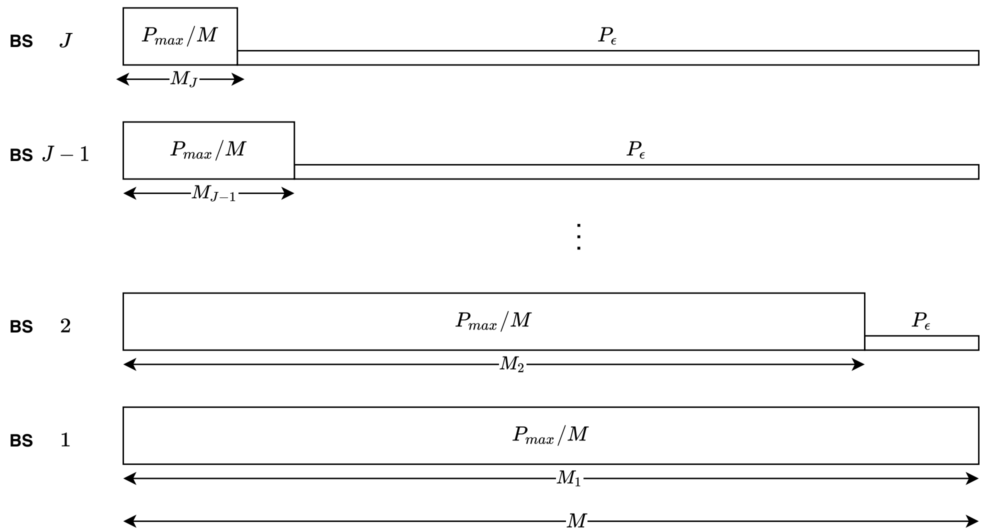

Figure 4.1: Per subchannel power for Reuse 1 + Smart Operation.

We will discuss how to compute ϵ later. The per subchannel rates $\gamma_{uj}(k)$ of user u associated to BS j in block k can be calculated as:

- If $k \geq j$

$$\gamma_{uj}(k) = f\Big(\frac{G_{uj}P_{max}/M}{\mu + \sum_{j'\neq j, j'\leq k} G_{uj'}P_{max}/M + \sum_{j'>k} G_{uj'}P_\epsilon}\Big) \tag{4.1}$$

- If $k < j$

$$\gamma_{uj}(k) = f\Big(\frac{G_{uj}P_\epsilon}{\mu + \sum_{j'\leq k} G_{uj'}P_{max}/M + \sum_{j'\neq j, j'>k} G_{uj'}P_\epsilon}\Big) \tag{4.2}$$

Again, BSs with no users are omitted from the interference calculation. We then do joint subchannel allocation and user scheduling problem per frame by solving $\mathcal{P}_{\text{reuse1\_SO}}$ given the $\mathcal{U}_j, \forall j \in \mathcal{J}$, the per subchannel rates $y_{u,j}(k), \forall u \in \mathcal{U}_j, \forall j \in \mathcal{J}$ on block k for $1 \leq k \leq J$ to compute the M_j's:

$$\mathcal{P}_{\text{reuse1\_SO}}: \max_{(\lambda_{u,j}),(M_j),(\alpha_{u,j}(k))} \sum_{j=1}^{J} \sum_{u \in \mathcal{U}_j} \log(\lambda_{u,j}) \tag{4.3}$$

$$\lambda_{u,j} = \sum_{k=1}^{J} \alpha_{u,j}(k)\gamma_{u,j}(k) \quad \forall u \in \mathcal{U}_j,\ \forall j \in \mathcal{J} \tag{4.4}$$

$$\sum_{u \in \mathcal{U}_j} \alpha_{u,j}(k) = M_k - M_{k+1} \quad \forall k, \forall j \in \mathcal{J} \tag{4.5}$$

$$0 \leq M_J \leq ... \leq M_1 = M \tag{4.6}$$

$$\alpha_{u,j}(k) \geq 0, \lambda_{u,j} \geq 0, \forall k, \forall u \in \mathcal{U}_j, \forall j \in \mathcal{J} \tag{4.7}$$

In this problem, $\alpha_{u,j}(k)$ is the number of subchannels allocated to user u associated to BS j in subchannel block k. Note that the problem to solve is global (making the problem large) but otherwise all constraints are linear. So it can be solved easily.

4.2 Reuse 2 with Smart Operation

Let $\mathcal{J}$ be the set of BSs in the system, and $\mathcal{J}_1, \mathcal{J}_2$ be the set of BSs coloured blue and orange respectively. Then J is the number of BSs in the system, and J_1, J_2 are the number of BSs in blue and orange groups respectively.

We then treat the blue and orange BSs independently.

Among the blue BSs It is the same as Reuse 1 with EP per subchannel but on set $\mathcal{J}_1$, twice as much per subchannel power, and a user receives interference only from the co-subchannel BSs.

Among the orange BSs It is the same as Reuse 1 with EP per subchannel but on set $\mathcal{J}_2$ and twice as much per subchannel power, and a user receives interference only from the co-subchannel BSs.

4.3 Generalized Reuse 1 with Smart Operation

We start with Generalized Reuse 1 where the P and δ are given. At a given time (same as Reuse 1 + Smart Operation), we want more subchannels with high transmit power allocated to crowded BSs in $\mathcal{J}$ in B_1. We also want the same in B_2 but for BSs in $\mathcal{J}_1$, and the same in B_3 but for BSs in $\mathcal{J}_2$.

To do so, we order the BSs so that the first BS o_1 is the one in $\mathcal{J}$ with the least users, the second one, o_2 is the BS in $\mathcal{J}$ with the second least users, etc. Let $\mathcal{O}$ be the order. We also have an order $\mathcal{O}_1$ for $\mathcal{J}_1$ only and an order $\mathcal{O}_2$ for $\mathcal{J}_2$ only. The nth element of $\mathcal{O}_1$ is called o_n^1, of $\mathcal{O}_2$ is called o_n^2, and of $\mathcal{O}$ is called o_n. We divide B_1 into J sub-bands of size k_j^1 subchannels. Then the first BS in $\mathcal{O}$ receives the subchannels in the first sub-band in B_1 (i.e., subchannels 1 to k_1^1 inclusive), the second BS receives the subchannels in the first and second sub-bands in B_1 (i.e., subchannels 1 to $k_1^1 + k_2^1$ inclusive), and the jth BS receives the subchannels in the first to jth sub-bands inclusive in B_1 (i.e., subchannels 1 to $\sum_{i=1}^{i=j} k_i^1$ inclusive). We do the same for the BSs in $\mathcal{O}_1$ but for sub-band B_2 (by dividing B_2 into J_1 sub-bands of size k_j^2 subchannels), and the same for the BSs in $\mathcal{O}_2$ but for sub-band B_3 (by dividing B_3 into J_2 sub-bands of size k_j^3 subchannels).

BS $o_n \in \mathcal{O}$ will transmit on sub-bands 1 to n inclusive in B_1 with per subchannel power P and in subband $n+1$ to J inclusive in B_1 with per subchannel power $P_\epsilon = \epsilon P$. We do the same for the BSs in $\mathcal{O}_1$ but for sub-band B_2, and for the BSs in $\mathcal{O}_2$ but for sub-band B_3. Additionally, BSs in $\mathcal{O}_2$ will transmit with per subchannnel power $P_\delta = \delta P$ in B_2, and BSs in $\mathcal{O}_3$ will transmit with per subchannel power P_δ in B_3 where δ is a small positive number. The per subchannel power is shown in Figures 4.2, 4.3, and 4.4 for B_1, B_2, and B_3 respectively.

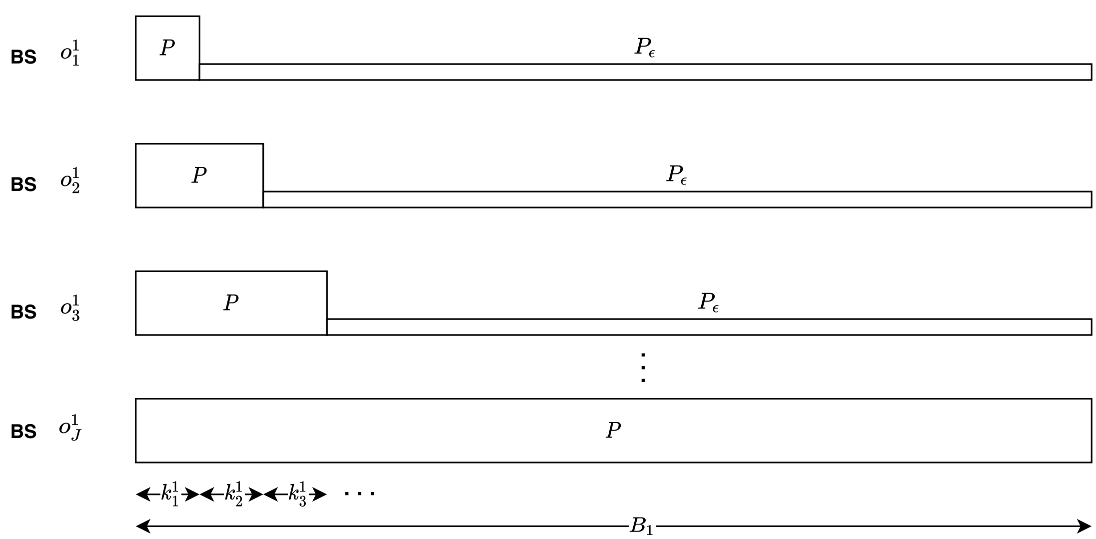

Figure 4.2: Per subchannel power for B_1 in Generalized Reuse 1 + Smart Operation.

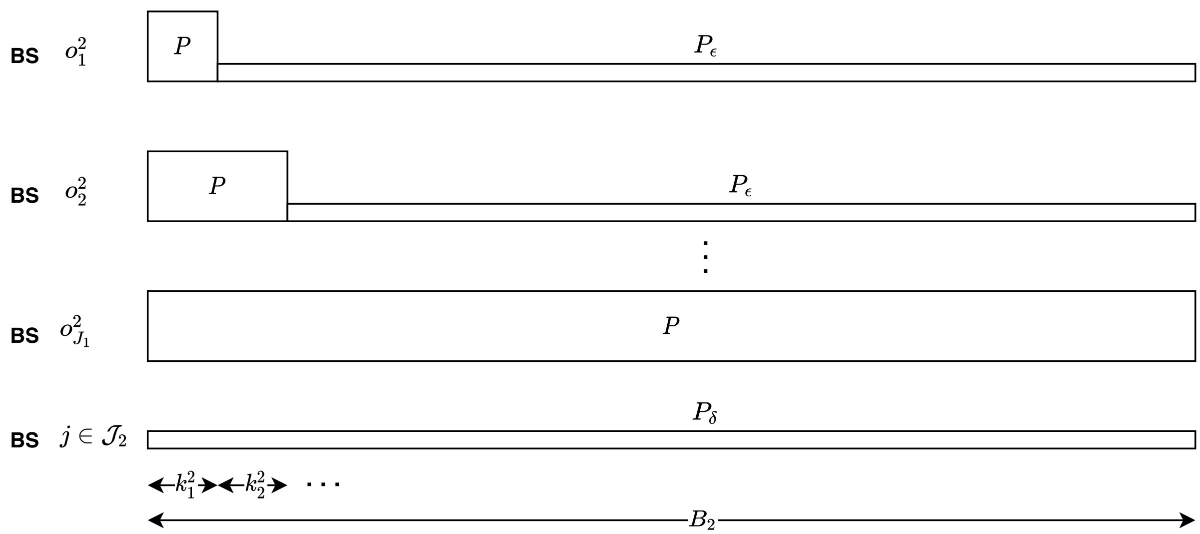

Figure 4.3: Per subchannel power for B_2 in Generalized Reuse 1 + Smart Operation.

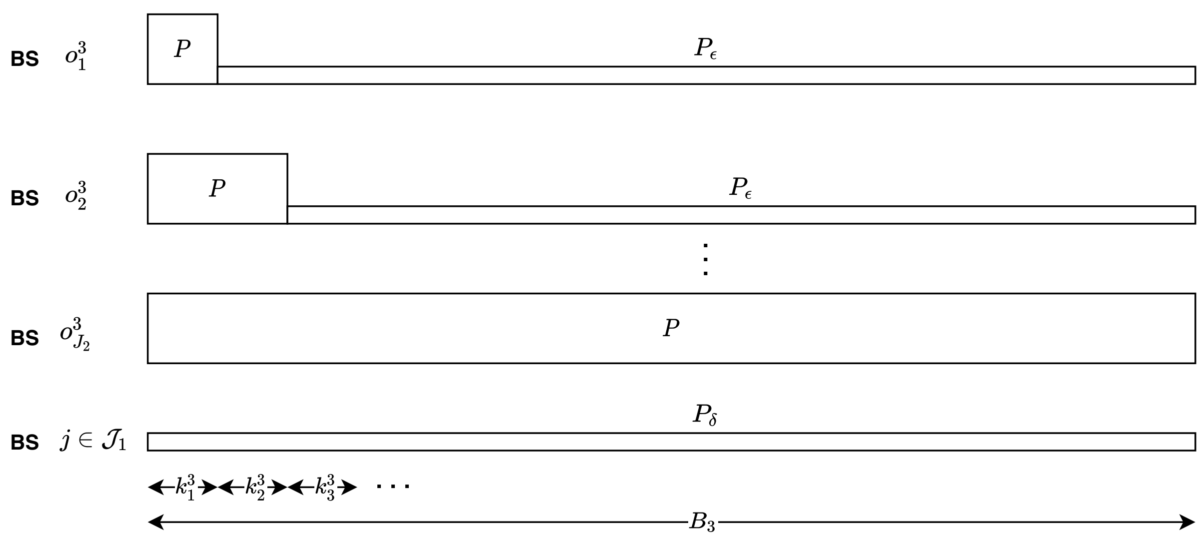

Figure 4.4: Per subchannel power for B_3 in Generalized Reuse 1 + Smart Operation.

Last but not least, we need to compute the sub-band sizes in B_1, B_2, and B_3 (i.e., the k_j^1's, k_j^2's and k_j^3's). In total, we have $2J$ sub-bands (i.e., J in B_1, J_1 in B_2, and J_2 in B_3) and for each sub-band, we can compute beforehand $\gamma_{u,j}(l)$ which is the per subchannel rate seen by user u of BS j on sub-band $1 \leq l \leq 2J$. Note that this rate depends on the position of BS j in the order $\mathcal{O}$ for sub-bands $1 \leq l \leq J$ and if $j \in \mathcal{J}_1$, its rate in sub-bands $J+1 \leq l \leq J+J_1$ depends on its place in $\mathcal{O}_1$ and if $j \in \mathcal{J}_2$, its rate in sub-bands $J+J_1+1 \leq l \leq 2J$ depends on its place in $\mathcal{O}_2$.

We will discuss how to compute ϵ later.

Rate calculation per BS per sub-band

In sub-band $1 \leq l \leq J$, given the ordering $\mathcal{O}$,

- $\forall u \in \mathcal{U}_j, \forall j \in \mathcal{O}$, if $l \leq n$

$$\gamma_{u,O_n}(l) = f\Big(\frac{G_{u,O_n}P}{\mu + \sum_{n' \neq n, l \leq n'} G_{u,O_{n'}}P + \sum_{l > n'} G_{u,O_{n'}}P_\epsilon}\Big) \tag{4.8}$$

- $\forall u \in \mathcal{U}_j, \forall j \in \mathcal{O}$, if $l > n$

$$\gamma_{u,O_n}(l) = f\Big(\frac{G_{u,O_n}P_\epsilon}{\mu + \sum_{l \leq n'} G_{u,O_{n'}}P + \sum_{n' \neq n, l > n'} G_{u,O_{n'}}P_\epsilon}\Big) \tag{4.9}$$

In sub-band $J+1 \leq l \leq J+J_1$, given the ordering $\mathcal{O}_1$,

- $\forall u \in \mathcal{U}_j, \forall j \in \mathcal{O}_1$, if $l \leq n+J$

$$\gamma_{u,O_n^1}(l) = f\Big(\frac{G_{u,O_n^1}P}{\mu + \sum_{n' \neq n, l \leq J+n'} G_{u,O_{n'}^1}P + \sum_{l > J+n'} G_{u,O_{n'}^1}P_\epsilon + \sum_{j \in \mathcal{J}_2} G_{u,j}P_\delta}\Big) \tag{4.10}$$

- $\forall u \in \mathcal{U}_j, \forall j \in \mathcal{O}_1$, if $l > n+J$

$$\gamma_{u,O_n^1}(l) = f\Big(\frac{G_{u,O_n^1}P_\epsilon}{\mu + \sum_{l \leq n'+J} G_{u,O_{n'}^1}P + \sum_{n' \neq n, l > J+n'} G_{u,O_{n'}^1}P_\epsilon + \sum_{j \in \mathcal{J}_2} G_{u,j}P_\delta}\Big) \tag{4.11}$$

- $\forall u \in \mathcal{U}_j, \forall j \in \mathcal{J}_2$

$$\gamma_{u,j}(l) = f\Big(\frac{G_{u,j}P_\delta}{\mu + \sum_{l \leq n+J} G_{u,O_n^1}P + \sum_{l > n+J} G_{u,O_n^1}P_\epsilon + \sum_{j' \in \mathcal{J}_2, j' \neq j} G_{u,j'}P_\delta}\Big) \tag{4.12}$$

In sub-band $J+J_1+1 \leq l \leq 2J$, given the ordering $\mathcal{O}_2$,

- $\forall u \in \mathcal{U}_j, \forall j \in \mathcal{O}_2$, if $l \leq n + J + J_1$

$$\gamma_{u,O_n^2}(l) = f\Big(\frac{G_{u,O_n^2}P}{\mu + \sum_{n' \neq n, l \leq n'+J+J_1} G_{u,O_{n'}^2}P + \sum_{l > n'+J+J_1} G_{u,O_{n'}^2}P_\epsilon + \sum_{j \in \mathcal{J}_1} G_{u,j}P_\delta}\Big) \tag{4.13}$$

- $\forall u \in \mathcal{U}_j, \forall j \in \mathcal{O}_2$, if $l > n + J + J_1$

$$\gamma_{u,O_n^2}(l) = f\Big(\frac{G_{u,O_n^2}P_\epsilon}{\mu + \sum_{l \leq n'+J+J_1} G_{u,O_{n'}^2}P + \sum_{n' \neq n, l > n'+J+J_1} G_{u,O_{n'}^2}P_\epsilon + \sum_{j \in \mathcal{J}_1} G_{u,j}P_\delta}\Big) \tag{4.14}$$

- $\forall u \in \mathcal{U}_j, \forall j \in \mathcal{J}_1$

$$\gamma_{u,j}(l) = f\Big(\frac{G_{u,j}P_\delta}{\mu + \sum_{l \leq n+J+J_1} G_{u,O_n^2}P + \sum_{l > n+J+J_1} G_{u,O_n^2}P_\epsilon + \sum_{j' \in \mathcal{J}_1, j' \neq j} G_{u,j'}P_\delta}\Big) \tag{4.15}$$

Again, BSs with no users are omitted from the interference calculation.

Optimization problem

We transition from the notation k_i^j to $k(l)$, the size of sub-band $l \in \{1, ..., 2J\}$. That is, $k(1) = k_1^1, k(2) = k_2^1, ..., k(J) = k_J^1, k(J+1) = k_1^2, ..., k(J+J_1) = k_{J_1}^2, k(J+J_1+1) = k_1^3, ..., k(2J) = k_{J_2}^3$. We compute the $\gamma_{u,j}(l), \forall u \in \mathcal{U}_j, \forall j \in \mathcal{J}, \forall l \in \{1, \ldots, 2J\}$, and then solve $\mathcal{P}_{\text{generalized\_reuse1\_SO}}$ to obtain the user scheduling (i.e., $\alpha_{u,j}(l)$'s) per frame and the sub-band sizes (i.e., $k(l)$'s).

$$\mathcal{P}_{\text{generalized\_reuse1\_SO}}: \max_{\alpha_{u,j}(l),\lambda_{u,j},k(l)} \quad \sum_{j=1}^{J}\sum_{u\in\mathcal{U}_j}\log(\lambda_{u,j}) \tag{4.16}$$

$$\text{subject to} \quad \lambda_{u,j} = \sum_{l=1}^{J+J_1+J_2}\alpha_{u,j}(l)\cdot\gamma_{u,j}(l), \qquad \forall u\in\mathcal{U}_j, \forall j\in\mathcal{J} \tag{4.17}$$

$$\sum_{u\in\mathcal{U}_j}\alpha_{u,j}(l)\le k(l), \qquad \forall l\in\{1,...,2J\}, \forall j\in\mathcal{J} \tag{4.18}$$

$$\sum_{l=1}^{J}k(l)\le\frac{M}{3}, \tag{4.19}$$

$$\sum_{l=J+1}^{J+J_1}k(l)\le\frac{M}{3}, \tag{4.20}$$

$$\sum_{l=J+J_1+1}^{2J}k(l)\le\frac{M}{3}, \tag{4.21}$$

$$\alpha_{u,j}(l)\ge 0, \lambda_{u,j}\ge 0, k(l)\ge 0, \forall u\in\mathcal{U}_j, \forall j\in\mathcal{J}, \forall l\in\{1,...,2J\} \tag{4.22}$$

In this problem, $\alpha_{u,l}(k)$ is the number of subchannels allocated to user u associated to BS j in sub-band l. This problem is also global but otherwise all constraints are linear. So it can be solved easily.

4.4 Finding the best ϵ

Notice that every Smart Operation optimization problem is a function of ϵ. Therefore we will find the best ϵ for every network and hotspot configuration. Since ϵ is just the ratio between the high and low power levels, its range is $0 \leq \epsilon \leq 1$. Therefore just like how we previously found the best δ, we will simulate in a dynamic setting to find the best ϵ by exhaustive search. We try 5 different values of ϵ: 0, 0.05, 0.1, 0.15, and 0.75.

We now present the simulation results for each network using the fixed delay scenario. We use the same system model parameters (Table 3.2), simulation parameters (Table 2.1), and networks. We compare cases with and without Smart Operation (SO). For the regular and lightly irregular networks, we compare Generalized Reuse 1, Reuse 1 + SO, and Generalized Reuse 1 + SO to the baseline Reuse 1 with EP per subchannel. For the highly irregular network, we compare Generalized Reuse 1, Reuse 2 + SO, and Generalized Reuse 1 + SO to the baseline Reuse 2 with EP per subchannel.

4.4.1 Regular network

We find the best ϵ for 0, 2, and 8 hotspots. The results are shown in Figures 4.5, 4.6, 4.7.

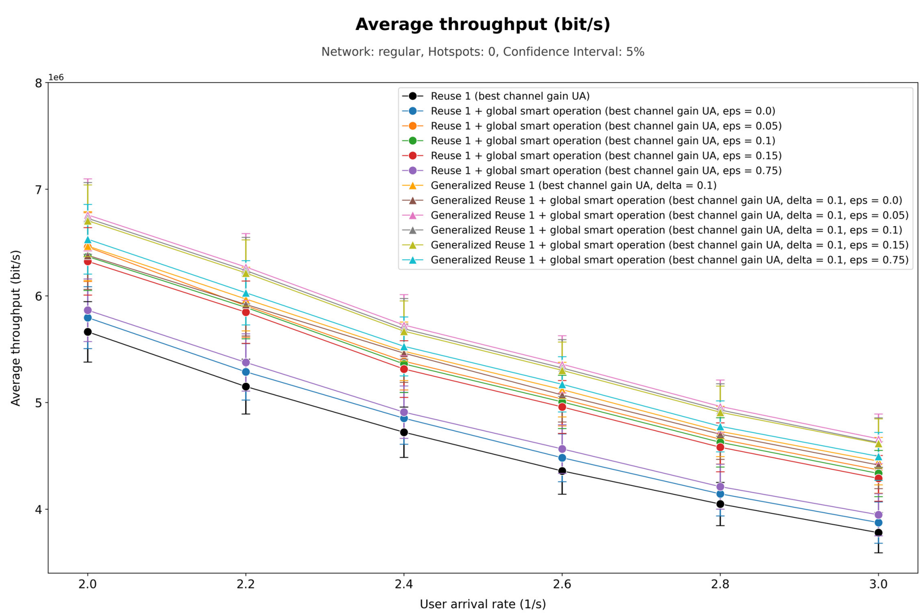

Figure 4.5: Finding the best ϵ for regular network (0 hotspot).

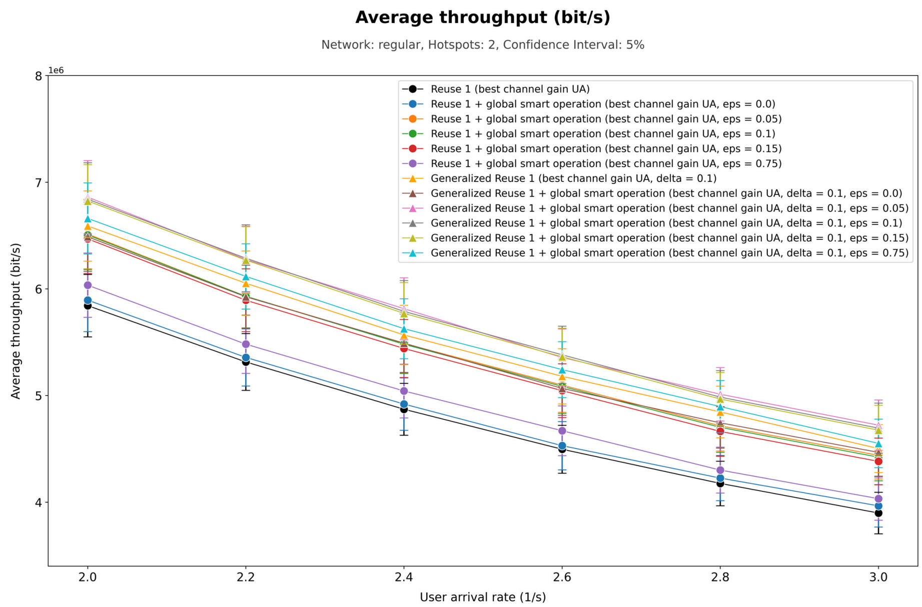

Figure 4.6: Finding the best ϵ for regular network (2 hotspots).

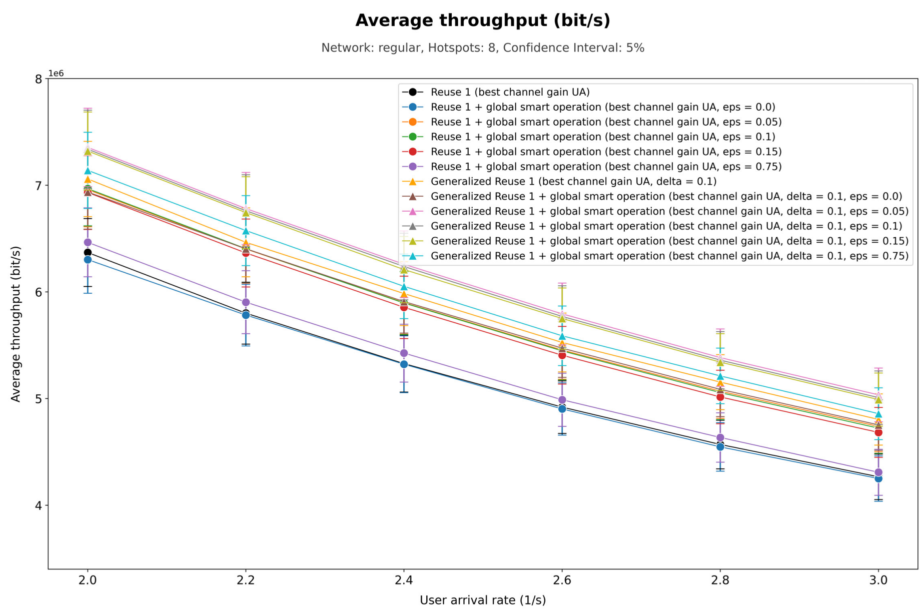

Figure 4.7: Finding the best ϵ for regular network (8 hotspots).

In all three figures, we see that Generalized Reuse 1 (light orange line) has slightly better performance than Reuse 1 + SO with $\epsilon = 0.05$ (dark orange line) which is the best performing Reuse 1 + SO ϵ-variant. Therefore Generalized Reuse 1 alone brings slightly better performance at lower complexity than Reuse 1 + SO. Generalized Reuse 1 + SO ($\epsilon = 0.05$) has higher performance than Generalized Reuse 1 by roughly 5% (relative to Reuse 1) which is not much.

Based on the results, performance peaks at about $\epsilon = 0.05$ for 0, 2, and 8 hotspots. Therefore we keep this value of ϵ for the regular network. To summarize, against the baseline Reuse 1, the gains were roughly 15-20% for the regular network with Generalized Reuse 1 + SO, and roughly 10-15% with Generalized Reuse 1 alone and Reuse 1 + SO (though it does slightly worse than Generalized Reuse 1).

4.4.2 Lightly irregular network

We find the best ϵ for 0, 2, and 8 hotspots. The results are shown in Figures 4.8, 4.9, 4.10.

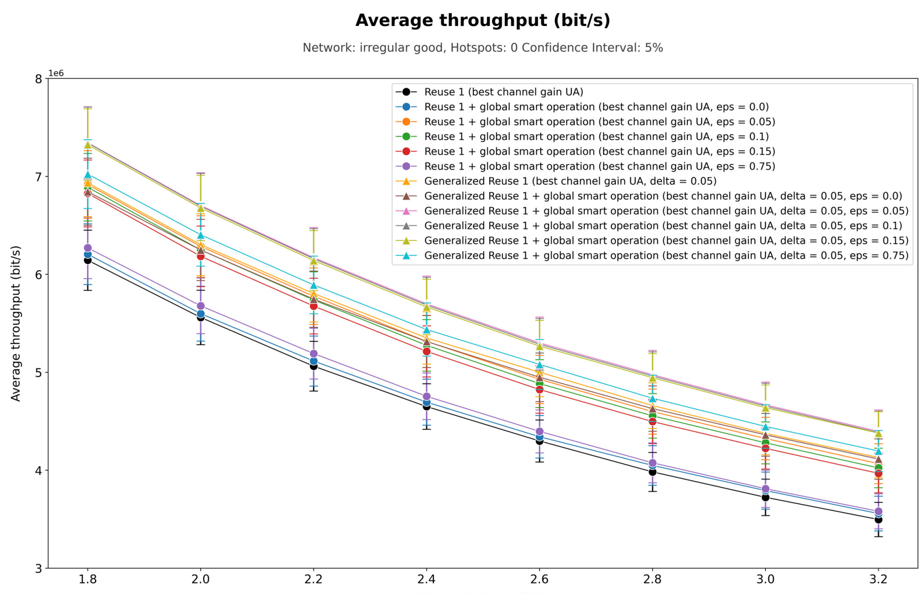

Figure 4.8: Finding the best ϵ for lightly irregular network (0 hotspot).

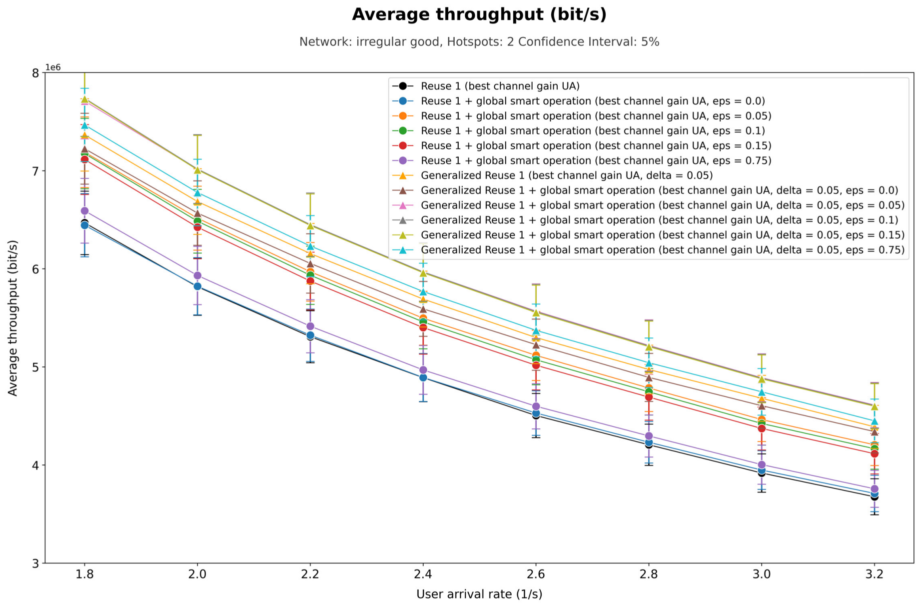

Figure 4.9: Finding the best ϵ for lightly irregular network (2 hotspots).

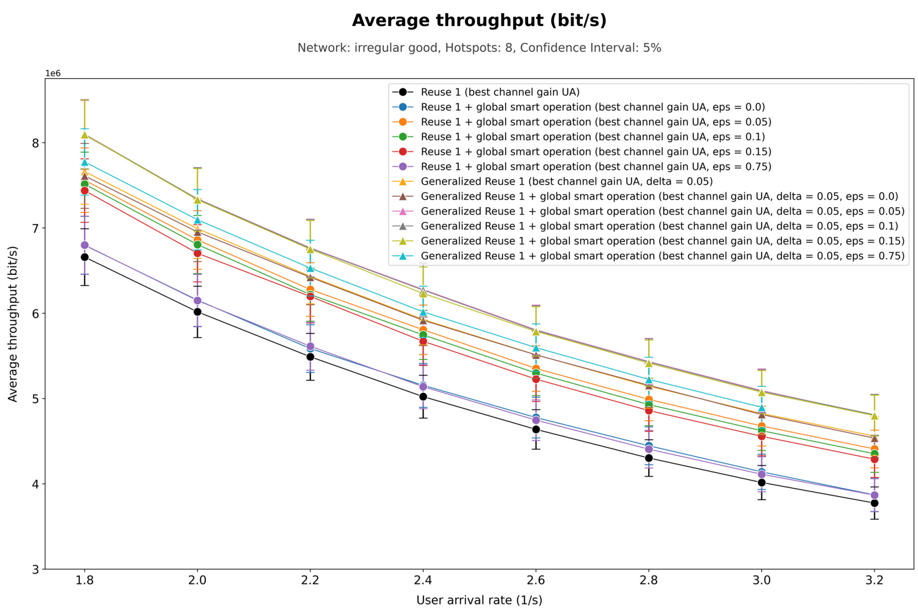

Figure 4.10: Finding the best ϵ for lightly irregular network (8 hotspots).

In the 0 hotspot case, we see that Generalized Reuse 1 (light orange line) has slightly better performance than Reuse 1 + SO with $\epsilon = 0.05$ (dark orange line) which is the best performing Reuse 1 + SO ϵ-variant. Moreover, Generalized Reuse 1 is easier to use than Reuse 1 + SO. In the 2 and 8 hotspots case, the performance gap is wider because Generalized Reuse 1 does better than Reuse 1 + SO by up to 5% (relative to Reuse 1). In all three figures, Generalized Reuse 1 + SO ($\epsilon = 0.05$) has higher performance than Generalized Reuse 1 by roughly 7% (relative to Reuse 1).

Based on the results, performance peaks at about $\epsilon = 0.05$ for 0, 2, and 8 hotspots. Therefore we keep this value of ϵ for the lightly irregular network. To summarize, against the baseline Reuse 1, the gains were roughly 20-25% for the lightly irregular network with Generalized Reuse 1 + SO, and roughly 13-18% with Generalized Reuse 1 alone. Reuse 1 + SO can perform up to 5% (relative to Reuse 1) worse than Generalized Reuse 1.

4.4.3 Highly irregular network

We find the best ϵ for 0, 2, and 8 hotspots. The results are shown in Figures 4.11, 4.12, 4.13.

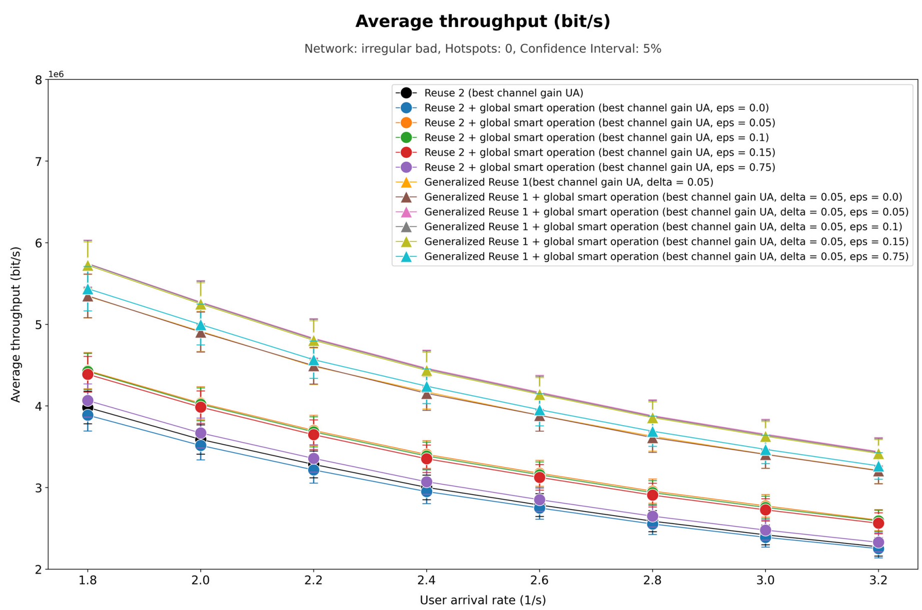

Figure 4.11: Finding the best ϵ for highly irregular network (0 hotspot).

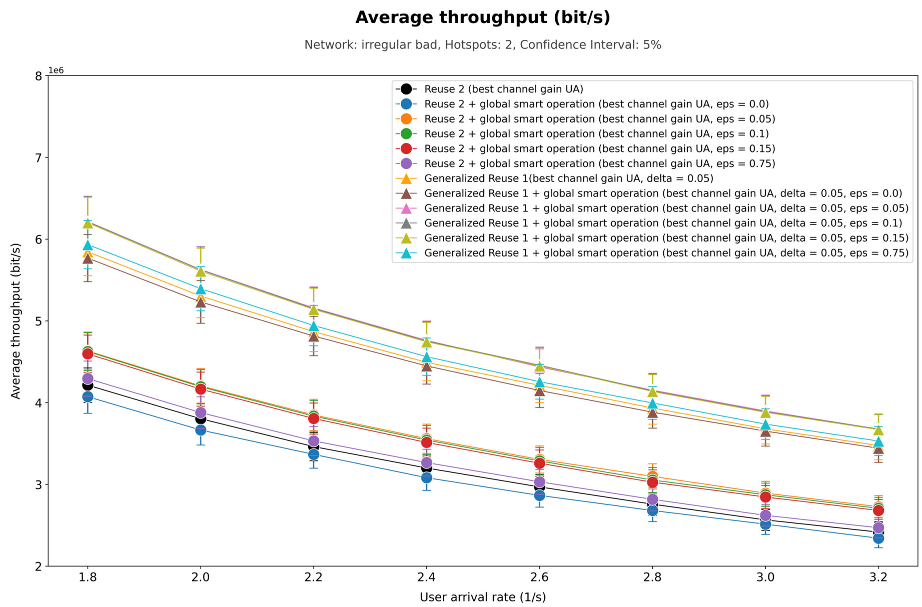

Figure 4.12: Finding the best ϵ for highly irregular network (2 hotspots).

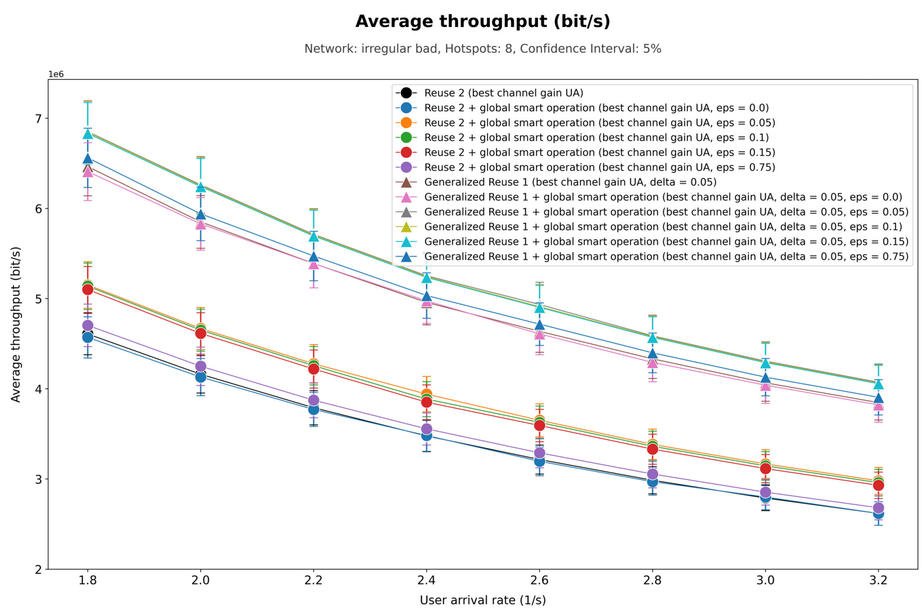

Figure 4.13: Finding the best ϵ for highly irregular network (8 hotspots).

In the 0 hotspot case, we see that Generalized Reuse 1 (light orange line) has better performance than Reuse 2 + SO by roughly 25% (relative to Reuse 2) with $\epsilon = 0.05$ (dark orange line) which is the best performing Reuse 2 + SO ϵ-variant. For 2 and 8 hotspots, Generalized Reuse 1 has better performance than Reuse 2 + SO ($\epsilon = 0.05$) by 30% (relative to Reuse 2). Therefore Generalized Reuse 1 brings better performance at lower complexity than Reuse 2 + SO. In all three figures, Generalized Reuse 1 + SO ($\epsilon = 0.05$) has higher performance than Generalized Reuse 1 by roughly 10% (relative to Reuse 2).

Based on the results, performance peaks at $\epsilon = 0.05$ for 0, 2, and 8 hotspots. Therefore we keep this value of ϵ for the highly irregular network. To summarize, against the baseline Reuse 2, the gains were roughly 45-55% for the highly irregular network with Generalized Reuse 1 + SO, roughly 35-45% with Generalized Reuse 1 alone, and roughly 10-15% with Reuse 2 + SO. The gains are higher in the highly irregular network.

We have only looked at the results for fixed delay so far. Next, we look at the file download results having found the best ϵ.

4.5 File download results

We now present the file download results for the regular, lightly irregular, and highly irregular networks.

4.5.1 Regular network

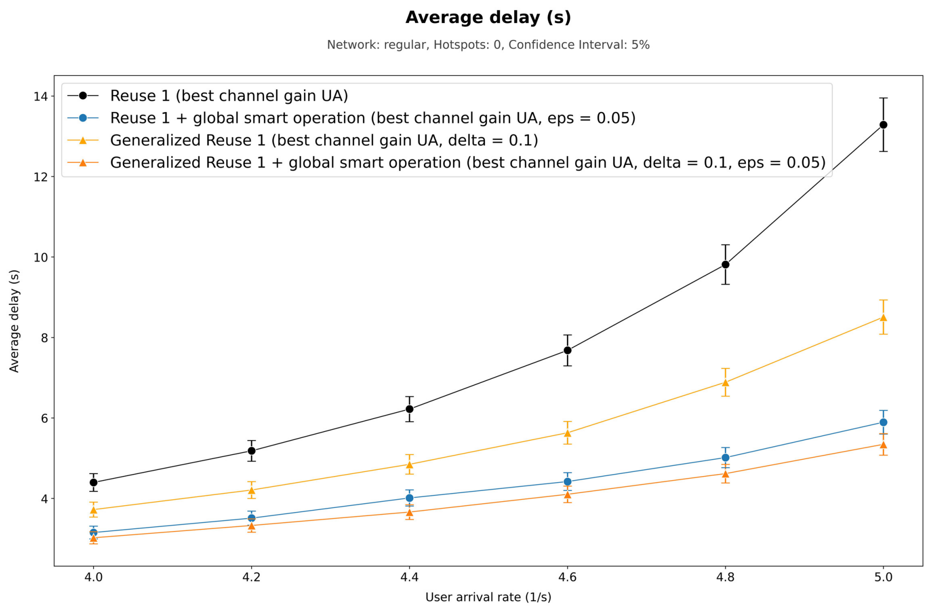

Figure 4.14: Average delay results for regular network (0 hotspot).

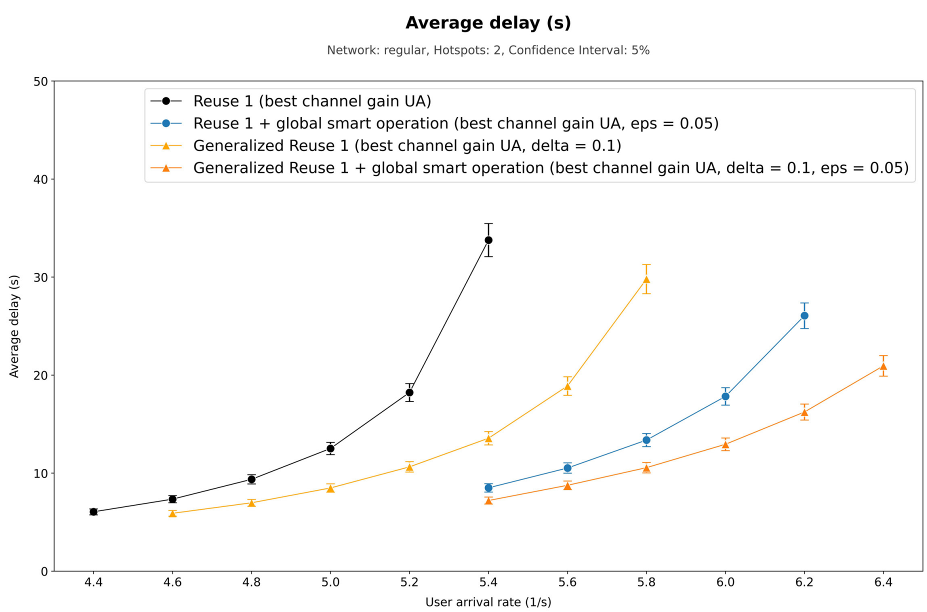

Figure 4.15: Average delay results for regular network (2 hotspots).

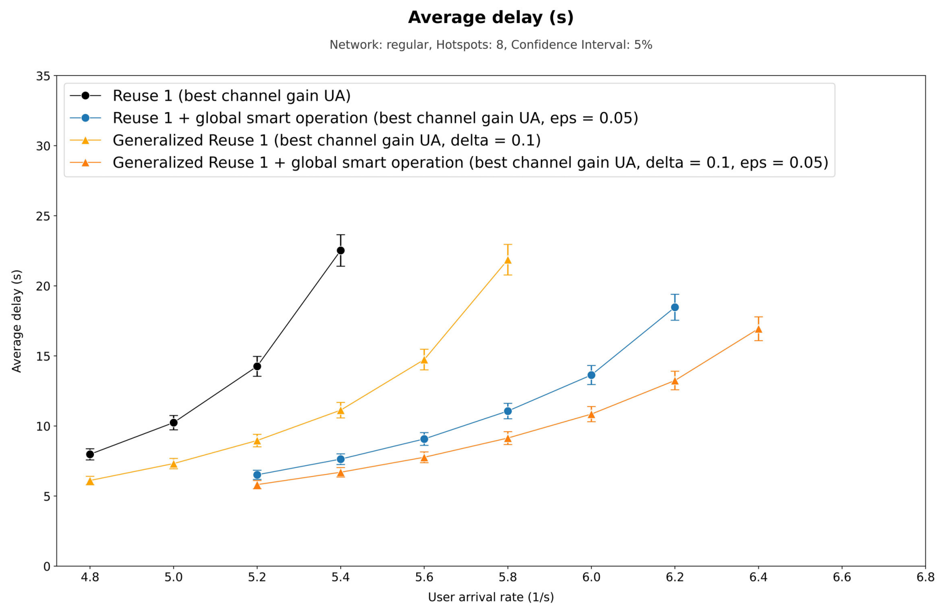

Figure 4.16: Average delay results for regular network (8 hotspots).

In all three figures, Smart Operation significantly improves the average delay for Reuse 1 and Generalized Reuse 1 as seen with the blue and dark orange lines. Reuse 1 + SO does better than Generalized Reuse 1 and performs close to Generalized Reuse 1 + SO. Therefore Reuse 1 + SO is good enough. These insights are different from the fixed delay scenario where Generalized Reuse 1 did better than Reuse 1 + SO.

4.5.2 Lightly irregular network

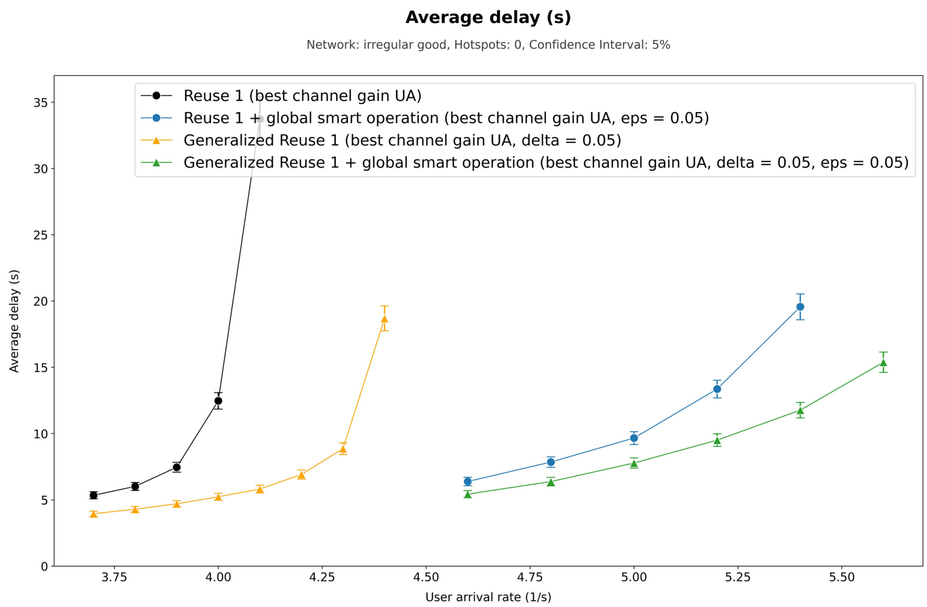

Figure 4.17: Average delay results for lightly irregular network (0 hotspot).

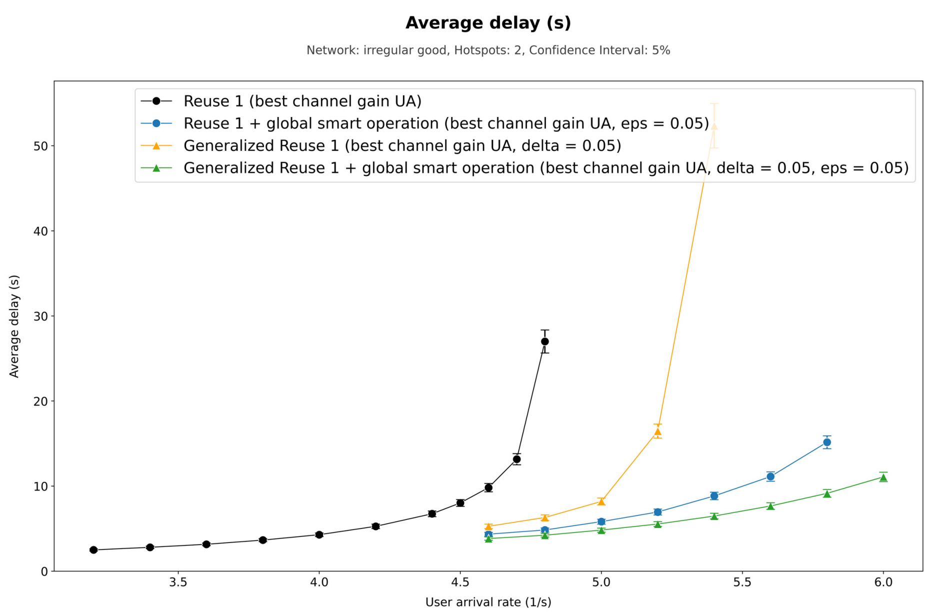

Figure 4.18: Average delay results for lightly irregular network (2 hotspots).

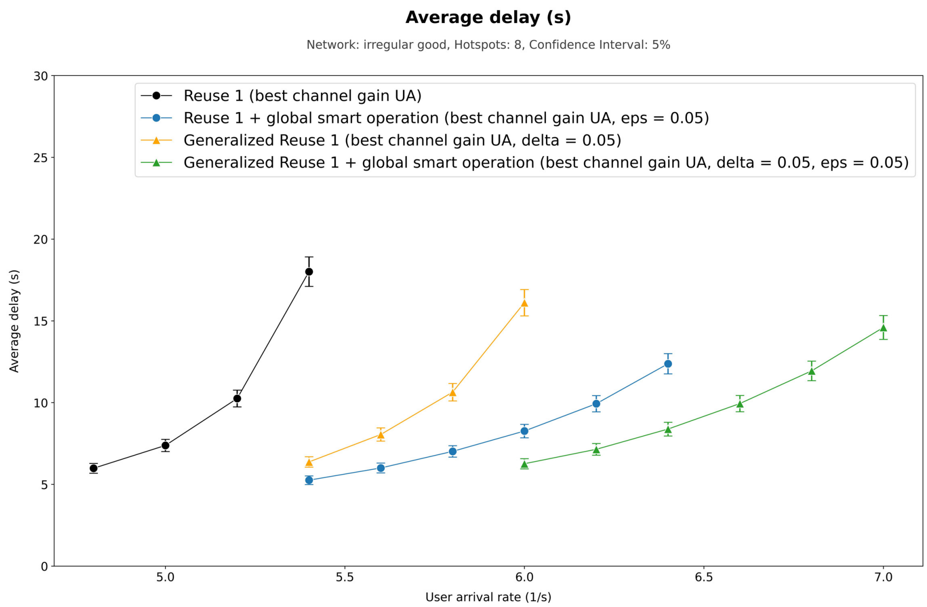

Figure 4.19: Average delay results for lightly irregular network (8 hotspots).

In all three figures, Smart Operation significantly improves the average delay for Reuse 1 and Generalized Reuse 1 as seen with the blue and green lines. Reuse 1 + SO does better than Generalized Reuse 1 and is almost good enough performing similar to Generalized Reuse 1 + SO. These insights are different from the fixed delay scenario where Generalized Reuse 1 did better than Reuse 1 + SO.

4.5.3 Highly irregular network

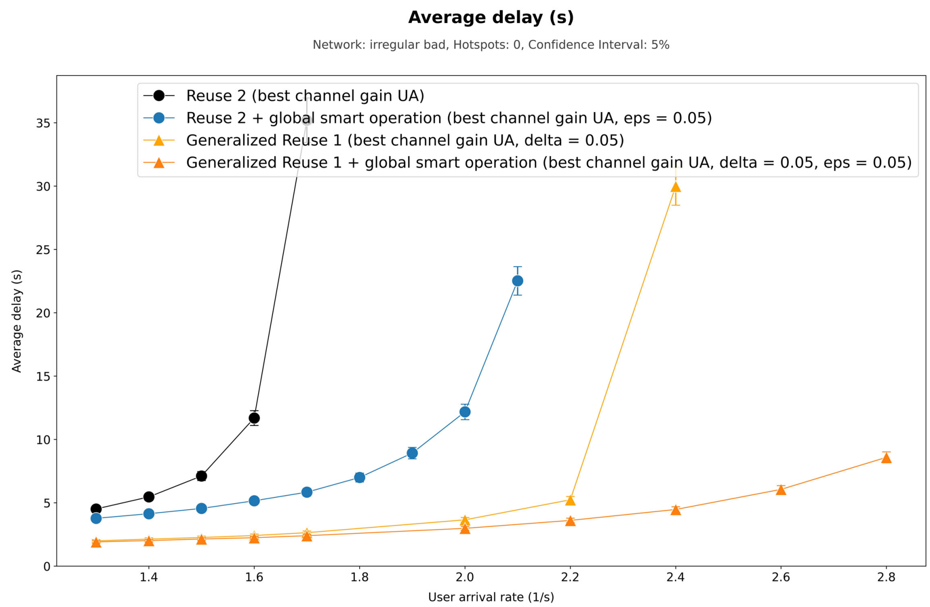

Figure 4.20: Average delay results for highly irregular network (0 hotspot).

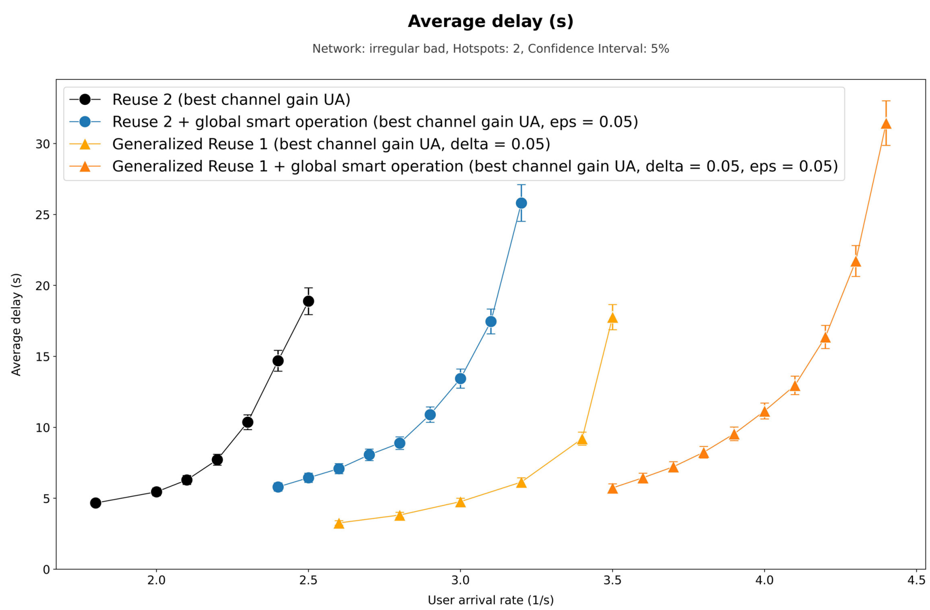

Figure 4.21: Average delay results for highly irregular network (2 hotspots).

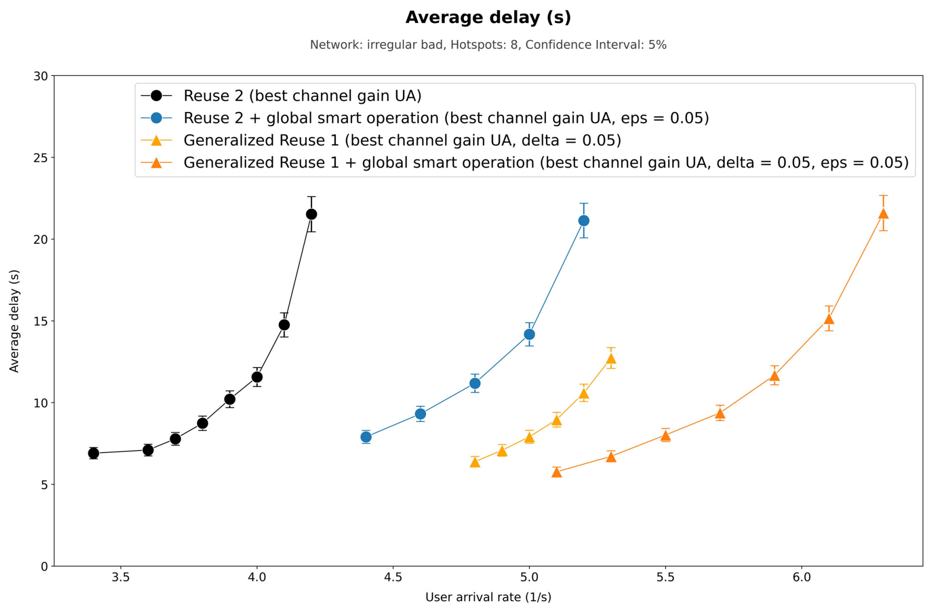

Figure 4.22: Average delay results for highly irregular network (8 hotspots).

In all three figures, Smart Operation significantly improves the average delay for Reuse 2 and Generalized Reuse 1 as seen with the blue and dark orange lines. Generalized Reuse 1 is better than Reuse 2 + SO. Generalized Reuse 1 + SO is the clear winner. This follows the fixed delay scenario where Generalized Reuse 1 also performed better than Reuse 2 + SO.

4.6 Results summary

The results are interesting because in the regular and lightly irregular networks, Generalized Reuse 1 had slightly better performance than Reuse 1 + SO in the fixed delay scenario. However, in the file download scenario, Reuse 1 + SO had significantly better performance than Generalized Reuse 1. Meanwhile for the highly irregular network, Generalized Reuse 1 had significantly better performance than Reuse 2 + SO in the fixed delay and file download scenario. In all scenarios and networks, Generalized Reuse 1 + SO had the best performance.

Why does Reuse 1 + SO perform much better in the file download scenario? The reason is that a user u associated BS j with low SINR stays longer in the network in the file download scenario. This contributes to overcrowding at BS j at which point SO will allocate more subchannels to BS j whereas Generalized Reuse 1 will take no action. However in the fixed delay scenario, user u's impact on the network is lessened because it will depart after Q seconds. This means there is no overcrowding in the fixed delay scenario and hence the benefits of SO are not fully exploited.

In the highly irregular network, Generalized Reuse 1 and Generalized Reuse 1 + SO are the top two performers in the fixed delay and file download scenario. This is due to the fact that BSs in Reuse 2 and Reuse 2 + SO only have access to $M/2$ subchannels.

For regular and lightly irregular networks when looking at performance and complexity, Generalized Reuse 1 is best for the fixed delay scenario, and Reuse 1 + SO is best for the file download scenario. For the highly irregular network, Generalized Reuse 1 is best for both fixed delay and file download scenarios.

Since using Generalized Reuse 1 alone might not be good enough in all scenarios, we look at its SO-variant and now turn to the practical implementation of Generalized Reuse 1 + SO.

4.7 Practical implementation

We now introduce practical implementation considerations for Smart Operation. Notice that the current form of Smart Operation is impractical because it relies on the central entity computing the subchannel allocation for all BSs and user scheduling for all users at every user arrival and departure. We assume for simplicity that the central entity is co-located with the centralized BBUs of the C-RAN. This creates a lot of internal traffic due to the constant exchange of data between the BBUs and central entity, and in practice, operators will not want to update the subchannel allocation for all BSs just because there is a new user entering or leaving the network.

We propose a practical implementation where the BS subchannel allocations are only updated periodically. Every T seconds, the BBUs send the instantaneous user rates to the central entity to perform global BS subchannel allocation and user scheduling. Then the central entity sends the BS subchannel allocations back to the BBUs. The result is that for the next T seconds, the BBUs will perform local user scheduling knowing the BS subchannel allocations. This significantly reduces the exchange of data between the BBUs and central entity but it relies on a periodic snapshot.

For Generalized Reuse 1 + Smart Operation Periodic Allocation, we solve the global BS subchannel allocation and user scheduling problem $\mathcal{P}_{\text{generalized\_reuse1\_SO}}$ every T seconds, and keep the computed BS subchannel allocations (i.e., the $k(l)$'s) for the next T seconds. This allows us to perform local user scheduling for the next T seconds. The local scheduling optimization problem $\mathcal{P}_{\text{generalized\_reuse1\_SO\_scheduling}}$ is then solved at each BS j every time there is a departure or arrival given the sub-band sizes $k(l)$, and per subchannel rates $\gamma_u(l), \forall u \in \mathcal{U}_j, \forall l \in \{1, \ldots, 2J\}$:

$$\mathcal{P}_{\text{generalized\_reuse1\_SO\_scheduling}} : \max_{(\lambda_u),(\alpha_u(l))} \sum_{u \in \mathcal{U}_j} \log(\lambda_u) \tag{4.23}$$

$$\lambda_u = \sum_{l=1}^{2J} \alpha_u(l) \cdot \gamma_u(l) \quad \forall u \in \mathcal{U}_j, \tag{4.24}$$

$$\sum_{u \in \mathcal{U}_j} \alpha_u(l) \leq k(l) \quad \forall l \in \{1, \ldots, 2J\} \tag{4.25}$$

$$\alpha_u(l) \geq 0, \lambda_u \geq 0, \forall u \in \mathcal{U}_j, \forall l \in \{1, \ldots, 2J\} \tag{4.26}$$

This approach is simple but has an edge case that occurs when a user arrives at a BS that had no users when $\mathcal{P}_{\text{generalized\_reuse1\_SO}}$ was solved. As a result, its subchannel allocation is unknown. To handle this edge case triggered at a BS, let's call it BS z, it will need to know how many subchannels to use in B_1 and either B_2 (if $z \in \mathcal{J}_1$) or B_3 (if $z \in \mathcal{J}_2$). BS z will be assigned the smallest known subchannel allocation in B_1, and B_2 (if $z \in \mathcal{J}_1$) or B_3 (if $z \in \mathcal{J}_2$). For example in B_1, if the known subchannel allocation is that BS 1 uses 10 subchannels, and BS 2 uses 30 subchannels, then BS z will use 10 subchannels in B_1.

We want to keep the computed BS subchannel allocations for the next T seconds instead of recomputing every time a user arrives and departs the system. Figure 4.23 illustrates the timing of the practical implementation setting.

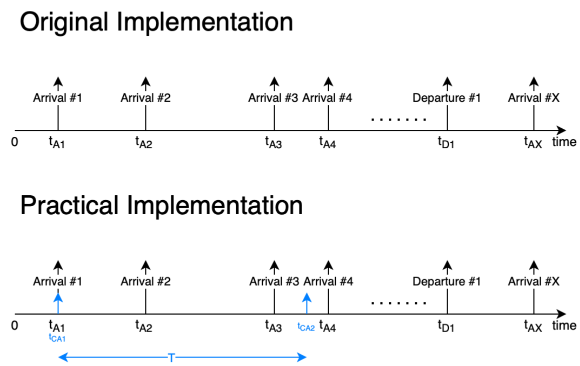

Figure 4.23: Smart Operation implementation (Top: Original. Bottom: Practical).

Let t_{An}, t_{Dn}, and t_{CAn} be the time of the nth arrival, departure and subchannel allocation respectively. Using Figure 4.23 as an example, at time t_{CA1} and t_{CA2}, we do global subchannel allocation and user scheduling. At time t_{A2}, t_{A3}, t_{A4}, and t_{D1}, we do local user scheduling only.

To evaluate the performance of the practical implementation, we simulate two scenarios: fixed delay, and file download. We try 3 different values of T: 10s, 30s, and 60s. The system model parameters are the same as in Table 3.2. The simulation parameters are the same as in Tables 2.1 and 2.2.

4.7.1 Regular network

Fixed delay

The results for the fixed delay scenario are shown in Figures 4.24, 4.25, and 4.26 for 0, 2, and 8 hotspots and the gains are summarized in Table 4.1 where Reuse 1 with EP per subchannel is the baseline.

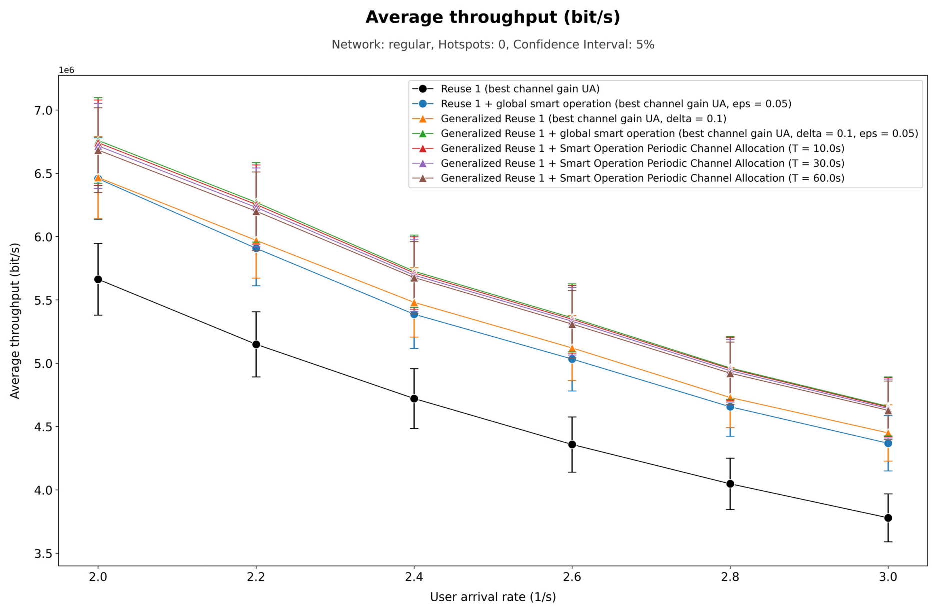

Figure 4.24: Average throughput for regular network (0 hotspot).

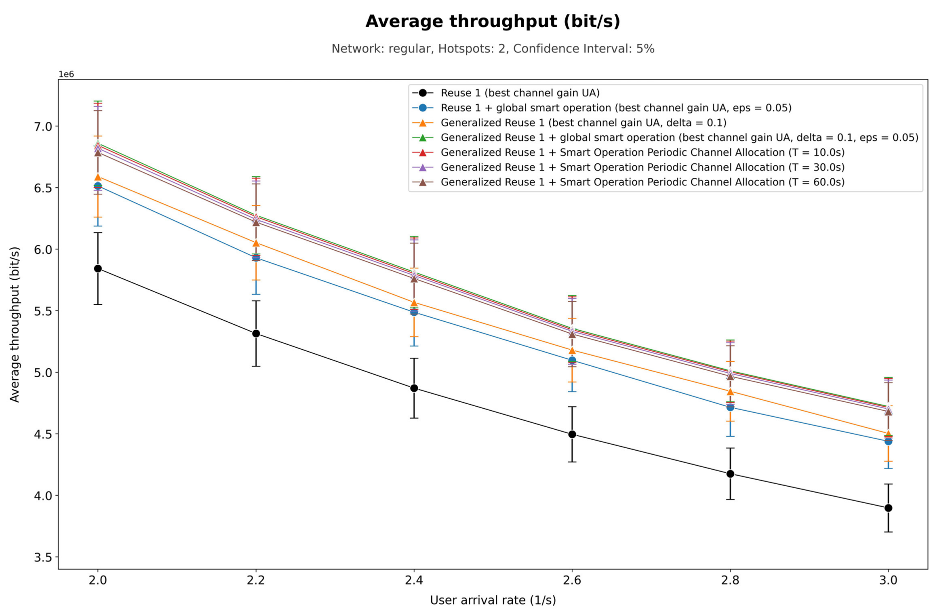

Figure 4.25: Average throughput for regular network (2 hotspots).

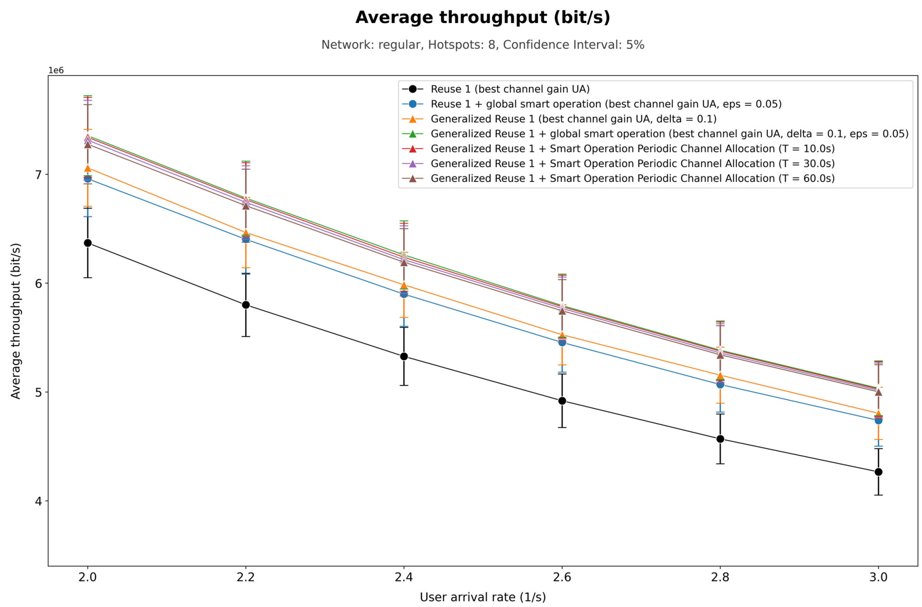

Figure 4.26: Average throughput for regular network (8 hotspots).

The main comment is that the impact of T is minimal but it is because the subchannel gains are time-invariant and users are fixed. If they were time-variant, we would expect to see SO periodic allocation perform worse.

Table 4.1: Gains for regular network with Smart Operation ($\epsilon = 0.05$).

	User arrival rate λ (1/s)					
Case	2.0	2.2	2.4	2.6	2.8	3.0
0 hotspot						
R1 + SO	1.140338	1.147199	1.141007	1.154822	1.150295	1.155703
GR1	1.142021	1.159446	1.160871	1.174973	1.168345	1.177413
GR1 + SO	1.193636	1.217744	1.212927	1.229602	1.226072	1.232884
GR1 + SO, T = 10s	1.190441	1.214385	1.210113	1.226952	1.224308	1.231062
GR1 + SO, T = 30s	1.185963	1.209925	1.206325	1.223325	1.220734	1.228410
GR1 + SO, T = 60s	1.180168	1.204080	1.202339	1.218159	1.215799	1.224522
2 hotspots						
R1 + SO	1.114848	1.115818	1.126589	1.133740	1.129192	1.138801
GR1	1.127850	1.138913	1.143027	1.152146	1.160497	1.155147
GR1 + SO	1.174135	1.180815	1.193571	1.191322	1.200239	1.211360
GR1 + SO, T = 10s	1.171259	1.178493	1.191025	1.188925	1.198285	1.209250
GR1 + SO, T = 30s	1.167176	1.174470	1.187893	1.185940	1.195046	1.206116
GR1 + SO, T = 60s	1.161468	1.170296	1.182801	1.181153	1.189645	1.200916
8 hotspots						
R1 + SO	1.092582	1.103776	1.107300	1.108832	1.109276	1.110775
GR1	1.108335	1.114536	1.123411	1.123241	1.128055	1.126067
GR1 + SO	1.154742	1.169087	1.174975	1.177713	1.178260	1.180113
GR1 + SO, T = 10s	1.152375	1.166708	1.170945	1.175631	1.176376	1.178274
GR1 + SO, T = 30s	1.148204	1.162232	1.166799	1.172371	1.172833	1.175610
GR1 + SO, T = 60s	1.142370	1.157106	1.162364	1.168014	1.169078	1.172363

We see that periodically updating the BS subchannel allocations in Smart Operation works well with almost no drop in performance. This makes sense because users stay for 60 seconds which keeps the relative number of users at the BSs consistent.

File download

The results for 0, 2, and 8 hotspots are shown in Figures 4.27, 4.28, 4.27 for practical Generalized Reuse 1 + SO where lower curves indicate better performance.

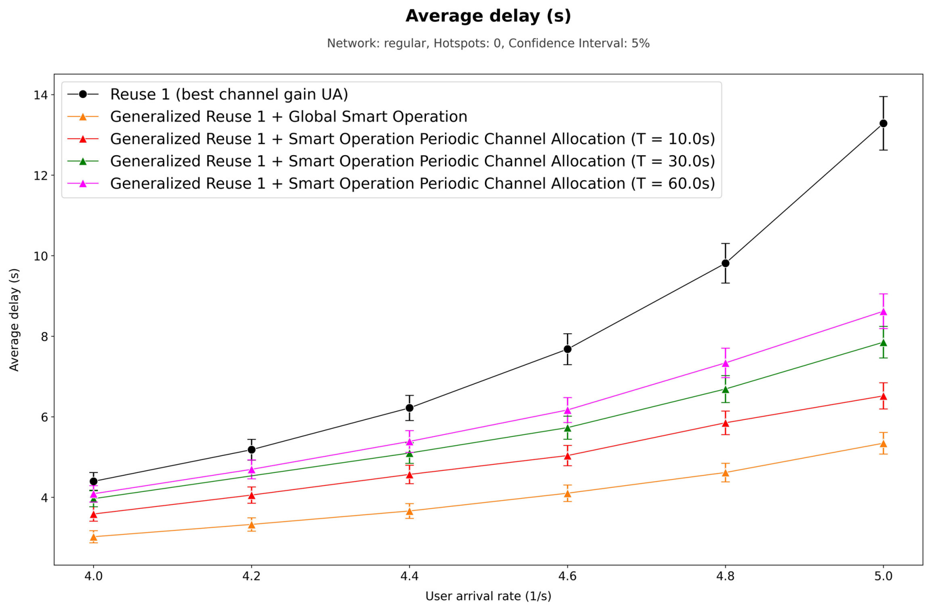

Figure 4.27: Average delay for practical Generalized Reuse 1 + SO in regular network (0 hotspot).

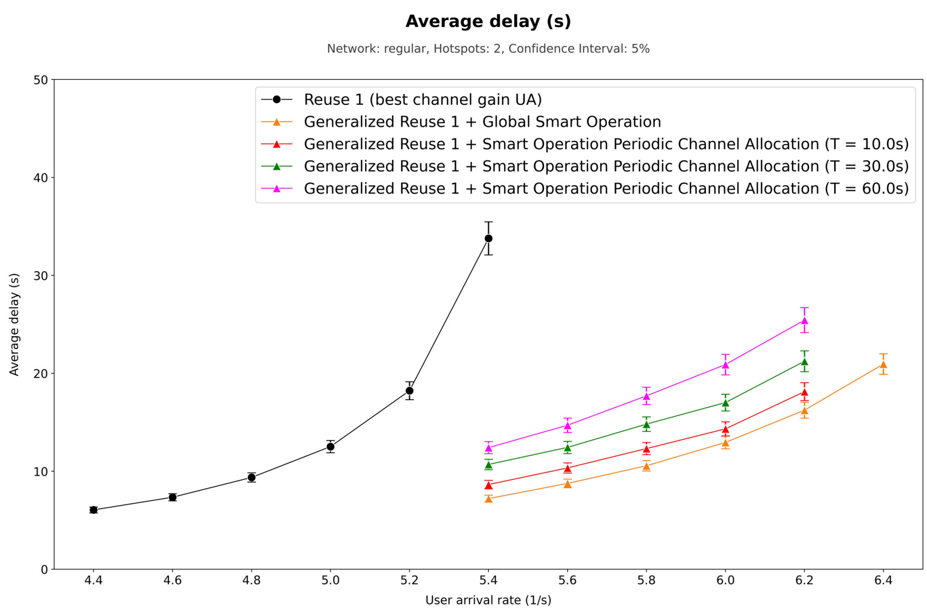

Figure 4.28: Average delay for practical Generalized Reuse 1 + SO in regular network (2 hotspots).

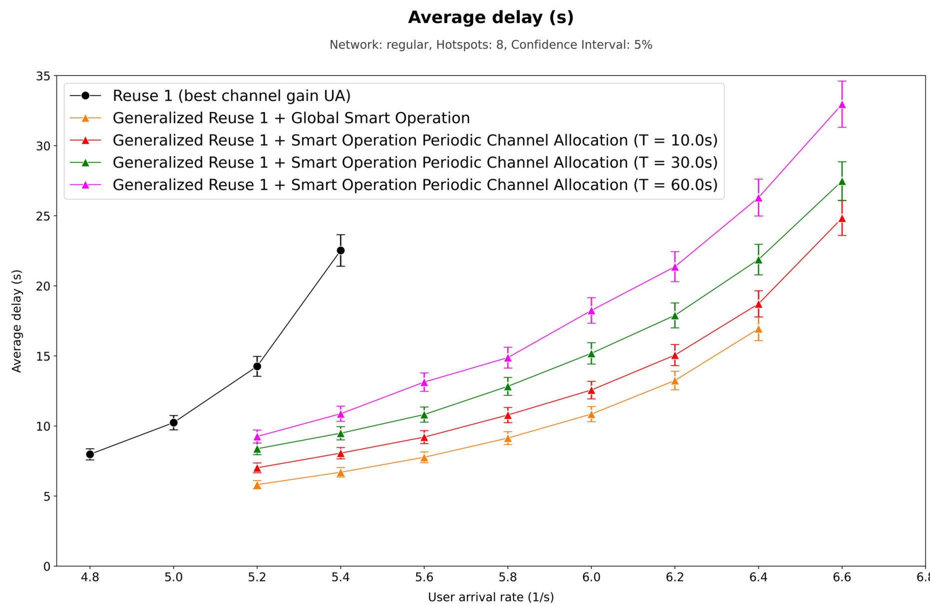

Figure 4.29: Average delay for practical Generalized Reuse 1 + SO in regular network (8 hotspots).

In all three figures, the practical implementation still performs significantly better than Reuse 1. As expected, the lowest periodicity performs best because it quickly adapts to the highly dynamic file download scenario.

4.7.2 Lightly irregular network

Fixed delay

The results for the fixed delay scenario are shown in Figures 4.30, 4.31, and 4.32, and the gains are summarized in Table 4.2 where Reuse 1 with EP per subchannel is the baseline.

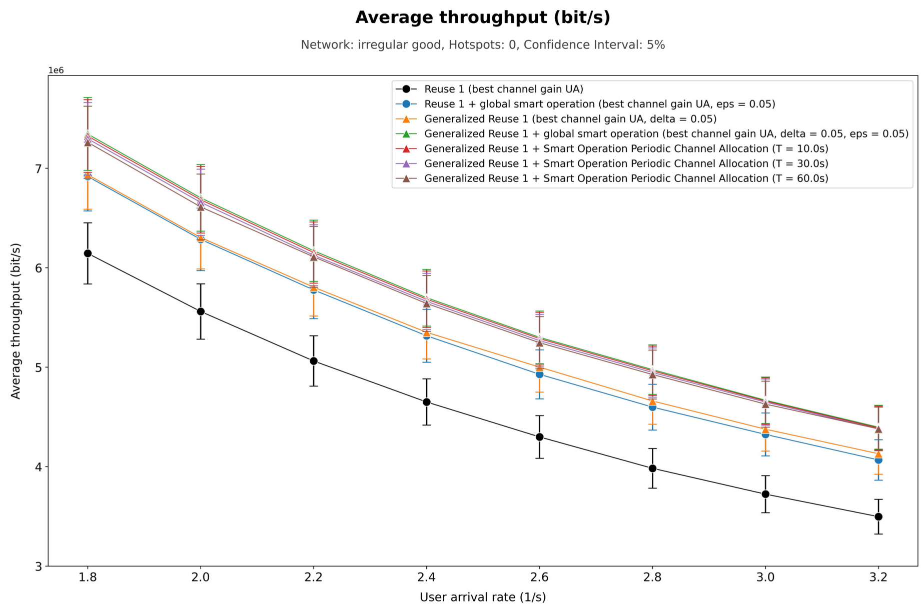

Figure 4.30: Average throughput for lightly irregular network (0 hotspot).

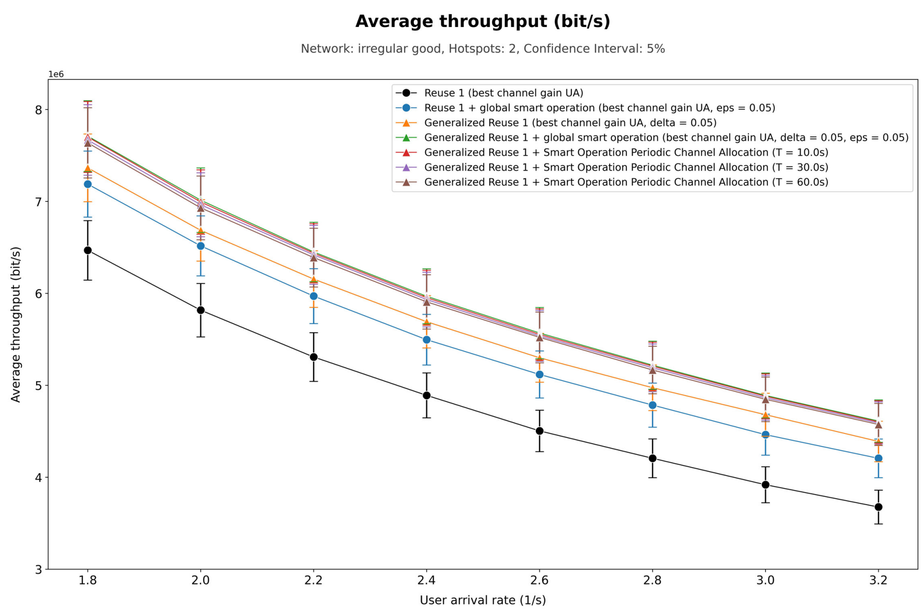

Figure 4.31: Average throughput for lightly irregular network (2 hotspots).

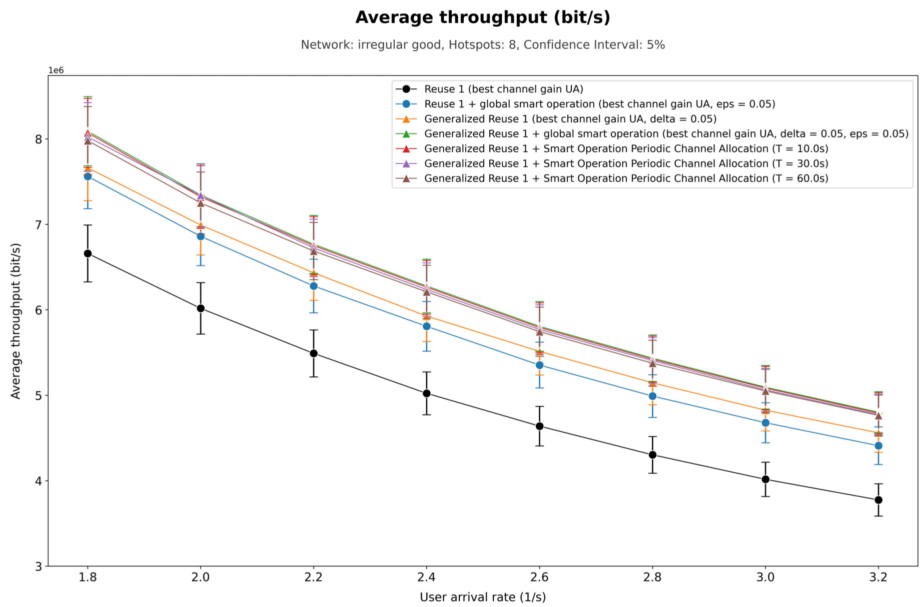

Figure 4.32: Average throughput for lightly irregular network (8 hotspots).

Again, we see that the impact of T is minimal because the subchannel gains are time-invariant and users are fixed.

Table 4.2: Gains for lightly irregular network with Smart Operation ($\epsilon = 0.05$).

Case	User arrival rate λ (1/s) 1.8	2.0	2.2	2.4	2.6	2.8	3.0	3.2
0 hotspot								
R1 + SO	1.1258	1.1303	1.1411	1.1431	1.1463	1.1544	1.1612	1.1630
GR1	1.1287	1.1336	1.1465	1.1506	1.1632	1.1699	1.1753	1.1809
GR1 + SO	1.1952	1.2054	1.2188	1.2254	1.2328	1.2490	1.2534	1.2571
GR1 + SO, T = 10s	1.1919	1.2020	1.2153	1.2221	1.2299	1.2461	1.2513	1.2548
GR1 + SO, T = 30s	1.1874	1.1973	1.2100	1.2174	1.2251	1.2418	1.2485	1.2522
GR1 + SO, T = 60s	1.1817	1.1890	1.2067	1.2128	1.22036	1.2367	1.2430	1.2522
2 hotspots								
R1 + SO	1.1113	1.1202	1.1247	1.1238	1.1362	1.1375	1.1390	1.1440
GR1	1.1386	1.1492	1.1596	1.1637	1.1764	1.1824	1.1944	1.1940
GR1 + SO	1.1919	1.2056	1.2151	1.2203	1.2362	1.2407	1.2478	1.2543
GR1 + SO, T = 10s	1.1905	1.2023	1.2126	1.2172	1.2329	1.2381	1.2456	1.2519
GR1 + SO, T = 30s	1.1855	1.1971	1.2092	1.2131	1.2292	1.2339	1.2414	1.2486
GR1 + SO, T = 60s	1.1806	1.1913	1.2037	1.2079	1.2257	1.2282	1.2371	1.2443
8 hotspots								
R1 + SO	1.1353	1.1401	1.1437	1.1561	1.1539	1.1597	1.1648	1.1680
GR1	1.1504	1.1620	1.1717	1.1800	1.1885	1.1958	1.2013	1.2079
GR1 + SO	1.2148	1.2202	1.2325	1.2501	1.2516	1.2628	1.2683	1.2717
GR1 + SO, T = 10s	1.2118	1.2168	1.2297	1.2472	1.2487	1.2599	1.2658	1.2689
GR1 + SO, T = 30s	1.2048	1.2197	1.2248	1.2418	1.2438	1.2561	1.2607	1.2649
GR1 + SO, T = 60s	1.1983	1.2050	1.2182	1.2365	1.2383	1.2492	1.2575	1.2618

File download

The results for 0, 2, and 8 hotspots are shown in Figures 4.33, 4.34, 4.35 for practical Generalized Reuse 1 + SO where lower curves indicate better performance.

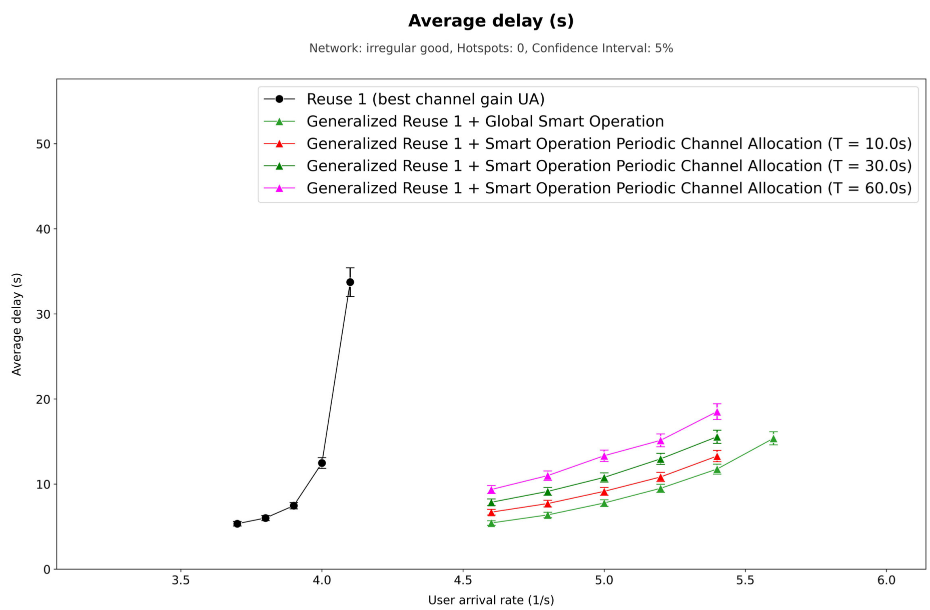

Figure 4.33: Average delay for practical Generalized Reuse 1 + SO in lightly irregular network (0 hotspot).

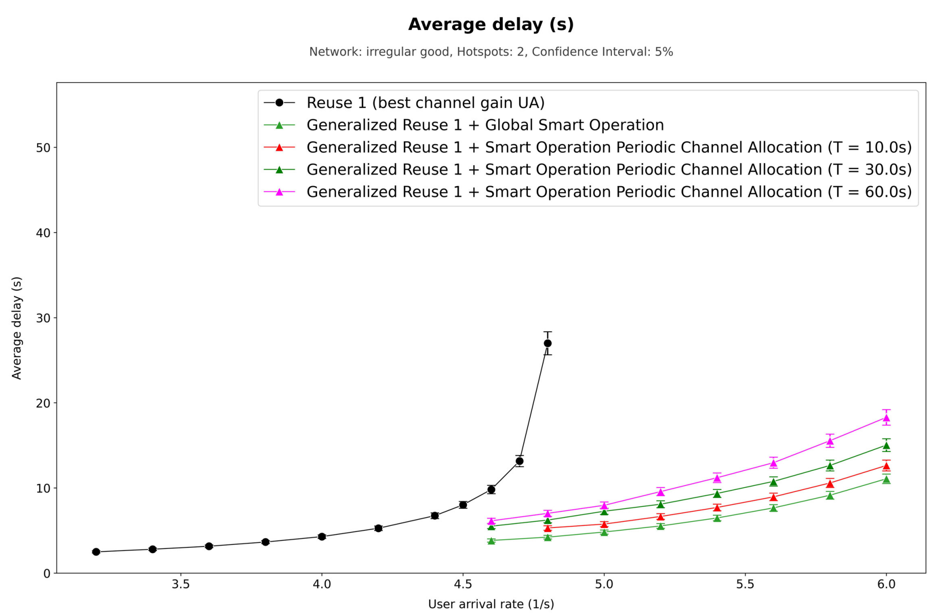

Figure 4.34: Average delay for practical Generalized Reuse 1 + SO in lightly irregular network (2 hotspots).

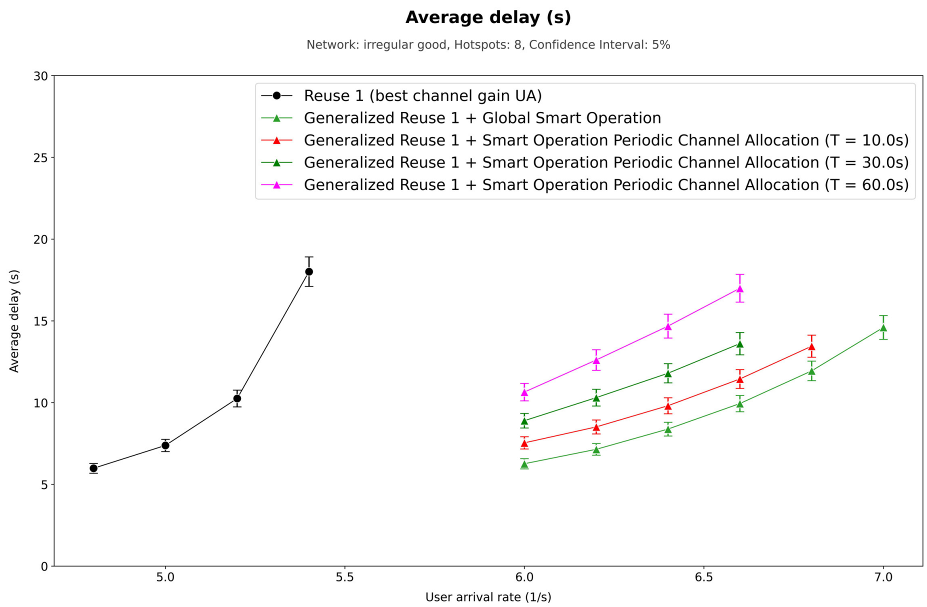

Figure 4.35: Average delay for practical Generalized Reuse 1 + SO in lightly irregular network (8 hotspots).

In all three figures, the practical implementation still performs significantly better than Reuse 1. As expected, the lowest periodicity performs best because it quickly adapts to the highly dynamic file download scenario.

4.7.3 Highly irregular network

Fixed delay

The results for the fixed delay scenario are shown in Figures 4.36, 4.37, and 4.38, and the gains are summarized in Table 4.3 where Reuse 2 with EP per subchannel is the baseline.

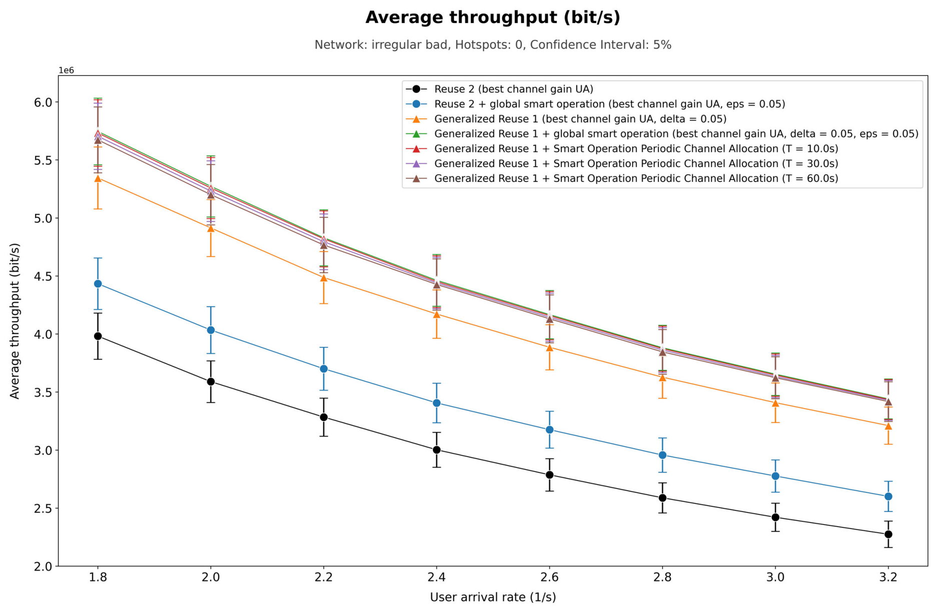

Figure 4.36: Average throughput for highly irregular network (0 hotspot).

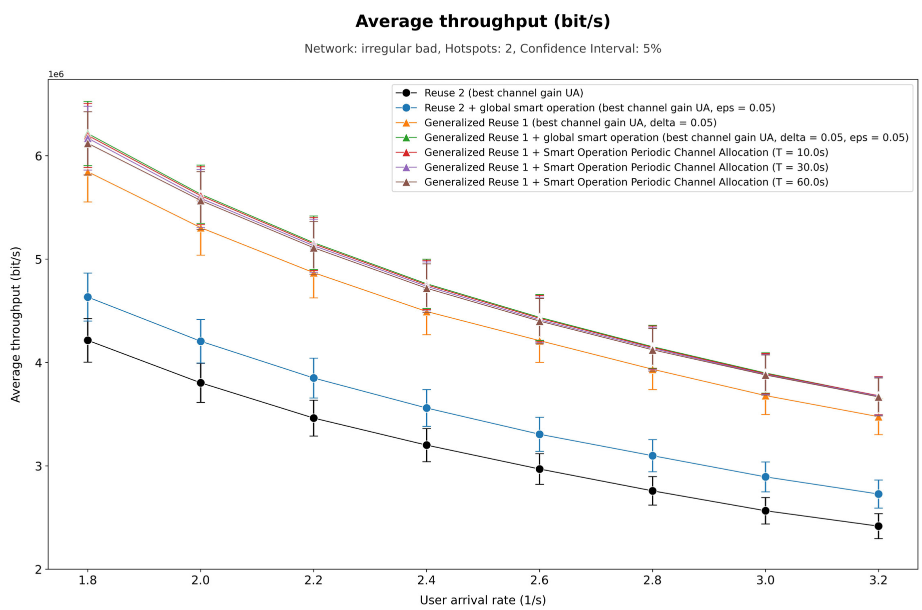

Figure 4.37: Average throughput for highly irregular network (2 hotspots).

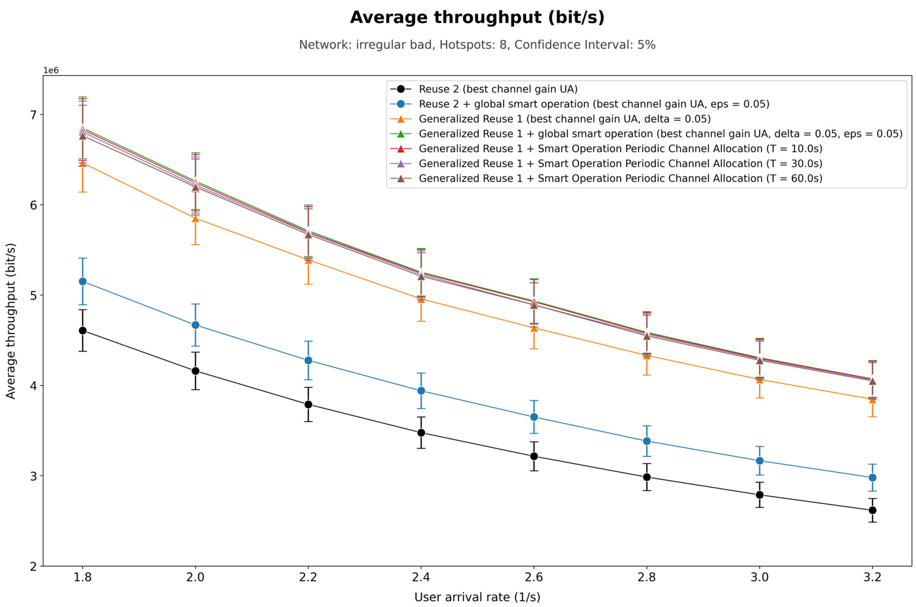

Figure 4.38: Average throughput for highly irregular network (8 hotspots).

Again, we see that the impact of T is minimal because the subchannel gains are time-invariant and users are fixed.

Table 4.3: Gains for highly irregular network with Smart Operation ($\epsilon = 0.05$).

	User arrival rate λ (1/s)							
Case	1.8	2.0	2.2	2.4	2.6	2.8	3.0	3.2
0 hotspot								
R2 + SO	1.1134	1.1238	1.1268	1.1344	1.1395	1.1423	1.1468	1.1434
GR1	1.3422	1.3689	1.3662	1.3895	1.3943	1.4015	1.4079	1.4115
GR1 + SO	1.4429	1.4688	1.4704	1.4861	1.4953	1.4993	1.5093	1.5125
GR1 + SO, T = 10s	1.4396	1.4647	1.4676	1.4826	1.4921	1.4965	1.5060	1.5104
GR1 + SO, T = 30s	1.4325	1.4574	1.4600	1.4787	1.4873	1.4918	1.5010	1.5073
GR1 + SO, T = 60s	1.4247	1.4488	1.4515	1.4743	1.4823	1.4856	1.4967	1.5025
2 hotspots								
R2 + SO	1.0993	1.1057	1.1119	1.1121	1.1132	1.1232	1.1277	1.1285
GR1	1.3870	1.3946	1.4062	1.4038	1.4182	1.4263	1.4341	1.4382
GR1 + SO	1.4747	1.4797	1.4899	1.4877	1.4941	1.5054	1.5193	1.5212
GR1 + SO, T = 10s	1.4704	1.4760	1.4865	1.4845	1.4909	1.5028	1.5167	1.5222
GR1 + SO, T = 30s	1.4641	1.4692	1.4815	1.4799	1.4859	1.4991	1.5139	1.5205
GR1 + SO, T = 60s	1.4523	1.4637	1.4757	1.4741	1.4817	1.4945	1.5117	1.5173
8 hotspots								
R2 + SO	1.1179	1.1220	1.1285	1.1332	1.1353	1.1333	1.1354	1.1383
GR1	1.4026	1.4060	1.4218	1.4255	1.4419	1.4507	1.4579	1.4690
GR1 + SO	1.4867	1.5047	1.5070	1.5105	1.5345	1.5363	1.5441	1.5554
GR1 + SO, T = 10s	1.4826	1.5007	1.5031	1.5079	1.5318	1.5332	1.5416	1.5538
GR1 + SO, T = 30s	1.4768	1.4941	1.5015	1.5036	1.5211	1.5290	1.5386	1.5513
GR1 + SO, T = 60s	1.4679	1.4891	1.4963	1.4979	1.5210	1.5234	1.5338	1.5468

File download

The results for 0, 2, and 8 hotspots are shown in Figures 4.39, 4.40, 4.41 for practical Generalized Reuse 1 + SO.

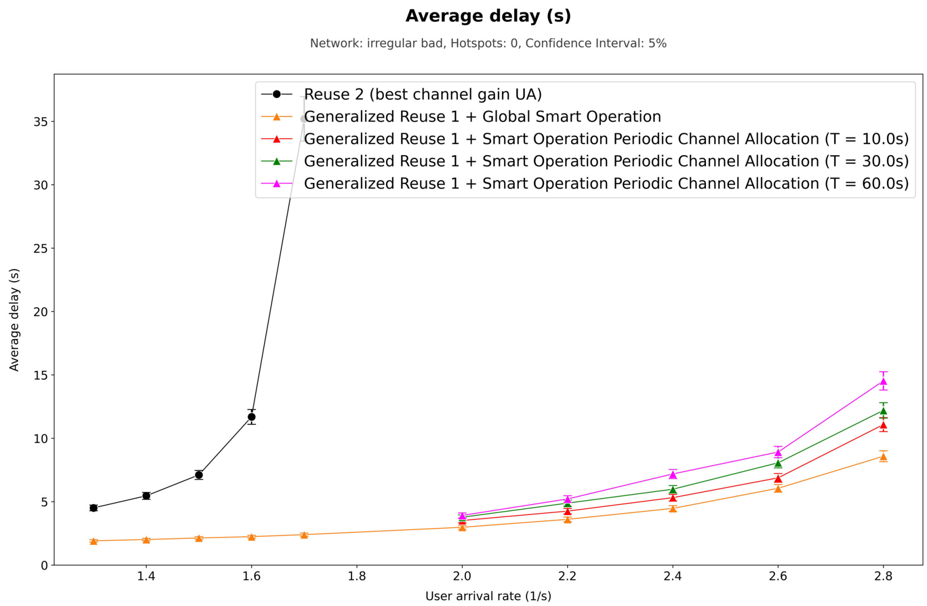

Figure 4.39: Average delay for practical Generalized Reuse 1 + SO in highly irregular network (0 hotspot).

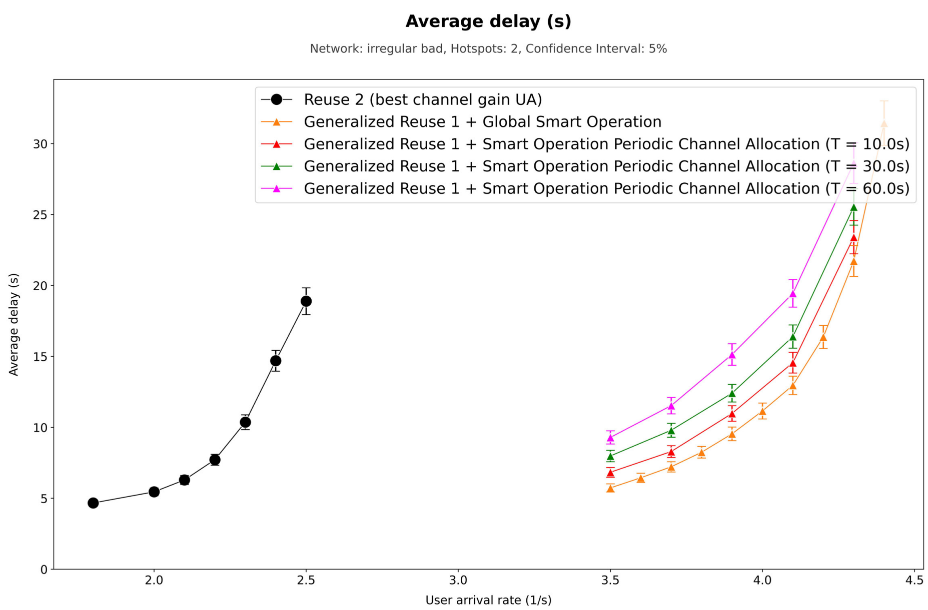

Figure 4.40: Average delay for practical Generalized Reuse 1 + SO in highly irregular network (2 hotspots).

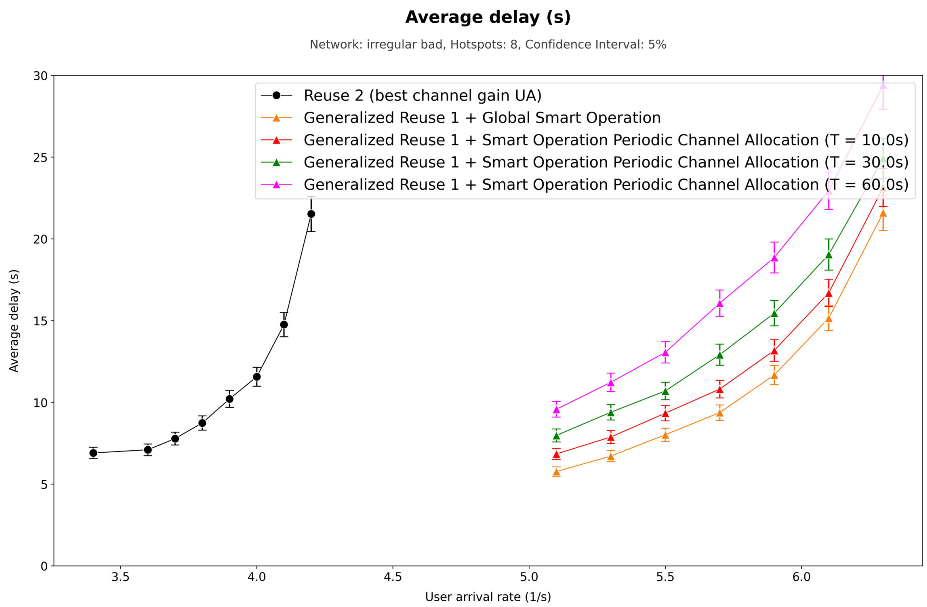

Figure 4.41: Average delay for practical Generalized Reuse 1 + SO in highly irregular network (8 hotspots).

In all three figures, the practical implementation still performs significantly better than Reuse 2. As expected, the lowest periodicity performs best because it quickly adapts to the highly dynamic file download scenario.

4.7.4 Results summary

The practical implementation for SO works well. There is very little drop off in performance in the fixed delay scenario for all networks and hotspot configurations. In the file download scenario, there is a noticeable drop in performance but it still does better than the baseline Reuse 1 in the regular and lightly irregular networks, and Reuse 2 in the highly irregular network.

Chapter 5

Conclusions

We re-visited planning and operation in cellular networks by looking at regular, lightly irregular, and highly irregular networks. In planning, we proposed Generalized Reuse 1, a simple power map which improved performance and coverage in the regular and lightly irregular networks with respect to Reuse 1. In the highly irregular network, it significantly improved performance while only slightly decreasing coverage with respect to Reuse 2. In operation, we looked at further increasing the performance of the network by taking into account the instantaneous number of users at the base stations in the presence of hotspots. We proposed different Smart Operation variants for the benchmarks and Generalized Reuse 1.

The results for the regular and lightly irregular networks showed that Generalized Reuse 1 had slightly better performance than Reuse 1 + Smart Operation in the fixed delay scenario. However, Reuse 1 + Smart Operation had significantly better performance in the file download scenario. Meanwhile in the highly irregular network, Generalized Reuse 1 performed better than Reuse 2 + Smart Operation in both fixed delay and file download scenarios. As a result, although we would have liked to use Generalized Reuse 1 for all scenarios since it is simple, we realized that in some cases, Smart Operation was needed to achieve better performance. Hence we proposed a practical implementation of Smart Operation.

The gains in performance can be very significant depending on the scenario (fixed delay or file download), network, and the existence of hotspots. For example, Generalized Reuse 1 for the highly irregular network, showed huge gains (35-45%) in the fixed delay scenario compared to other networks (up to 18%), and its gains were highest in the 8 hotspot case. In another example, in the file download scenario for the regular and lightly irregular networks, Reuse 1 + Smart Operation performed significantly better than Generalized Reuse 1. However, Generalized Reuse 1 performed slightly better in the fixed delay case.

References

[1] Minos for ampl. URL: https://ampl.com/products/solvers/solvers-we-sell/minos/.

[2] 3rd generation partnership project; technical specification group radio access network; evolved universal terrestrial radio access (e-utra); user equipment (ue) procedures in idle mode (release 8), dec 2007. URL: http://www.3gpp.org/ftp/Specs/archive/36_series/36.304/36304-800.zip.

[3] Importance of serving cell association in hetnets (r1-100701). Technical report, 3GPP, jan 2010.

[4] 3rd generation partnership project; technical specification group radio access network; evolved universal terrestrial radio access (e-utra); user equipment (ue) procedures in idle mode (release 10), jun 2012. URL: http://www.3gpp.org/ftp/Specs/archive/36_series/36.304/36304-a60.zip.

[5] 3rd generation partnership project; technical specification group radio access network; evolved universal terrestrial radio access (e-utra); user equipment (ue) procedures in idle mode (release 16), jul 2020. URL: http://www.3gpp.org/ftp//Specs/archive/36_series/36.304/36304-g10.zip.

[6] A. Adejo, J. Hussein, and S. Boussakta. Optimal transmit power configuration for soft frequency reuse in irregular cellular networks. In *2017 Ninth International Conference on Ubiquitous and Future Networks (ICUFN)*, pages 711–713, 2017.

[7] Vittoria Mignone Alberto Morello Assunta De Vita, Rossella Gaffoglio. Application of the wib concept to dvb-t2. *n/a*, jul 2014.

[8] G. Boudreau, J. Panicker, N. Guo, R. Chang, N. Wang, and S. Vrzic. Interference coordination and cancellation for 4g networks. *IEEE Communications Magazine*, 47(4):74–81, 2009.

[9] S. V. Budihal and R. M. Banakar. Evidence-based dynamic radio resource allocation to mitigate inter cell interference employing cooperative communication. *IET Communications*, 14(12):1848–1857, 2020.

[10] U. Challita, L. Dong, and W. Saad. Proactive resource management for lte in unlicensed spectrum: A deep learning perspective. *IEEE Transactions on Wireless Communications*, 17(7):4674–4689, 2018.

[11] H. Chang and I. Rubin. Optimal downlink and uplink fractional frequency reuse in cellular wireless networks. *IEEE Transactions on Vehicular Technology*, 65(4):2295–2308, 2016.

[12] S. Chang, S. Kim, and J. P. Choi. The optimal distance threshold for fractional frequency reuse in size-scalable networks. *IEEE Transactions on Aerospace and Electronic Systems*, 56(1):527–546, 2020.

[13] L. Chen and D. Yuan. Soft frequency reuse in large networks with irregular cell pattern: How much gain to expect? In *2009 IEEE 20th International Symposium on Personal, Indoor and Mobile Radio Communications*, pages 1467–1471, 2009.

[14] L. Chen and D. Yuan. Beyond conventional fractional frequency reuse for networks with irregular cell layout: An optimization approach and performance evaluation. In *2010 The 5th Annual ICST Wireless Internet Conference (WICON)*, pages 1–7, 2010.

[15] K. Doppler, C. Wijting, and K. Valkealahti. Interference aware scheduling for soft frequency reuse. In *VTC Spring 2009 - IEEE 69th Vehicular Technology Conference*, pages 1–5, 2009.

[16] Mohamed Elwekeil, Masoud Alghoniemy, Osamu Muta, Adel B Abdel-Rahman, Haris Gacanin, and Hiroshi Furukawa. Performance evaluation of an adaptive self-organizing frequency reuse approach for ofdma downlink. *Wireless networks*, 25(2):507–519, 2019.

[17] D. Fooladivanda and C. Rosenberg. Joint resource allocation and user association for heterogeneous wireless cellular networks. *IEEE Transactions on Wireless Communications*, 12(1):248–257, 2013.

[18] D. González G., H. Hakula, A. Rasila, and J. Hämäläinen. Spatial mappings for planning and optimization of cellular networks. *IEEE/ACM Transactions on Networking*, 26(1):175–188, 2018.

[19] Weisi Guo, Siyi Wang, Xiaoli Chu, Jiming Chen, Hui Song, and Jie Zhang. Automated small-cell deployment for heterogeneous cellular networks. *Communications Magazine, IEEE*, 51, 07 2013. doi:10.1109/MCOM.2013.6515046.

[20] F. Hamdani, A. Maurizka, M. M. Ulfah, and Iskandar. Power ratio evaluation for soft frequency reuse technique in lte-a heterogeneous networks. In *2017 11th International Conference on Telecommunication Systems Services and Applications (TSSA)*, pages 1–5, 2017.

[21] Harri Holma, Antti Toskala, Takehiro Nakamura, and Tommi Uitto. *Introduction*, chapter 1, pages 1–11. John Wiley & Sons, Ltd, 2019. URL: https://onlinelibrary.wiley.com/doi/abs/10.1002/9781119236306.ch1, arXiv:https://onlinelibrary.wiley.com/doi/pdf/10.1002/9781119236306.ch1, doi:10.1002/9781119236306.ch1.

[22] A. Idris, S. S. Md Yusoff, N. Fadzlina Naim, S. S. Sarnin, M. Kassim, and M. D. Rozaini. Reduction of inter-cell interference (ici) by fractional frequency reuse (ffr) in orthogonal frequency division multiple access (ofdma). In *2019 International Conference on Information and Communications Technology (ICOIACT)*, pages 123–128, 2019.

[23] Jianfeng Ding, Lingge Jiang, and Chen He. Spectrum allocation and interference alignment for fractional frequency reuse based hetnets. In *2015 10th International Conference on Communications and Networking in China (ChinaCom)*, pages 205–210, 2015.

[24] Frank Kelly. Charging and rate control for elastic traffic. *European Transactions on Telecommunications*, 8(1):33–37, 1997. URL: https://onlinelibrary.wiley.com/doi/abs/10.1002/ett.4460080106, arXiv:https://onlinelibrary.wiley.com/doi/pdf/10.1002/ett.4460080106, doi:10.1002/ett.4460080106.

[25] Mamoru Machida Kimio Watanabe. Outdoor lte infrastructure equipment (enodeb). Technical report, Fujitsu, jan 2012.

[26] T. Kudo and T. Ohtsuki. Cell selection using distributed q-learning in heterogeneous networks. In *2013 Asia-Pacific Signal and Information Processing Association Annual Summit and Conference*, pages 1–6, 2013.

[27] J. Li, N. B. Shroff, and E. K. P. Chong. A reduced-power channel reuse scheme for wireless packet cellular networks. *IEEE/ACM Transactions on Networking*, 7(6):818–832, 1999.

[28] Hector Menendez. Enabling c-ran and transport convergence with time-sensitive networking. *n/a*, jul 2019.

[29] T. D. Novlan, R. K. Ganti, A. Ghosh, and J. G. Andrews. Analytical evaluation of fractional frequency reuse for ofdma cellular networks. *IEEE Transactions on Wireless Communications*, 10(12):4294–4305, 2011.

[30] Thomas Novlan, Radha Ganti, Arunabha Ghosh, and Jeffrey Andrews. Analytical evaluation of fractional frequency reuse for heterogeneous cellular networks. *Communications, IEEE Transactions on*, 60:2029–2039, 07 2012. doi:10.1109/TCOMM.2012.061112.110477.

[31] European Communications Office. *SEAMCAT Handbook*, jun 2017.

[32] Greger Blennerud Jason Kyohun Shim Brian Arendse Ahmad Husseini Per Lindberg Kati Öhman Peter Jonsson, Stephen Carson. Ericsson mobillity report november 2019. Technical report, Ericsson, nov 2019.

[33] B. Post and S. Borst. Joint load-driven frequency allocation and user association in dense cellular networks. In *2019 31st International Teletraffic Congress (ITC 31)*, pages 75–83, 2019.

[34] A. M. Saleh, N. T. Le, and A. B. Sesay. Inter-cell interference coordination using fractional frequency reuse scheme in multi-relay multi-cell ofdma systems. In *2018 IEEE Canadian Conference on Electrical Computer Engineering (CCECE)*, pages 1–5, 2018.

[35] Sandvine. The mobile internet phenomena report (february 2020). Technical report, Sandvine, feb 2020.

[36] N. Sapountzis, T. Spyropoulos, N. Nikaein, and U. Salim. Optimal downlink and uplink user association in backhaul-limited hetnets. In *IEEE INFOCOM 2016 - The 35th Annual IEEE International Conference on Computer Communications*, pages 1–9, 2016.

[37] N. Sapountzis, T. Spyropoulos, N. Nikaein, and U. Salim. Joint optimization of user association and dynamic tdd for ultra-dense networks. In *IEEE INFOCOM 2018 - IEEE Conference on Computer Communications*, pages 2681–2689, 2018.

[38] Catherine Sbeglia. Mobile ar market to hit $24 billion by 2030, says report, jul 2020. URL: https://www.rcrwireless.com/20200707/wireless/mobile-ar-market-24-billion-by-2030.

[39] P. Wang, H. Jiang, W. Zhuang, and H. V. Poor. Redefinition of max-min fairness in multi-hop wireless networks. *IEEE Transactions on Wireless Communications*, 7(12):4786–4791, 2008.

[40] Z. Wang, R. Schoenen, H. Yanikomeroglu, and M. St-Hilaire. Load balancing in cellular networks with user-in-the-loop: A spatial traffic shaping approach. In *2015 IEEE International Conference on Communications (ICC)*, pages 2638–2643, 2015.

[41] Z. Xu, G. Y. Li, C. Yang, and X. Zhu. Throughput and optimal threshold for ffr schemes in ofdma cellular networks. *IEEE Transactions on Wireless Communications*, 11(8):2776–2785, 2012.

[42] Mohamad Yassin, Mohamed Aboulhassan, Samer Lahoud, Marc Ibrahim, Dany Mezher, Bernard Cousin, and Essam Sourour. Survey of icic techniques in lte networks under various mobile environment parameters. *Wireless Networks*, 23:403–418, 02 2017. `doi:10.1007/s11276-015-1165-z`.

[43] Mohamad Yassin, Mohamed Aboulhassan, Samer Lahoud, Marc Ibrahim, Dany Mezher, Bernard Cousin, and Essam Sourour. Survey of icic techniques in lte networks under various mobile environment parameters. *Wireless Networks*, 23:403–418, 02 2017. `doi:10.1007/s11276-015-1165-z`.

[44] Y. Özcan, J. Oueis, C. Rosenberg, R. Stanica, and F. Valois. Robust planning and operation of multi-cell homogeneous and heterogeneous networks. *IEEE Transactions on Network and Service Management*, pages 1–1, 2020.